Dissertation

submitted to the

Combined Faculties for the Natural Sciences and for Mathematics

of the Ruperto-Carola University of Heidelberg, Germany

for the degree of

Doctor of Natural Sciences

Presented by

M.Sc. Biology Weijun Feng

Born in: Zhejiang, China

Oral-examination:

The Jumonji-C domain containing proteins PHF2 and PHF8 act in concert to stimulate transcription of rRNA genes

Referees: Prof. Dr. Ingrid Grummt

PD Dr. Karsten Rippe

Acknowledgements

I would like to express my sincere gratitude to my Ph.D. supervisor Prof. Dr. Ingrid Grummt and to thank her for giving me the opportunity to pursue my Ph.D. in her group. I am indebted to her for her incomparable guidance, stimulating discussion and unconditional support. I am also very grateful for her great patience while tutoring my scientific writing during the preparation of manuscripts and this thesis. Her insistence on the pursue of accuracy and perfection is a precious gift not only for my scientific career but also for my whole life.

I owe my gratitude to Dr. Yonggang Zhou for precious advice and technical assistance from the very beginning of my study in Grummt's group. Many thanks go to Dr. Jing Ye, from whom I have received a lot of help both in the lab and privately. I am indebted to all my colleagues in the group for their indispensable help and numerous discussions. In particular, I would like to express my gratitude to Dr. Holger Bierhoff for his helpful suggestions and critical reading of my thesis. I also would like to thank Mr. Urs Hoffmann-Rohrer and Mrs. Anne Wohlfahrt for their administrative support and help during my stay in Heidelberg.

I wish to thank Dr. Masato Yonezawa and Prof. Dr. Thomas Jenuwein, Reserch Institute of Molecular Pathology (IMP), The Vienna Biocenter, Austria, not only for providing constructs of PHF2 and PHF8 and other experimental materials, but also for making this very productive cooperation possible. I am especially thankful to Dr. Masato Yonezawa for sharing his valuable scientific experiences, his helpful advice and his active participation in this project.

I would like to extend my gratitude to my Ph.D. thesis committee members PD Dr. Renate Voit and PD Dr. Karsten Rippe for their scientific input, insightful discussion, and generous support of my thesis.

I am indebted to all my friends for their kind help and encouragement during my whole study. My final heartfelt acknowledgement goes to my parents for their endless support, understanding and constant inspiration through years.

Abbreviations

aa	amino acid
Asn	Asparagine
ATP	Adenosine-5'-triphosphate
bp	base pairs
BSA	Bovine serum albumin
cDNA	complementary deoxyribonucleic acid
ChIP	Chromatin immunoprecipitation
Ci	Curie
C-terminus	Carboxyl-terminus
CTP	Cytidine-triphosphate
DMEM	Dulbecco's modified Eagle's medium
DMSO	Dimethylsulphoxide
DNA	Deoxyribonucleic acid
DNase	Deoxyribonuclease
DTT	Dithiothreitol
ECL	Enhanced chemi-luminescence
E. coli	Escherichia coli
EDTA	Ethlylene diamine tetraacetic acid
EGTA	Ethyleneglycol-bis- (2-aminoethylether)-tetraacetic acid
FCS	Fetal calf serum
g	gram
Glu	Glutamic acid
GST	Glutothionine S-transferase
GTP	Guanine-triphosphate
H3	Histone H3
H4	Histone H4
HA	Hemagglutinin
HEPES	4-(2-hydroxethyl)-1-piperazineethanesulphonic acid
His	Histidine
hr	hour
HRP	Horseradish peroxidase
IF	Immunofluorescence

IgG	Immunoglobulin G
IP	Immunoprecipitation
IPTG	Isopropyl-ß-D-thiogalatopyranoside
JmjC	Jumonji C
KDa	Kilo Dalton
KDM	Lysine demethylase
KMT	Lysine methyltransferase
KAT	Lysine acetyltransferase
l	liter
LB medium	Luria-bertani-broth medium
Lys	Lysine
m-, µ-, n-, f-, p-	milli-, micro-, nano-, feto-, pico-
min	minute
MOPS	3-(N-Morpholino) propanesulfonic acid
N-terminus	Amino-terminus
NB	Northern Blot
NP-40	Nonidet P-40
Nt	Nucleotide
OD	Optical density
PAGE	Polyacrylamide gel electrophoresis
PBS	Phosphate-buffered saline
PCR	Polymerase chain reaction
PHD	Plant homeobox domain
Phe	Phenylalanine
PHF2	PHD finger protein 2
PHF8	PHD finger protein 8
Pol I	RNA polymerase I
rDNA	Ribosomal DNA
RNA	Ribonucleic acid
rRNA	Ribosomal RNA
RNase	Ribonuclease
RNasin	Ribonuclease inhibitor
rpm	radiations per minute
RT	Room temperature

RT-PCR	Reverse transcription polymerase chain reaction
SDS	Sodium dedocyl sulphate
SDS-PAGE	SDS-polyacrylamide gel electrophoresis
shRNA	short hairpin RNA
siRNA	small interfering RNA
SSC	Saline-sodium citrate buffer
TAF	TATA-binding proteins associated factor
TBE	Tris-EDTA-borate buffer
TBP	TATA-binding factor
TCA	Trichloroacetic acid
TE	Tris-EDTA buffer
Thr	Threonine
TIF	Transcription initiation factor
Tris	Tris (hydroxymethyl)-amino-methane
Tyr	Tyrosine
Tween 20	Polyoxyethylene-sorbitan-monolaurate
UBF	Upstream binding factor
UTP	Uridine-triphosphate
WB	Westerm blots
WT	Wild-type
w/v	Weight/volume
v/v	Volume/volume
XLMR	X chromosome-linked mental retardation

Zusammenfassung

Die Gene, die für rRNA kodieren (rDNA), liegen in Säugerzellen in mehreren hundert Kopien vor, von denen etwa die Hälfte transkriptionell aktiv, die andere Hälfte inaktiv ist. Aktive und inaktive rDNA Kopien weisen eine unterschiedliche Chromatinstruktur auf. Aktive Gene liegen in ‚offener' euchromatischer Konfiguration vor, während inaktive Gene eine kompakte heterochromatische Struktur aufweisen. Nukleosomen an aktiven rDNA Promotoren sind durch spezifische Histonmodifikationen charakterisiert, die sich von Histonmodifikationen an inaktiven Genen unterscheiden. So ist z.B. Histon H3 am Promotor aktiver Gene an Lysin 4 methyliert (H3K4me), während Histon H3 an inaktiven Gene an Lysin 9 methyliert (H3K9me) ist. Das Gleichgewicht zwischen H3K4me und H3K9me wird durch das koordinierte Zusammenspiel von verschiedenen Histon-Methyltransferasen und -Demethylasen etabliert und aufrechterhalten. Für verschiedene Histon-H3K9-Methyltransferasen wie G9a, SETDB1 und Suv39H1 konnte gezeigt werden, dass sie die Chromatinstruktur von rDNA modulieren. Enzyme, die reprimierende Methylgruppen von H3K9 am rDNA Promotor entfernen, sind bislang unbekannt. In der vorliegenden Arbeit wird die Funktion von zwei putativen Histon-Demethylasen, PHF2 und PHF8, charakterisiert.

Sowohl PHF2 als auch PHF8 lokalisieren in Nukleoli und sind mit aktiven rRNA Genen assoziiert. Depletierungs- und Überexpressions-Experimente demonstrieren, dass PHF2 und PHF8 die Pol I Transkription aktivieren. Die transkriptionelle Aktivierung hängt von der Präsenz eines funktionellen PHD-Fingers und der JmjC-Domäne ab. PHF2 und PHF8 werden durch Interaktion mit der Pol I Transkriptionsmaschinerie an die rDNA rekrutiert. Zusätzlich binden die PHD-Finger von PHF2 und PHF8 an H3K4me3, ein Befund der die Bindung von PHF2 und PHF8 an aktive rRNA Gene unterstützt. Wird PHF8 durch siRNA depletiert, wird H3K9 am rDNA Promotor verstärkt methyliert. Dies weist darauf hin, dass PHF8 eine H3K9me1/2 Demethylase ist. Im Gegensatz dazu zeigt PHF2 keine Histon-demethylierende Aktivität, sondern scheint der H3K4 Demethylase KDM2B entgegenzuwirken. Mutationen in dem humanen PHF8 Gen korrelieren mit der Erbkrankheit XLMR (*X-linked mental retardation*). Eine mit XLMR-assoziierte

Punktmutation in der JmjC-Domäne von PHF8 (F279S) verhindert sowohl die Interaktion mit der Pol I-Transkriptionsmaschinerie als auch die nukleoläre Lokalisation und die PHF8-vermittelte Aktivierung der prä-rRNA. Es ist daher sehr wahrscheinlich, dass Inaktivierung von PHF8 zur ineffizienten rDNA Transkription führt und dies zur Entstehung von XLMR beiträgt.

Die vorliegenden Ergebnisse zeigen eine wichtige Rolle von PHF2 und PHF8 in der epigenetischen Regulation von rRNA Genen. Diese Regulation ist essentiell für die effiziente Transkription von rRNA Genen, und deren Dysregulation führt zu schweren genetischen Krankheiten.

Summary

In mammalian cells, actively transcribed rRNA genes (rDNA) exist in a euchromatic configuration, whereas silent rDNA repeats form a heterochromatic structure. A hallmark of active rDNA is methylation of histone H3 lysine K4 (H3K4me), while silent genes are characterized by methylation of histone H3 lysine K9 (H3K9me). The balance between H3K4me and H3K9me is established and maintained by the coordinated interplay of different histone methyltransferases and demethylases. Several histone H3K9 methyltransferases such as G9a, SETDB1 and Suv39H1, have been shown to modulate the chromatin structure of rRNA genes. However, the enzymes that remove repressive methyl groups from H3K9 at the rDNA promoter are yet unknown. In the present study, the function of two putative Jumonji-C (JmjC) domain-containing histone demethylases PHF2 (PHD finger protein 2) and PHF8 (PHD finger protein 8) has been characterized.

Both PHF2 and PHF8 localize to nucleoli and are associated with active rRNA genes. Gain-of-function and loss-of-function experiments demonstrate that PHF2 and PHF8 activate rDNA transcription. Transcriptional activation depends on the presence of a functional PHD finger and the JmjC domain. Recruitment of PHF2 and PHF8 to rDNA is mediated by the interaction with the RNA polymerase I (Pol I) transcription machinery. In addition, the PHD fingers of PHF2 and PHF8 bind to the euchromatic histone mark, H3K4me3, which may facilitate the association of both proteins with active rDNA. Depletion of PHF8 leads to increased levels of the repressive marks H3K9me1 and H3K9me2 (H3K9me1/2) at the rDNA promoter, suggesting that PHF8 demethylates H3K9me1/2. In contrast, PHF2 shows no histone demethylase activity on itself but appears to antagonize a transcriptional repressor, the H3K4me3 demethylase KDM2B. The association of PHF2 with rDNA depends on PHF8, indicating that PHF2 and PHF8 function as a complex that is able to remove H3K9me1/2 and to maintain H3K4me3 at active rDNA repeats.

Mutations in the human *PHF8* gene are associated with an inherited disease termed X-linked mental retardation (XLMR). As demonstrated in this study, an XLMR-associated point mutation in the JmjC domain of PHF8

(F279S) impairs the interaction with the Pol I transcription machinery, the nucleolar localization and PHF8-dependent transcriptional activation. Thus, impairment of PHF8-mediated activation of rDNA transcription might contribute to the development of XLMR.

Together, the results uncover an important function of PHF2 and PHF8 in nucleoli, adding a new layer of epigenetic regulation of rRNA genes. This regulation is vital for proper rRNA synthesis and its disruption is likely to cause severe diseases in humans.

1. Introduction

1.1. Epigenetic regulation of gene expression

The genome of a diploid human cell contains approximately 3 billion base pairs of DNA, which is about 2 meters in length. To fit the large genome into the microscopic space of eukaryotic nucleus, DNA is compacted by histones to form chromatin. Chromatin is the physiological template for all kinds of DNA-dependent processes such as transcription, replication, recombination, and DNA repair. Histones are a family of positively charged proteins, termed histone H1, H2A, H2B, H3 and H4. As DNA is negatively charged, histones bind to DNA very tightly. The fundamental unit of chromatin is the nucleosome, an octamer containing two of each of the core histones (H2A, H2B, H3, H4) wrapped around 146 base pairs of DNA. The linker histone H1 binds the nucleosome at the entry and exit sites of the DNA, thus locking the DNA into place and allowing the formation of higher order structure.

Like other DNA-related metabolic processes, all stages of transcription from initiation to termination are affected by the packaging of DNA into chromatin. The presence of nucleosomes poses barriers to RNA polymerases. It is therefore important for cells to have means of ‘‘opening’’ chromatin and/or removing histones transiently to permit transcription. There are two major mechanisms by which chromatin becomes more accessible. First, histones can be modified by addition of acetyl or phosphate groups that reduce the DNA-histone interaction; second, histones can be displaced by chromatin remodeling complexes, thereby exposing underlying DNA sequences to DNA binding proteins.

The core histones are predominantly globular except for their unstructured N-terminal “tails”. One of the most important features of histones is that histone tails and to a less extent also globular domains are subjected to a wide range of posttranslational modifications. The most common modifications include methylation, acetylation and ubiquitylation of lysine (K) residues; methylation of arginine (R) residues; and phosphorylation of serine (S) and threonine (T) residues (Fig. 1.1). As most, if not all, histone modifications are reversible, this post-translational histone marking system represents a

fundamental regulatory mechanism for chromatin function (Jenuwein and Allis 2001). Histone modifications regulate transcription by affecting higher-order chromatin structure or by recruiting effector proteins that further modify chromatin. While acetylation and phosphorylation increase the negative charge of histones and therefore reduce the DNA-histone interaction, methylation does not influence the net charge of histones, and hence, has no effect on DNA-histone interaction. Instead, histone methylations function as recognition marks for effector proteins.

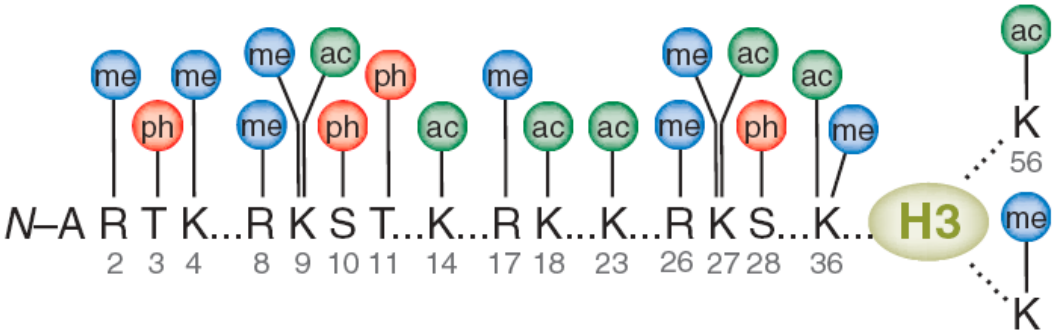

Figure 1.1. Common posttranslational modifications in histone H3
A scheme outlines the common posttranslational modifications in histone H3, including acetylation (ac), methylation (me), and phosphorylation (ph). The numbers below residues indicate the positions of individual amino acids. Figure from Bhaumik et al. 2007.

There are two distinct chromatin structures, transcriptional silent heterochomatin and active euchromatin, which are demonstrated by a distinct set of chromatin modifications. Histone modifications like acetylation and phosphorylation are generally related to active transcription. Methylation and ubiquitylation of lysine and arginine methylation can both activate and repress transcription, depending on the particular residue that is modified. The transcriptional outcome of certain histone modification is dependent on the context, i.e. the information has to be decoded by downstream effector proteins. Effector proteins are recruited to certain chromatin areas by recognizing specific histone modifications. After recruitment, these effector proteins either modify the chromatin by themselves or recruit other factors that directly impact chromatin structure. An increasingly growing number of chromatin-recognition motifs have been identified. For example, histone methylation is recognized by

PHD-, chromo-, tudor- and MBT-domains. Acetylation of histones is recognized by bromodomains, and phosphorylation by a domain within 14-3-3 proteins (Taverna et al. 2007).

Covalent modifications do not only occur on histones, but also on DNA. In mammalian cells, DNA can be methylated at cytosine residues that reside in CpG dinucleotide sequences. The majority of CpGs are methylated in mammals, whereas unmethylated CpGs are grouped in clusters, termed "CpG islands", which are present in the 5' regulatory regions of many genes (Cedar and Bergman 2009). DNA methylation usually results in heritable transcriptional silencing at least partly by preventing association of general transcription factors with gene promoters. Like histone methylation, the methylation state of CpGs is recognized by specific proteins. Methylated CpG dinucleotides are recognized by methyl-CpG binding domain (MBD) containing-proteins, such as MBD1-MBD4 and MECP2, whereas the CXXC zinc-finger domain specifically binds to unmethylated CpG-rich regions (Voo et al. 2000).

Generally, nucleosomes present a barrier for the transcription machinery to pass through DNA. To overcome this, a family of chromatin remodeling factors that are able to alter the histone-DNA contacts at the expense of ATP-hydrolysis, has evolved. The dynamics of nucleosome remodeling regulate DNA accessibility that is key to proper gene regulation. For instance, a positioned nucleosome directly upstream of the transcription start site of many genes has to be repositioned or evicted to expose regulatory elements to transcription factors upon gene activation (Henikoff 2008).

1.2. Establishment and interpretation of histone lysine methylation

1.2.1. Histone lysine methylation and transcription

Histone lysine methylation has been shown to play important roles in maintaining genome integrity, transcription and epigenetic memory (Martin and Zhang 2005). Methylation occurs on several lysine residues in the N-terminal

tails of histone H3 and H4 and in the globular domain of histones as well. There are three different methylation states of lysine residues: mono-, di-, or trimethyl. Each methylation state is often associated with a distinct biological outcome. Consequently, protein modules that bind methylated lysines should be selective not only towards a given lysine residue but also for its methylation state. The same holds true for enzymes that catalyze the transfer or removal of the methyl groups. Thus, a complex regulatory network establishes a specific pattern of histone lysine methylation (Kustatscher and Ladurner 2007). With the exception of methylation of H3K79, histone lysine methylations are catalyzed by a family of SET domain-containing proteins (Qian and Zhou 2006). In contrast to histone acetyltransferases, which have a broad substrate specificity, most histone methyltransferases only modify a defined lysine residue to a specific methylation state.

Histone methylation can both activate or repress transcription, depending on the particular lysine residue that is methylated. In most cases, methylation on histone H3K4, H3K36 and H3K79 is associated with euchromatic regions, whereas H3K9me, H3K27me and H4K20me are found in heterochromatin. However, there are increasing evidences showing that the transcriptional outcome of a particular histone methylation is context dependent, relying on both the localization of this modification and the effector proteins that recognize the modification (Li et al. 2007; Kouzarides 2007). Different histone methylaton marks exhibit a distinct localized pattern within a gene, with preference either at the enhancer region, the core promoter or the gene body. Indeed, the location of a given modification is tightly regulated and is crucial for its effect on transcription. For example, methylation at H3K36 or H3K9 has a positive effect when it is localized within the coding region of certain gene but has a negative effect when it is present in the promoter (Landry et al. 2003; Vakoc et al. 2005). Moreover, histone lysine methylation appears to function as a nucleation site for effector proteins (Taverna et al. 2007). These effector proteins recognize specific histone lysine methylation and impact chromatin by themselves or by recruiting downstream proteins, which either activate or repress gene expression. For instance, BPTF, the largest subunit of nucleosome remodeling factor (NURF), binds to chromatin by recognizing H3K4me3 via its

PHD finger, leading to activation of *Hox* gene expression (Wysocka et al. 2006).

1.2.2. Histone demethylases

Similar to DNA methylation, methylation of histones has been regarded as irreversible because of the high thermodynamic stability of the N-CH_3 bond. However, the recent identifications of histone demethylases have shown that histone methylation is reversible and dynamically regulated like other histone modifications (Shi et al. 2004; Yamane et al. 2006; reviewed by Cloos et al. 2008). So far, two groups of histone demethylases have been characterized, LSD1 and a family of Jumonji (JmjC) domain-containing proteins. LSD1 removes methyl group through a flavin adenine dinucleotide (FAD)-dependent amine oxidase reaction (Fig. 1.2, upper panel). However, as this reaction requires a protonated methyl ε-ammonium group for oxidation, LSD1 is not able to catalyze the demethylation of trimethylated lysine residues. Unlike LSD1, the JmjC domain-containing histone demethylases are able to remove all three methyl groups from histones. The JmjC domain cooperates with cofactor iron Fe(II) and α-ketoglutarate (αKG) to produce highly reactive oxoferryl species that hydroxylate the methylated substrate, allowing spontaneous loss of the methyl group as formaldehyde (Fig. 1.2, lower panel).

The JmjC domain is structurally conserved, each of the two layered β sheets containing four antiparellel β strands that produce the typical jellyroll-like structure (Fig. 1.3). A highly conserved His-X-ASP/GLU-Xn-His motif (X: any amino acid; Xn: various number of amino acid in between) supplies three chelating positions for the iron. αKG interacts with the iron and is further stabilized by the interaction with two additional conserved residues (Phe/Thr/Tyr for the first and Lys for the second amino acid). All these residues are conserved in the JmjC domains of active histone demethylases and mutation of these critical residues results in loss of demethylation activity.

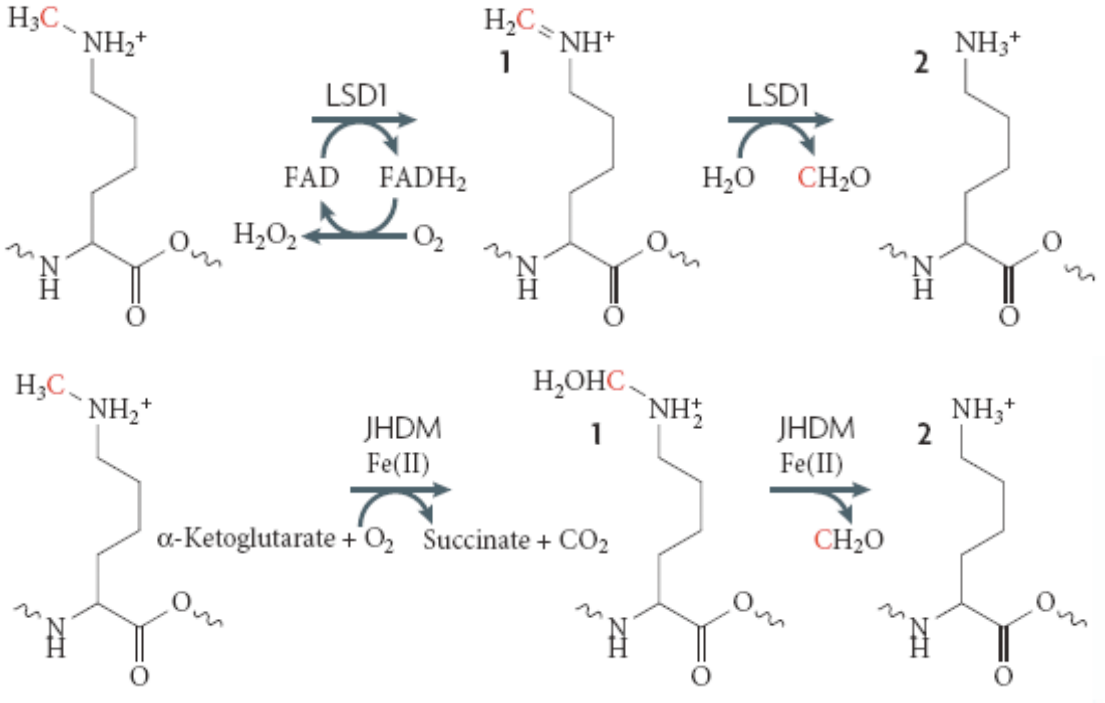

Figure 1.2. The mechanisms of removing methyl group by demethylases
(Upper) LSD1 mediates histone demethylation through an amine oxidation reaction using FAD as a cofactor. Loss of the methyl group from mono-methyl lysine occurs through an imine intermediate, which is hydrolysed to form formadelhyde. (Lower) The JmjC domain-containing proteins use iron and αKG as cofactors in an oxidative demethylation reaction that produces hydroxymethyl-lysine, succinate and CO_2 as reaction products. The hydroxymethyl group is then spontaneously lost as formaldehyde. Figure from Klose and Zhang. 2007.

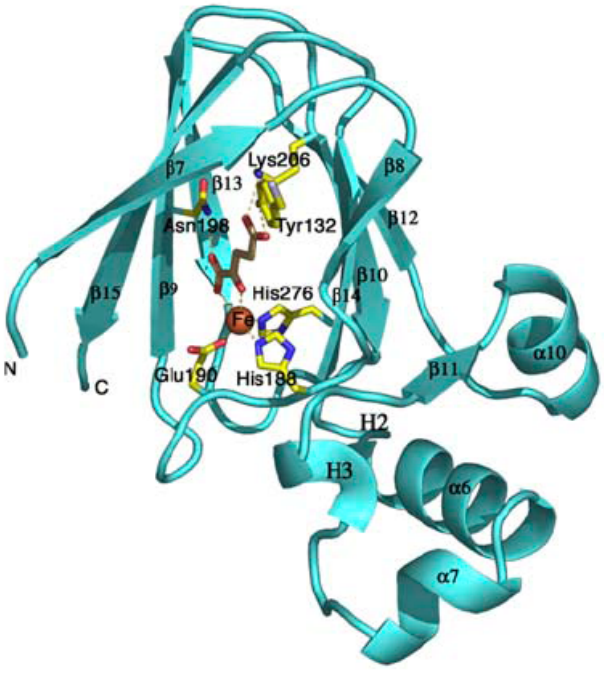

Figure 1.3. Structure of the JmjC domain of KDM4A
The scheme demonstrates the structure of the JmjC domain of the histone H3K9 demethylase KDM4A. Residues that are involved in the interactions with the cofactors iron (His188, Glu190 and His276) and the αKG molecule (Tyr132, Asn198, and Lys206) are displayed and labeled. Figure from Chen et al. 2006.

There are about 27 different JmjC domain-containing proteins encoded in the human genome, and 15 of them have been shown to be active histone demethylases (Fig. 1.4). JMJD6 is the only histone demethylase that removes methyl groups from arginine residues on histones (Chang et al. 2007), whereas the other histone demethylases remove methyl groups from lysine residues. An obvious feature of these enzymes is that they often contain chromatin-binding modules, such as the PHD finger (PHD), tudor (Tdr) domain or CXXC zinc-finger domain (CXXC), which may facilitate targeting the histone demethylases to specific genomic regions. Most of these enzymes localize to nuclei consistent with a role in regulating chromatin structure.

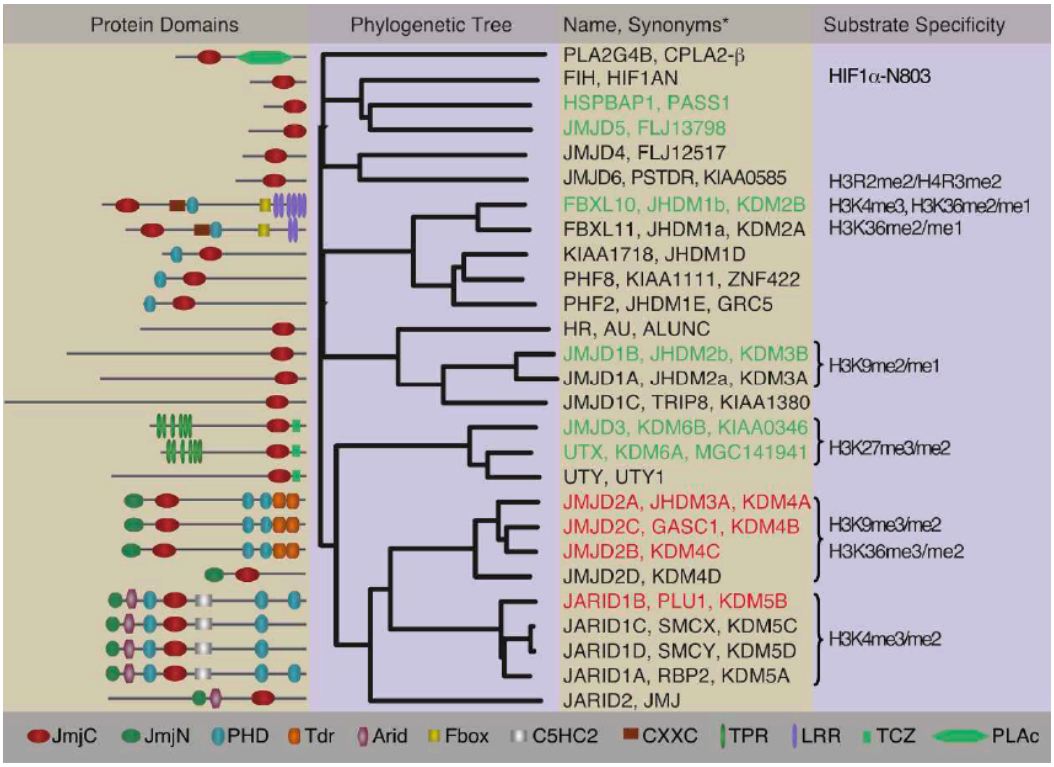

Figure 1.4. Phylogenetic tree of the JmjC family of demethylases
The names, synonyms, substrates specificities, and domain structures of the JmjC family proteins are provided. Figure from Cloos et al. 2007.

JmjC domain-containing proteins have been shown to play a crucial role in various physiological processes, including nuclear hormone signaling (Yamane et al. 2006; Wissmann et al. 2007), spermatogenesis (Okada et al. 2007) and cell differentiation (Loh et al. 2007). Consequently, dysregulation of

these enzymes has been connected to various human diseases, such as neurological disorders and several types of cancer (Shi 2007; Cloos et al. 2008).

1.2.3. The PHD fingers of chromatin-associated protein recognize different state of histone lysine methylation

The PHD finger is a conserved zinc finger domain that is present in a large number of chromatin-associated factors and has emerged as a motif that recognizes different methylation state of lysine residues on histone H3 tails (Adams-Cioaba and Min 2009). The typical PHD finger consists of a Cys_4-His-Cys_3 containing segment coordinated to two Zn^{2+} ions (Fig 1.5, left panel). According to their methyl lysine-binding specificity, the PHD fingers can be divided into several subclasses. The first subclass of PHD fingers, represented by BPTF and ING2, recognizes H3K4me3 (Li et al. 2006; Pena et al. 2006; Shi et al. 2006; Wysocka et al. 2006), engages H3K4me3 and H3R2 simultaneously in two adjacent channels that are separated by a conserved tryptophan residue (Fig. 1.5, middle panel). A second subclass of PHD fingers, including those of BHC80 and DNMT3L, specifically interacts with unmodified H3K4 (Ooi et al. 2007; Lan et al. 2007). Instead of utilizing an aromatic cage/channel, the specificity for the association is established through an electrostatic bridge between the unmodified epsilon amino group of H3K4 and an acidic residue in the PHD finger (Fig. 1.5, right panel). It seems that many other PHD fingers do not fit into the two subclasses above, and therefore may be associated with yet to be characterized methyl-lysine residues on histones. In support of this, one of the two PHD fingers of the histone demethylase SMCX/KDM4C has been shown to recognize H3K9me3 (Iwase et al. 2007).

The PHD fingers are not only present in histone modifying enzymes but also in general transcription factors. A recent report has revealed that the basal Pol II-specific transcription factor TFIID directly binds to H3K4me3 via the PHD finger of TAF3 (Vermeulen et al. 2007). Consistent with misinterpretation of histone modifications being detrimental to the cell, mutations within the PHD fingers have been associated with a wide variety of human diseases. For instance, point mutations, deletions or chromosomal translocations of the PHD fingers of RAG2 and ING1 have been associated with

immunological disorders, cancers and neurological diseases (Baker et al. 2008). Moreover, a recent study has demonstrated that fusing an H3K4me3-binding PHD finger to NUP98 is sufficient to induce leukaemia (Wang et al. 2009).

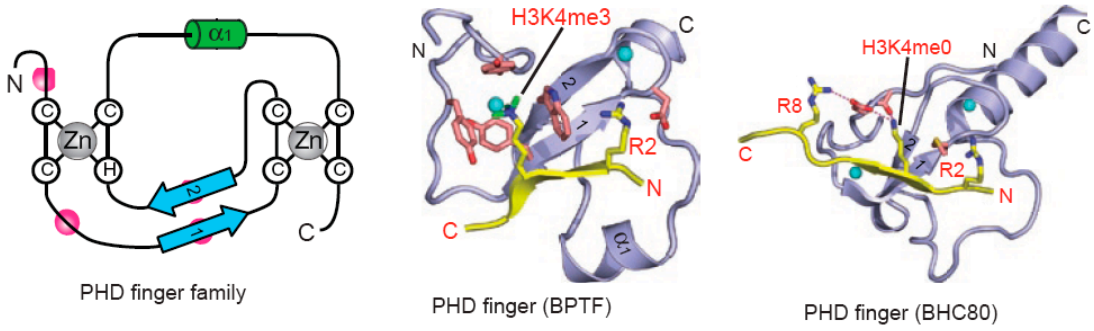

Figure 1.5. Readout of histone lysine methylation by the PHD finger
(Left panel) Topology of the PHD finger fold. Blue arrows, two small β-strands that bridge the interleaved zinc-finger motifs; labeled white circles, zinc-coordinated cysteine and histidine residue; green cylinder, short α-helix (α1) near the C terminus; pink circles, the caging residues for readout of methyl-lysine or unmodified lysine mark. (Middle panel) Specific recognition of H3K4me3 by the PHD finger of BPTF. The H3 peptide resides in a surface groove between α1 and β1-strand upon formation of the antiparallel β-sheet with the core β-strands. Note the full aromatic cage formed at the protein surface for trimethyl-specific readout. H3K4 site specificity is achieved by simultaneous recognition of H3K4me3 and H3R2, as well as by anchoring of the N terminus zinc ions within the zinc-finger motifs. (Right panel) Specific readout of unmodified H3K4 peptide by the PHD finger of BHC80. The module has a surface patch of acidic residues for unmodified H3K4 mark recognition. Figure from Taverna et al. 2007.

1.3. The structure of rRNA genes and the Pol I transcription apparatus

The rate of cell growth and proliferation depends on the cellular capacity of protein synthesis, which in turn is linked to ribosome biogenesis. Ribosomal RNA (rRNA) is the major catalytic and architectural component of a ribosome, and therefore transcription of rRNA genes (rDNA) is a central step of ribosome biogenesis. In cycling cells, about 50% of cellular transcription activity is expended in the synthesis of rRNA. Thus, it is not surprising that the cell has evolved complex regulatory mechanisms to control rRNA synthesis. Practically all signaling pathways that affect cell growth also regulate rDNA transcription by modulating the activity of Pol I-specific transcription factors. In addition,

regulation of rDNA transcription occurs also by modulating the chromatin structure of rDNA.

Mammalian cells contain 200-400 copies of tandemly repeated rRNA genes located in specific nuclear compartments, the nucleoli. Clusters of rDNA repeats, termed nucleolar organizer regions (NORs), are located on different chromosomes, e.g. in humans on the short arms of acrocentric chromosomes 13, 14, 15, 21 and 22. Each rRNA gene encodes a precursor transcript (45S pre-rRNA) that is subsequently processed into mature 18S, 5.8S and 28S rRNAs. The 43 kb human rDNA transcription units comprise sequences encoding pre-rRNA (13 kb) that are separated by intergenic spacer (IGS) sequences (30 kb). Multiple regulatory elements reside within the IGS, including the rDNA promoter, the upstream terminator T_0 and the downstream terminators (T_{1-10}) (Fig. 1.6).

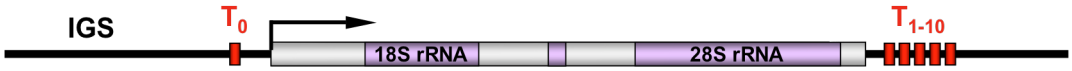

Figure 1.6. The mammalian rDNA transcription unit
The scheme outlines a representative mammalian rDNA repeat, illustrating the rDNA promoter, the upstream terminator (T_0), the pre-rRNA coding region, the downstream terminators (T_{1-10}), and the intergenic spacer (IGS).

rRNA genes are transcribed by RNA polymerase I (Pol I). In mammals, Pol I is found in a complex of >1MDa consisting at least 13 core subunits and several Pol I-associated factors (Miller et al. 2001). Interestingly, cellular Pol I exists in two functionally distinct complexes (Pol Iα and Pol Iβ). Pol Iα, which comprises the majority (>90%) of the total cellular Pol I, is unable to initiate transcription at the rDNA promoter but rather catalyzes the random synthesis of RNA. Therefore, Pol Iα probably represents the elongating Pol I complex. In the other hand, the initiation-competent form Pol Iβ contains Pol I-specific transcription factor TIF-IA and is able to direct accurate initiation of transcription from the rDNA promoter.

UBF is a Pol I-specific transcription activator that contains six HMG (high mobility group) DNA binding motifs. The HMG boxes enable UBF to

bend DNA to form the enhancesome, a nucleosome-like structure thought to be required for rDNA transcription (Stefanovsky et al. 2001). In addition, UBF has been shown to be involved in the formation of preinitiation complex (Bell et al. 1988), promoter escape (Panov et al. 2006), transcription elongation (Stefanovsky et al. 2006) and the determination of the number of active rRNA genes (Sanij et al. 2008).

1.4. rRNA genes exist in two distinct epigenetic states

Despite rDNA transcription is limiting for cell growth, less than 50% of the rRNA genes are transcriptionally active. The proportion of active and silent rRNA genes can be identified by their different susceptibility to the DNA cross-linking agent psoralen (Sogo and Thoma 1989). Transcriptionally active rRNA genes are accessible to psoralen and are free of regularly spaced nucleosomes, whereas inactive rDNA gene copies are inaccessible to psoralen and display regularly spaced nucleosomes (Conconi et al. 1989). The ratio of active and inactive rRNA genes is stably propagated through cell cycle, which suggests that epigenetic regulation mechanism is involved in modulating the chromatin structure of rDNA.

Distinct chromatin modifications are associated with transcriptionally active and silent rDNA repeats (Fig. 1.7). Typical euchromatic marks, such as DNA hypomethylation of CpG residues, acetylation of histones and methylation at H3K4 are present at active rRNA genes, whereas hypermethylated CpG residues, histone hypoacetylation, methylation at H3K9, H3K27 and H4K20 are associated with silent rDNA repeats (Santoro et al. 2002; Zhou et al. 2002; Santoro and Grummt. 2005). A key factor that establishes heterochromatin at the rDNA promoter is an ATP-dependent chromatin remodeling complex, termed NoRC (Nucleolar Remodeling Complex). NoRC is composed of the regulatory subunit TIP5 and the ATPase SNF2h. TIP5 binds exclusively to inactive rDNA repeats and serves as a scaffold to recruit the Sin3a-HDAC corepressor complex, the histone H3K9 methyltransferase SETDB1, as well as DNA methyltransferases DNMT1 and DNMT3 (Santoro et al. 2002; Zhou et al. 2002). In addition, NoRC is capable to shift the promoter-bound nucleosome

into the silent position, which impairs binding of the Pol I-specific transcription factor UBF to the rDNA promoter (Li et al. 2006).

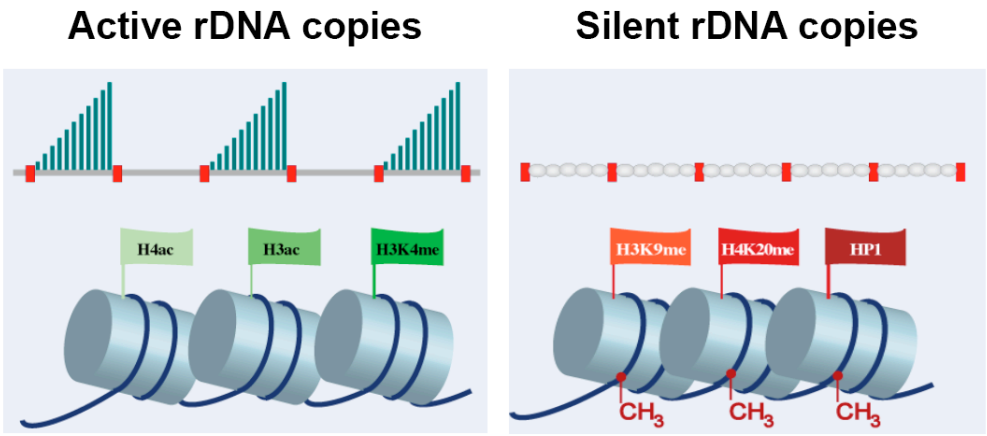

Figure 1.7. rDNA repeats exist in two distinct chromatin states
Active rRNA genes possess a typical euchromatical structure consisting of acetylation of histones, methylation of H3K4 and hypomethylated CpG residues. In contrast, silent rRNA genes are packaged into heterochromatin containing methylation at H3K9, H4K20, hypermethylated CpG residues and are also bound by heterochromatin protein HP1.

Compared to NoRC-dependent silencing of rDNA, little is known about the molecular mechanism that establishes the epigenetically active state of rDNA repeats. A putative candidate for an active chromatin remodeler is CSB (Cockayne Syndrome Protein B), a DNA-dependent ATPase that activates rDNA transcription in an ATP-dependent manner. CSB is capable to recruit the histone methyltransferase G9a to the pre-rRNA coding region, where G9a methylates H3K9, a mark that is associated with transcription elongation (Bradsher et al. 2002; Yuan et al. 2007). Moreover, other ATP-dependent remodelers have also been shown to stimulate rDNA transcription, such as WICH, a complex comprising WSTF (Williams Syndrome Transcription Factor) and the ATPase SNF2h, and Mi2β (Percipalle et al. 2006; Shimono et al. 2005). However, the molecular mechanism underlying is not well known.

Regulation of histone lysine methylation is required for proper transcription of rRNA genes. Several histone H3K9 methyltransferases, i.e. SETDB1, SUV39H1 and G9a have been shown to modulate the chromatin structure of rDNA (Santoro et al. 2002; Yuan et al. 2007; Murayama et al.

2008). To dynamically regulate H3K9 methylation, one would predict that there is a histone demethylase removing H3K9me. Previous studies have shown that the histone demethylases KDM3 and KDM4 are capable to demethylate H3K9me (Yamane et al. 2006; Cloos et al. 2006; Fodor et al. 2006; Klose et al. 2006; Whetstine et al. 2006). However, it is not known whether these demethylases serve a function at rDNA. The first identified JmjC domain-containing protein that modifies nucleolar chromatin is KDM2B (also known as JHDM1B or FBXL10). KDM2B was shown to repress rDNA transcription by demethylating the active histone mark H3K4me3 (Frescas et al. 2007). In other studies KDM2B has been shown to demethylate H3K36me2 and to inhibit cell proliferation and senescence through silencing of the $p15^{ink4b}$ tumor suppressor gene (He et al. 2008; Tzatsos et al. 2009). Moreover, KDM2B has also been reported to repress c-Jun expression and to protect cells from H_2O_2-induced apoptosis and G_2/M arrest. The biological role of other JmjC family proteins in the context of rDNA transcription is yet to be elucidated.

1.5. The PHF2/PHF8/KIAA1718 subfamily of JmjC domain-containing proteins

The PHF2/PHF8/KIAA1718 subfamily of JmjC domain-containing proteins contains a PHD finger in addition to the JmjC domain (Fig. 1.4). The presence of a PHD finger, a module recognizing different methylation state of lysine residues on histones, suggests a function of this group of proteins in the regulation of chromatin structure and transcription. No enzymatic activity has yet been assigned to these proteins and very little is known about their function. Proteins of the PHF2/8/KIAA1718 subfamily are evolutionarily conserved from yeast to humans. Interestingly, deletion of the *C. elegans PHF2/PHF8* ortholog *4F429* causes embryonic lethality with a low penetrance (Fernandez et al. 2005), suggesting that this protein plays a role in development. A genome-wide screen of MoMuLV-induced T cell lymphomas have revealed provirus insertions upstream of *PHF2* and *PHF8* (Pfau et al. 2008), suggesting that both proteins may be involved in the development of lymphomas. The last member of this subfamily is KIAA1718, which lies on human chromosome 7q34

encoding a 941 aa protein. The biological function of KIAA1718 is unknown.

Human *PHF2* lies on chromosome 9q22 and encodes a 1099 aa protein. In mice, PHF2 is ubiquitously expressed, particularly concentrated in the embryonic neural tube and root ganglia. The expression pattern and chromosomal localization suggest that PHF2 is a candidate gene for hereditary sensory neuropathy type 1, HSN1 (Hasenbusch-Theil et al. 1999). Moreover, a variety of chromosome aberrations at chr.9q22 have been related to different malignancies including breast cancer, and mutations in *PHF2* has been identified in these patients (Sinha et al. 2008).

The gene encoding human PHF8 is located on the X-chromosome at p11.22. It contains 22 exons encoding a 1024 aa protein. Mutations of *PHF8* are associated with a disease termed X-linked mental retardation (XLMR) (Siderius et al. 1999; Laumonnier et al. 2005; Abidi et al. 2007; Koivisto et al. 2007). XLMR is an inherited disease that causes failure to develop cognitive abilities because of mutations in numerous genes on the X chromosome. This disease is a highly heterogeneous condition affecting around 1.6/1000 males, with a carrier frequency of 2.4/1000 females. Over the years, more than 60 XLMR-associated genes have been identified (Ropers 2006). Mutation in some of these genes give rise to clinically distinguishable syndromic forms of mental retardation, such as fragile X syndrome and Rett syndrome, whereas others have been implicated in non-syndromic XLMR. Intriguingly, many XLMR-related genes have a direct role in modulation of chromatin structure, such as *MECP2, JARID1C, ATRX, PHF6 and PHF8*. In particular, *JARID1C* encodes a JmjC domain-containing histone demethylase that specifically targets H3K4me2/3. Over twenty mutations in *JARID1C* have been reported in patients with XLMR (Jensen et al. 2005; Tzschach et al. 2006; Abidi et al. 2008). Although most of these mutations are not located in the functional PHD finger and JmjC domain, they indeed impair chromatin binding and demethylation activity of JARID1C (Iwase et al. 2007; Tahiliani et al. 2007). In support of specific histone demethylases being involved in XLMR, disease-causing mutations result in truncations of PHF8 that apparently compromise its demethylation function. *PHF8* is ubiquitously expressed in mouse embryos, especially in the embryonic and early postnatal stages of brain development. A higher expression is observed in the cerebellum (granular layer) and hippocampus of the adult brain

(Laumonnier et al. 2005), i.e. are structures that are potentially involved in processes underlying memory and learning abilities.

1.6. Objectives

Active and silent rDNA repeats exhibit two distinct states of chromatin structure, euchromatic marks, i.e. acetylation of histone H4 and methylation of H3K4 correlate with transcriptional activation, whereas CpG hypermethylation and methylation of H3K9 and H4K20 are characteristic of transcriptional silencing. The specific pattern of histone methylation is established and maintained by a coordinated interplay of histone methyltransferases and demethylases. Several histone H3K9 methyltransferases i.e. G9a, SETDB1 and SUV39H1, have been shown to methylate H3K9 at rRNA genes, whereas the enzyme that removes methyl groups from H3K9 at rDNA is yet unknown. GFP-tagging of JmjC domain-containing proteins revealed that two putative histone demethylases PHF2 and PHF8, localize in nucleoli, suggesting a function in nucleolar chromatin dynamics and epigenetic regulation. To investigate the role of PHF2 and PHF8 in rDNA transcription, the following issues should be addressed.

- Generation of antibodies against PHF2 and PHF8, and expression constructs of PHF2 and PHF8.
- Examination of the cellular distribution of PHF2 and PHF8 as well as their association with rDNA and the Pol I transcription machinery.
- Gain-of-function and loss-of-function assays should reveal whether PHF2 and PHF8 serve a function on rDNA transcription. If so, point mutants in the functional important PHD finger and JmjC domain should be generated and their effects on rDNA transcription have to be assayed.
- Examination of the methyl-lysine binding specificity of the PHD fingers of PHF2 and PHF8.
- Identification of the specific methylated lysine residues on histones that can be demethylated by PHF2 and PHF8.
- Study of the functional link of PHF2 and PHF8 with the identified nucleolar JmjC domain-containing histone demethylase KDM2B.

- Mutations of human *PHF8* are associated with the disease X-linked mental retardation (XLMR). Therefore, the PHF8 point mutant (PHF8-F279S) that is found in XLMR patients should be generated and its nucleolar function has to be examined.

2. Materials and Methods

2.1. Materials

2.1.1. Antibodies

Table 1 Primary antibodies

Name	Type	Source	Application
Anti-PHF2	Rabbit, polyclonal	T. Jenuwein's lab	WB (1:1000)
Anti-PHF8	Rabbit, polyclonal	Home made (W. Feng)	WB (1:2000)
Anti-HA	Mouse, monoclonal	Munich	ChIP
Anti-HA (agarose)	Mouse, monoclonal	Sigma-Aldrich (Cat. A2095)	IP
Anti-Flag (M2)	Mouse, monoclonal, IgG1	Sigma-Aldrich (Cat. F2426)	WB (1:3000)
Anti-Flag (M2) (agarose)	Mouse, monoclonal, IgG1	Sigma-Aldrich (Cat. A2220)	IP
Anti-Flag-Cy3	Mouse, monoclonal, IgG1, conjugate	Sigma-Aldrich (Cat. A9594)	IF
Anti-V5	Mouse, monoclonal	Invitrogen (Cat. 46-0705)	WB (1:5000)
Anti-V5	Rabbit, polyclonal	Bethyl (Cat. A190-220A)	WB (1:5000), IP, ChIP
Anti-V5 (agarose)	Mouse, monoclonal	Sigma-Aldrich (Cat. A7345)	IP
Anti-RPA116	Rabbit, polyclonal	Home made (Seither et al.)	WB (1:1000), IP, ChIP
Anti-UBF	Rabbit, polyclonal	Home made	ChIP
Anti-Pol I	Human, polyclonal	Autoimmune serum #S57299	IP, IF
Anti-UBF	Human, polyclonal	Autoimmune serum (Zatsepina et al. 1993)	IP
Anti-UBF (F-9)	Mouse, monoclonal	SantaCruz (Cat, sc-13125)	WB (1:500), IF
Anti-α-Tubulin	Mouse, monoclonal	Calbiochem (Cat. CP06)	WB (1:1000)
Anti-MLL1	Rabbit, polyclonal	Bethyl (Cat. A300-086A-1)	WB (1:500)
Anti-H3	Rabbit, polyclonal	Abcam (Cat. ab1791)	ChIP

Anti-H3K4me1	Rabbit, polyclonal	Abcam (Cat. ab8895)	ChIP
Anti-H3K4me2	Rabbit, polyclonal	Upstate (Cat. 07-030)	ChIP
Anti-H3K4me3	Rabbit, polyclonal	Abcam (Cat. ab8580)	ChIP
Anti-H3K9me1	Rabbit, polyclonal	T. Jenuwein's lab	ChIP
Anti-H3K9me2	Rabbit, polyclonal	T. Jenuwein's lab	ChIP
Anti-H3K9me3	Rabbit, polyclonal	Upstate (Cat. 07-442)	ChIP
Anti-H3K27me2	Rabbit, polyclonal	T. Jenuwein's lab	ChIP
Anti-H3K27me3	Rabbit, polyclonal	Upstate (Cat. 07-449)	ChIP
Anti-H3K36me1	Rabbit, polyclonal	Abcam (Cat. ab1783)	ChIP
Anti-H3K36me2	Rabbit, polyclonal	Upstate (Cat. 07-369)	ChIP
Anti-H3K36me3	Rabbit, polyclonal	Abcam (Cat. ab1785)	ChIP
Anti-H4K20me3	Rabbit, polyclonal	Abcam (Cat. ab9053)	ChIP
Anti-acetyl-H4	Rabbit, polyclonal	Upstate (Cat. 06-866)	ChIP

Table 2 Secondary antibodies and IgGs

Name	**Type**	**Source**	**Application**
Goat anti-mouse HRP-conjugated	IgG (H+L)	Jackson Immunoresearch Laboratories, Inc	WB (1:5000)
Goat anti-rabbit HRP-conjugated	IgG (H+L)	Jackson Immunoresearch Laboratories, Inc	WB (1:5000)
Mouse IgGs		Dianova	IP, ChIP
Rabbit IgGs		Dianova	IP, ChIP
Human IgGs		Dianova	IP, ChIP

2.1.2. Primers

Table 3. Primers for qPCR

Name	Sequence	Applicaton
hrDNA (promoter) (-49 / +32)	Forward: 5'-GGTATATCTTTCGCTCCGAG-3' Reverse: 5'-GACGACAGGTCGCCAGAGGA-3'	ChIP
hrDNA (promoter) (-150 / +32)	Forward: 5'-CGATGGTGGCGTTTTT-3' Reverse: 5'-GACGACAGGTCGCCAGAGGA-3'	ChIP
HrDNA (18S rRNA) (+3990 / +4092)	Forward: 5'-CGACGACCCATTCGAACGTCT-3' Reverse: 5'-CTCTCCGGAATCGAACCCTGA-3'	ChIP
hrDNA (28S rRNA) (+7936 / +8036)	Forward: 5'-GCGACCTCAGATCAGACGTGG-3' Reverse: 5'-CTGTTCACTCGCCGTTACTGAG-3'	ChIP
hrDNA (IGS-1) (+18155 / +18280)	Forward: 5'-GTTGACGTACAGGGTGGACTG-3' Reverse: 5'-GGAAGTTGTCTTCACGCCTGA-3'	ChIP
hrDNA (IGS-2) (+27365 / +27475)	Forward: 5'-CCTTCCACGAGAGTGAGAAGC-3' Reverse: 5'-TCGACCTCCCGAAATCGTACA-3'	ChIP
hrDNA (Enhancer) (-1020 / -927)	Forward: 5'-AGAGGGGCTGCGTTTTCGGCC-3' Reverse: 5'-CGAGACAGATCCGGCTGGCAG-3'	ChIP
hrDNA (5' ETS) (+307 / +442)	Forward: 5'-TGTCAGGCGTTCTCGTCTC-3' Reverse: 5'-AGCACGACGTCACCACATC-3'	RT-PCR
hPHF2	Forward: 5'-AAGAGTGCAGGCAAACGACT-3' Reverse: 5'-TCGACCGGGACTTAAAGATG-3'	RT-PCR
hPHF8	Forward: 5'-TGGATGAACAGGACAGCTTG-3' Reverse: 5'-GGGTCGAGATTTCAAAGCAG-3'	RT-PCR
hKDM2B	Forward: 5'-GAGGAGAAGAAGAAGGTGAAG-3' Reverse: 5'-TTGATGGGCTGCTGGTTC-3'	RT-PCR
hβ–actin	Forward: 5'-CGTCACCAACTGGGACGACA-3' Reverse: 5'-CTTCTCGCGGTTGGCCTTGG-3'	RT-PCR
hGAPDH	Forward: 5'-CCCATCACCATCTTCCAGGAG-3' Reverse: 5'-CTTCTCCATGGTGGTGAAGACG-3'	RT-PCR

Table 4. Primers for mutagenesis

hPHF8-Y7A	Sense: 5'-CTCGGTGCCGGTGGCTTGCCTCTGCCGG-3' Antisense: 5'-CCGGCAGAGGCAAGCCACCGGCACCGAG-3'
hPHF8-H247A	Sense: 5'-GAGATAGCTATACAGACTTTGCCATTGACTTTG-GTGGCACCT-3' Antisense: 5'-AGGTGCCACCAAAGTCAATGGCAAAGTCTGTA-TAGCTATCT-3'
hPHF8-H247A, I248A, D249A	Sense: 5'-GTGCGAGATAGCTATACAGACTTTGCCGCTG-CCTTTGGTGGCACCTCTGTCTGGTA-3' Antisense: 5'-TACCAGACAGAGGTGCCACCAAAGGCAGCGGC-AAAGTCTGTATAGCTATCTCGCAC-3'
hPHF8-F279S	Sense: 5'-AAATGCCAATCTGACTCTCAGTGAGTGCTGG-AGCAGTTCC-3' Antisense: 5'-GGAACTGCTCCAGCACTCACTGAGAGTCAGAT-TGGCATTT-3'
mPHF8-Y7A	Sense: 5'-GCCTCGGTGCCTGTGGCTTGCCTCTGTCGACT-3' Antisense: 5'-AGTCGACAGAGGCAAGCCACAGGCACCGA-GGC-3'
mPHF2-Y7A	Sense: 5'-GACGGTGCCCGTGGCCTGCGTCTGCCGG-3' Antisense: 5'-CCGGCAGACGCAGGCCACGGGCACCGTC-3'

2.1.3. siRNA oligos

Table 5 siRNA oligos

Name	**Target sequence**
si-hPHF2 (1943)	5'-GAGGCCAAGTGGAAGTACA-3'
si-hPHF2 (1966)	5'-CAGCAAACCTGACTCCTTA-3'
si-hPHF8 (2202)	5'-GGAGGACTATACAACAGAT-3'
si-hPHF8 siGENOME SMARTpool, Dharmacon, D-004291-01	5'-GAACCAAGAUAGCAAAGAA-3' 5'-CAGCAGACCUCUUCAGAUU-3' 5'-GGAGGGAACUUCUUACACA-3' 5'-GGACAUCUUUCGCGGUUUG-3'
si-hKDM2B siGENOME SMARTpool, Dharmacon, D-014930-01	5'-GCAAUAAGGUCACUGAUCA-3' 5'-GACCUCAGCUGGACCAAUA-3' 5'-GGGAGUCGAUGCUUAUUGA-3' 5'-CAGCAUAGACGGCUUCUCU-3'

2.1.4. Standard buffers and solutions

MOPS (10 x)	200 mM MOPS 50 mM NaAc 10 mM EDTA
Laemmli buffer (2 x)	125 mM Tris-HCl pH 6.8 4% SDS 20% Glycerol 10% 2-mercaptoethanol 0.004% Bromophenol blue
PBS	137 mM NaCl 2.7 mM KCl 10 mM Na_2HPO_4, 2 mM KH_2PO_4
PBST	PBS containing 0.1% Tween 20
Ponceau S	5% Acetic acid (v/v) 30% Trichloroacetic acid (TCA) (v/v), 2% Ponceau S (w/v)
RNA loading buffer	50% Glycerol 1 mM EDTA 0.25% Bromophenol blue
SDS running buffer (10 x)	250 mM Tris base 1% SDS 1.9 M Glycine
SSC (20 x)	3 M NaCl 0.3 M Na-Citrate
TBE buffer	90 mM Tris-HCl pH 8.3 2.5 mM EDTA 90 mM Boric acid
TE buffer	10 mM Tris-HCl pH 8.0 1 mM EDTA
WB transfer buffer	25 mM Tris base 192 mM Glycine 20 % Methanol

2.2. Methods

2.2.1. Cloning and constructs

2.2.1.1. Plasmid DNA

A cDNA clone, hj04651s1, encoding the open reading frame (ORF) of human PHD finger protein 8 (PHF8) (KIAA1111, GenBank accession number AB029034), was obtained from the cDNA Bank Section Kazusa DNA Research Institute, Japan. The coding sequence of human PHF8 was PCR-amplified and cloned into the Gateway entry vector pDONR/Zeo (Invitrogen). The entry vectors pDONR/Zeo-PHF2, encoding murine PHD finger protein 2 (PHF2) (GenBank accession number BC051633) and pDONR/Zeo-KDM2B, encoding murine lysine demethylase 2B (KDM2B) (GenBank accession number NM_001003953.1) were provided by T. Jenuwein, Vienna, Austria. The Gateway entry vetor pDONR-WDR5, encoding human WD40-repeat protein (WDR5) was obtained from the clone library of the core facility of DKFZ. To generate expression vectors, the entry clones were transferred into Gateway compatible destination vectors, i.e. pI-GW-GFP, pcDNA4.0-FLAG-HA-GW, pEF-GW-V5 (Invitrogen). Point mutants of PHF2 and PHF8 were generated with QuickChange site-directed mutagenesis kit (Stratagene) and verified by DNA sequencing. pHrP2-BH is an artificial ribosomal minigene containing a 5'-terminal human rDNA fragment (from -411 to +375) fused to two rDNA terminator elements.

2.2.1.2. Transformation of bacteria

Competent *E. coli* cells, such as DH5α and BL21 CodenPlus (DE3), were incubated with plasmid DNA on ice for 30 minutes. After heated at 42^{o}C for 90 seconds and cooled on ice for 2 minutes, the cells were mixed with 1 ml of LB medium and incubated at 37^{o}C for 1 hour with shaking. The transformed cells were then plated on LB agar plates containing appropriate antibiotics.

2.2.1.3. Gateway BP reaction

The Gateway entry vector pDONR/Zeo (70 ng), PCR products (20-50 fmol),

and 1 µl of 5x BP Clonase II Enzyme mix (Invitrogen) were mixed and incubated at room temperature for 1-12 hr. The sample was digested with proteinase K (0.2 µg) at 37°C for 10 min before transformation. The transformed cells were plated onto low salt LB plates containing zeocin (50 µg/ml).

2.2.1.4. Gateway LR reaction

The Gateway destination vector (50 ng), entry vector (50 ng) and 1 µl of 5x LR Clonase II Enzyme mix (Invitrogen) were mixed and incubated at room temperature for 1-12 hr. After digestion with proteinase K (0.2 µg) at 37°C for 10 min, 1 µl of the reaction was used to transform DH5α competent cells. The transformed cells were plated onto LB plates containing ampicillin (50 ng/ml).

2.2.2. Cell culture and transfection

2.2.2.1. Cell culture

HEK293 is an epithelial cell line that is derived from primary human embryonic kidney transformed by sheared human adenovirus E1A gene product. HEK293T is a derivative of the HEK293 cell line into which the temperature sensitive SV40 T-antigen was inserted. Due to the expression of SV40 large T-antigen in HEK293T cells that allows episomal replication of plasmids containing the SV40 origin and early promoter region, HEK293T cells have higher transfection efficiency than HEK293 cells. Human osteosarcoma U2OS is a cell line derived from a moderately differentiated sarcoma. HEK293T cells and U2OS cells were cultured in Dulbecco's modified Eagle's medium (DMEM, GibcoBRL) supplemented with 10% heat-inactivated (15 min at 65°C) fetal calf serum (FCS, GibcoBRL), 1 mM sodium pyruvate (Biochrom AG), 100 U/ml of penicillin-streptomycin (Lonza) and 2 mM of glutamine (Lonza).

2.2.2.2. Transient plasmid DNA transfection in HEK293T cells

Transfection of HEK293T cells was performed with calcium phosphate-DNA precipitation method. Approximately 20 hours before transfection, cells were seeded in 10 ml of DMEM in 10 cm dishes at a density of 1 x 10^6 cells per

plate. Plasmid DNA was diluted in 500 µl of TE/Ca^{2+} buffer (2 mM Tris-HCl, pH 7.4, 0.01 mM EDTA, 0.25 mM $CaCl_2$) and the mix was added drop-wise into 500 µl of 2 x HeBS buffer (50 mM HEPES, 280 mM NaCl, 1.5 mM Na_2HPO_4, pH 7.05-7.10). The calcium phosphate-DNA complex was then applied to the cells. The original medium was replaced with 10 ml of fresh DMEM after 8-10 hours. Cells were harvested 36-48 hours after transfection.

2.2.2.3. siRNA transfection in HEK293T cells

To transfect cells in a 6-well dish, 2.5 µl of Lipofectamine 2000 transfection reagent (Invitrogen) was diluted in 250 µl of Opti-MEM I medium (Invitrogen) without serum in a sterile tube. In another tube, 60 µmol of siRNA oligos (the final concentration of RNA when added to the cells is 40 nM) were added in 250 µl of Opti-MEM I medium. After incubation at room temperature for 15 min, the diluted transfection reagent and siRNA oligos were combined and incubated at room temperature for 20 min. Meanwhile, the cells were trypsinized and plated in 1 ml of DMEM at a density of 4.5 x 10^5 cells per well. After incubation, RNA oligo-Lipofectamin 2000 complexes were applied to the cells. Cells were harvested 72- 96 hours after the initial transfection.

2.2.3. RNA analysis

2.2.3.1. RNA extraction

Cells were washed twice with ice-cold PBS, and lysed in 1 ml of TRIzol reagent (Invitrogen). The cell suspension was mixed with 200 µl of chloroform, shaken vigorously for 15 seconds, and incubated at room temperature for 5 min. After centrifugation (12,000 g, 15 min, 4^{o}C), the aqueous phase was transferred to a fresh tube and incubated at room temperature for 10 min after mixing with 400 µl of isopropanol. RNA was pelleted by centrifugation at 12,000 g, 4^{o}C for 10 min. The RNA pellet was washed once with 75% ethanol, air-dried and dissolved in water by incubating at 55^{o}C for 5-10 min.

2.2.3.2. Northern blot

Three to five microgram of cellular RNA was mixed with freshly prepared 2x

RNA denaturing buffer (59% Formamide, 8.7% Formaldehyde, 1.2 x MOPS and 58.8 µg/ml Ethidium bromide) and denatured at 65°C for 15 min. Denatured RNA was separated on a 1% agarose-MOPS gel and blotted to Hybond N^+ membrane (Amersham) for at least 16 hours in 10x SSC buffer. The transferred RNA was crosslinked to the filter by UV with Stratalinker (Stratagene). The filter was pre-hybridized in 10 ml of hybridization buffer containing 0.5 M Na-phosphate buffer pH 7.2, 10 mM EDTA, 7% SDS for 2-4 hours at 68°C and then hybridized with ^{32}P-labelled riboprobes at 68°C for at least 16 hours. After washing the filter three times (20 min at 68°C) in 15 ml 0.2 x SSC and 0.1% SDS, the blotted RNA was visualized by autoradiography.

2.2.3.3. Preparation of ^{32}P- labeled riboprobes

The DNA templates (200 ng) were mixed with 4 µl of 5 x transcription buffer (Promega), 2 µl of 100 mM DTT, 3 µl of 3.3 mM ATP, GTP and CTP mix, 0.3 µl of 1 mM UTP, 0.5 µl of RNasin (40 U/µl, Promega), 1 µl of T7 polymerase (18 U/µl, Promega), and 3 µl of α- [^{32}P] UTP (3000 Ci/mmol, Perkin Elmer). The sample was incubated at 37°C for 30 min, and DNA templates were digested by incubating with 20 units of RNase free DNase I (Roche) for 15 min at 37°C. The reaction was stopped by the addition of 25 µl of stop solution (400 mM ammonium acetate pH 5.5, 0.4% SDS, 0.2 mg/ml yeast tRNA). To precipitate RNA, the sample was mixed with 160 µl of absolute ethanol and kept at -20°C for 1 hr. The RNA was pelleted by centrifugation (13,000 rpm, room temperature, 15 min), air-dried, and dissolved in 100 µl of sterile water.

2.2.3.4. RT-PCR

Ten microgram of RNA was incubated at room temperature for 15 min with 10 units of DNase I (Roche) in the presence of 12 units of RNasin (Promega) in DNase I digestion buffer containing 40 mM Tris-HCl, pH 7.9, 10 mM NaCl, 6 mM $MgCl_2$, and 1 mM $CaCl_2$. The reaction was stopped by adding EDTA to the final concentration of 8 mM and heating to 75°C for 10 min. DNase I-treated RNA (500 ng) was hybridized to 1 µg of random primers dN6 (Roche) by incubating at 65°C for 30 min followed by another 30 min incubation at room temperature in hybridization buffer (10 mM Tris-HCl, pH 8.5, 150 mM KCl, 1

mM EDTA). Reverse transcription reaction was initiated by the addition of 10 µl of RT buffer (90 mM Tris-HCl, pH 8.5, 8 mM $MgCl_2$, 1.25 mM dNTP, 20 mM DTT and 12 units of RNasin), and incubated at 42^{o}C for 60 min. The cDNA sample was diluted 100 times with destilled H_2O before it was used as template for qRT-PCR.

2.2.4. Chromatin fractionation

HEK293T cells were washed with ice-cold PBS, resuspended in buffer A (10 mM HEPES, pH 7.9, 10 mM KCl, 1.5 mM $MgCl_2$, 0.5 mM DTT, complete protease inhibitor cocktail (Roche)) and incubated on ice for 5 min. The cell suspension was homogenized in a pre-cooled Dounce tissue homogenizer (Wheaton). The nuclei were collected by centrifugation (1,000 g, 5 min, 4^{o}C). The supernatant (the cytoplasmic fraction) was mixed with 250 µl of 10 x cytoplasmic extraction buffer (300 mM HEPES, pH 7.9, 1.4 M NaCl, 30 mM $MgCl_2$), incubated at 4^{o}C for 30 min and clarified by centrifugation (16,000 g, 5 min, 4^{o}C). The nuclei were washed once in buffer A, lysed for 30 min in extraction buffer (20 mM Tris-HCl, pH 8.0, 150 mM NaCl, 1 mM EDTA, 1 mM EGTA, 0.1% Triton X-100, complete protease inhibitor cocktail). The soluble nucleoplasmic fraction was separated from insoluble chromatin by centrifugation (2,000 g, 5 min, 4^{o}C). The chromatin was lysed in Laemmli buffer, sonicated for 5 min in the Bioruptor (15 sec on, 15 sec off, high level, Diagenode) and treated with Benzonase for 15 min at room temperature.

2.2.5. Cellular extract preparation

HEK293T cells were collected, washed with ice-cold PBS, and resuspended in a buffer containing 10 mM Tris-HCl, pH 8.0, 450 mM NaCl, 1 mM EDTA, 1 mM EGTA, 1% Triton X-100, complete protease inhibitor cocktail. The suspension was sonicated for 5 min in the Bioruptor (15 sec on, 15 sec off, high level), incubated at 4^{o}C for 30 min, and clarified by centrifugation (16,000 g, 10 min, 4^{o}C).

2.2.6. Glycerol gradient centrifugation

A total of 100 µl (380 µg) of nuclear extract from HEK293T cells were layed on top of a 3.8 ml of 12.5%-30% glycerol gradient in buffer AM-100 (20 mM Tris-HCl, pH 8.0, 100 mM NaCl, 5 mM $MgCl_2$, 0.1 mM EDTA, 10% glycerol, 0.5 mM DTT, complete protease inhibitor cocktail). Samples were ultracentrifuged at 4°C for 17 h at 45, 000 rpm in a SW60 rotor. Fractions (each of 200 µl) were collected, mixed with 22 µl of trichloroacetic acid (TCA) and incubated at 4°C for 45 min. After centrifugation (13,200 rpm/4°C/20min), the pellet was washed once with aceton, air-dried and dissolved in 1xLaemmli buffer.

2.2.7. Immunoblotting

Proteins were denatured for 5 min at 95 °C in Laemmli buffer, separated by SDS-PAGE using the Bio-Rad Mini protein gel system and transferred to nitrocellulose membrane (Protran, Schleicher & Schuell) using the ‘‘Trans-Blot Semi Dry Apparatus’’ (BioRad). The blots were blocked at room temperature for 1 hour in blocking solution (0.1% Tween 20 in PBS (PBST), 5% non-fat milk) and incubated with primary antibodies at 4 °C overnight. After washing three times for 15 min in PBST, the blots were incubated with secondary antibodies coupled to horseradish peroxidase (HRP) for 1 hour at room temperature followed by washing three times in PBST for 15 min. Proteins were detected by using Immobilon Western Chemiluminescent HRP Substrate (Millipore) and exposing in LAS-3000 (Fujifilm).

2.2.8. Coomassie staining

After SDS-PAGE, proteins were fixed in 30% ethanol, 10% acetic acid for at least 2 hours at room temperature and stained in 0.01% Coomassie Blue G250 w/v, 5% ethanol v/v, 8.5% H_3PO_4 v/v overnight. The gel was destained in distilled water for 4 hours and dried at 75°C for 1 hour with a gel dryer apparatus (Biorad).

2.2.9. Immunoprecipitation

HEK293T cells were washed with ice-cold PBS, resuspended in buffer A containing 0.1% Triton X-100. After incubation on ice for 7 min, nuclei were pelleted by centrifugaion (1,500 g/4^{o}C /5min). Nuclei were lysed in IP buffer (20 mM Tris-HCl, pH 8.0, 150 mM NaCl, 1 mM EDTA, 1 mM EGTA, 1% Triton X-100, complete protease inhibitor cocktail) at 4^{o}C for 30 min. The lysate was briefly centrifuged and supernatant was kept. The pellet was sonicated in IP buffer containg 450 mM NaCl, incubated at 4^{o}C for 20 min and diluted with 2 volumn of IP buffer containing no salt. The extract was combined with the supernatant from previous step and cleared by centrifugation (16,000 g, 15 min, 4^{o}C). Nuclear extracts were pre-cleared by incubation with protein A/G Sepharose (Amersham) at 4^{o}C for 1 hour. After pre-clearing, the lysates were incubated at 4^{o}C overnight with respective antibodies and protein A/G Sepharose blocked in IP buffer containing 1 mg/ml BSA for 1 hour at 4^{o}C. After successive washing with IP buffer, bound proteins were eluted from beads in 1.5 x Laemmli buffer and analyzed on western blots.

2.2.10. Chromatin immunoprecipitation (ChIP)

Cells were crosslinked with 1% formaldehyde at room temperature for 10 min and the reaction was quenched with 125 mM glycine for 5 min. Cells were collected, homogenized in PBS containing 1% Triton X-100, and transferred to 0.5 ml thin wall PCR tubes (Eppendorf). The pellets were resuspended in SDS lysis buffer (50 mM Tris-HCl, pH 8.0, 10 mM EDTA, 1% SDS, complete protease inhibitor cocktail) and sonicated to yield DNA fragments of 0.2-0.5 kb in the Bioruptor (10-20 min, 30 seconds on, 30 seconds off, high level). The lysates were diluted at least 10-fold in ChIP dilution buffer (20 mM Tris-HCl, pH 8.0, 150 mM NaCl, 2 mM EDTA, 1% Triton X-100, complete protease inhibitor cocktail) and pre-cleared with protein A/G Sepharose at 4^{o}C for 1 hour. After keeping 10% of cleared lysate as the “input” samples, the rest of lysates were incubated with the respective primary antibodies overnight at 4^{o}C and the immuno-complexes were precipitated with protein A/G Sepharose (blocked in ChIP dilution buffer containing 0.5 mg/ml BSA and 0.2 mg/ml sonicated salmon sperm DNA) for 2 hours at 4^{o}C. The beads were washed sequentially with three-times of high salt washing buffer (20 mM Tris-HCl, pH

8.0, 500 mM NaCl, 2 mM EDTA, 1% Triton X-100), three-times of LiCl washing buffer (10 mM Tris-HCl, pH 8.0, 250 mM LiCl, 1% Na-deoxycholate, 1% NP40) and 1 time of TE buffer. Bead-bound DNA was extracted by boiling for 10 min in 100 µl of 10% Chelex slurry (Biorad). Proteins were removed with digestion with 10 µg of proteinase K at 55°C for 30 min. After boiling for 10 min to inactivate proteinase K, 60 µl of the supernatant was transferred to a fresh tube. The Chelex resin was mixed with 100 µl of destilled H_2O, centrifuged at 12,000 g for 30 seconds, and 100 µl of the supernatant was combined with the previous supernatant. The DNA was analyzed by qPCR in the LightCycler 480 apparatus (Roche).

2.2.11. Methylation-sensitive ChIP-chop

The ChIP DNA samples (15 µl each) were either mock-treated or digested with 20 units of *HpaII* (New England Lab) overnight at 37°C. The DNA was amplified using primers that amplify human rDNA from -150 to +32 (the transcription start site was set as +1), a region covering four *HpaII* restriction sites. For normalization, a DNA fragment harboring rDNA sequence from +7936 to +8036 containing no *HpaII* restriction site was also amplified. Quantification of the percentage of *HpaII* resistance was calculated as follows:

$R_{HpaII}=((X_{HpaII}/X_{mock}) / (C_{HpaII}/C_{mock})) \times 100$

X, analyzed fragment and C, control fragment.

2.2.12. Immunofluorescence

U2OS cells grown on coverslips were rinsed briefly in PBS and fixed with either 4% paraformaldehyde (PFA) in PBS for 10 min at room temperature, or with methanol for 6 min and aceton for 1 min at -20°C. After washing twice with PBS, the PFA-fixed cells were permeabilized with PBS containing 0.2% Triton X-100 for 5 min at room temperature. After washing three times with PBS, cells were blocked in 5% horse serum (Invitrogen) for 1 hour at room temperature and incubated with the primary antibodies overnight at 4°C in a humidified chamber. The cells were washed three times with PBS and incubated with the secondary antibodies for 1 hour at room temperature in dark. After

three times of washing with PBS, the cells were counterstained with 1 µg/ml Hoechst for 5 min. The coverslips were rinsed in PBS and mounted onto slides with mounting medium. The stained cells were analyzed by fluorescence microscopy on a Carl Zeis, Axiophot microscope.

2.2.13. Expression of GST fusion proteins

E. coli BL21 CodenPlus (DE3) competent cells were transformed with the plasmid DNA pGEX6P-mPHF2$_{1-120}$-His$_6$ and pGEX6P-mPHF8$_{1-110}$-His$_6$, and single colony from the transformation was picked up and grown in LB medium overnight at 37^{o}C. Fifteen ml of overnight bacterial culture was seeded into 800 ml of LB medium containing 50 µg/ml of ampicillin. After the bacterial cells grown at 37^{o}C to an OD_{600} of 0.6, the expression of specific proteins was induced overnight at 18^{o}C with 0.5 mM IPTG. Cells were harvested by centrifugation (2,000 g, 20 min, 4^{o}C) and lysed in 20 ml ice-cold STE buffer (10 mM Tris-HCl pH8.0, 1 mM EDTA, 150 mM NaCl) containing 2 mg of lysozyme. After addition of 200 µl 1 M DTT and 2.8 ml 10% Sarkosyl, the sample was sonicated for 2 min (output: 4-4.5 duty: 50%, Branson Sonifier 250). After removal of cell debris by centrifugation (12,000 rpm, 4^{o}C, 30 min), Triton X-100 was added to the supernatant to a final concentration of 2%, and the final volume was adjusted to 40 ml with STE buffer. Aliquotes of the lysates were frozen in liquid nitrogen and stored at –80^{o}C.

3. Results

3.1. Generation of antibodies against PHF2 and PHF8

PHF2 and PHF8 belong to the family of JmjC domain-containing lysine demethylases but so far no cellular function of either protein is known. Recently, the closely related lysine demethylase JHDM1B/KDM2B has been shown to localize to nucleoli and to repress rDNA transcription via demethylating the euchromatic histone mark H3K4me3 (Frescas et al. 2007). To study the function of PHF2 and PHF8, polyclonal antibodies against both proteins were generated. For this, cDNAs encoding aa 452-750 of human PHF2 and aa 448-650 of human PHF8 were cloned into the bacterial expression vector pGex6P-His_6. The fusion proteins GST-$PHF2_{452-750}$-His_6 and GST-$PHF8_{448-650}$-His_6 (Fig. 3.1A) were expressed in *E. coli* and purified by affinity chromatography using either a glutathione or a Ni^{2+}-NTA resin. The purified recombinant proteins were injected into rabbits to produce polyclonal antisera.

As a first approach to characterize the anti-PHF2 and anti-PHF8 antisera, Flag-tagged PHF2 (Fl-PHF2) and PHF8 (Fl-PHF8) were expressed in HEK293T cells, immunoprecipitated with anti-Flag antibodies and detected on western blots. As shown in Fig. 3.1B, anti-Flag antibodies detected about 150 kDa proteins whose size corresponds to recombinant PHF2 and PHF8. Importantly, the antibodies against PHF2 and PHF8 recognized proteins of the same size, indicating that both antibodies are specific for the respective protein. Moreover, the antibodies were not only capable to detect endogenous PHF2 and PHF8 in nuclear extracts from HEK293T cells but also immunoprecipitated PHF2 and PHF8 from these extracts (Fig. 3.1C). In contrast, the respective pre-immune sera neither detect endogenous PHF2 and PHF8 in nuclear extracts nor immunoprecipitated them from these extracts, indicating that the generated antibodies faithful detect cellular PHF2 and PHF8.

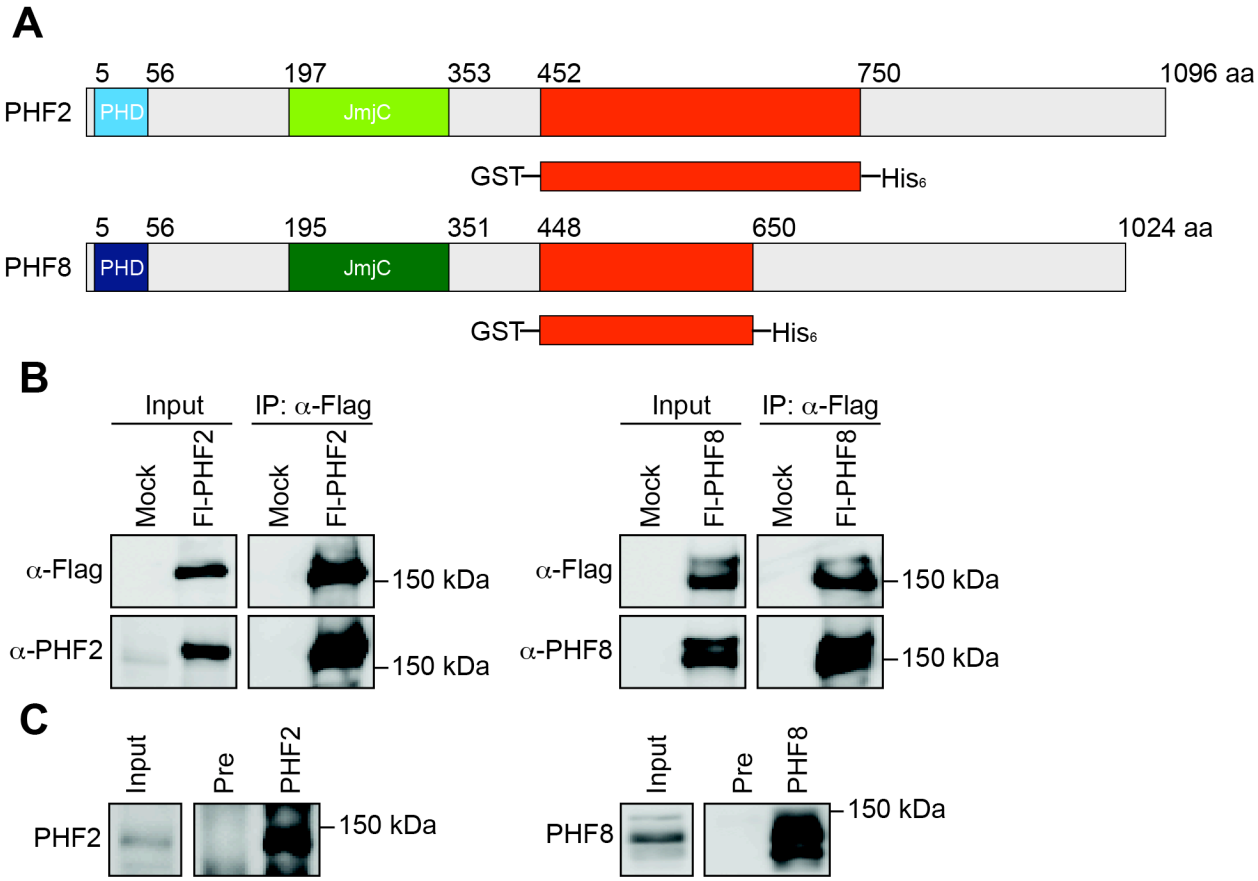

Figure 3.1. Anti-PHF2 and anti-PHF8 antibodies specifically recognize PHF2 and PHF8

(A) Schemes of human PHF2 and PHF8 show the PHD finger and the JmjC domain. The fragments used as antigens for immunization are indicated.

(B) Antisera against PHF2 and PHF8 recognize PHF2 and PHF8, respectively. Nuclear extracts from HEK293T cells overexpressing Flag-tagged PHF2 (Fl-PHF2) or PHF8 (Fl-PHF8) were precipitated with anti-Flag antibodies, and bound proteins were analyzed on western blots with anti-Flag antibodies and antisera against PHF2 and PHF8. Two percent of input and 30% of immunoprecipitated samples were analyzed. The molecular weight marker is indicated on the right.

(C) Anti-PHF2 and anti-PHF8 antibodies immunoprecipitate endogenous PHF2 and PHF8. Nuclear extracts from HEK293T cells were subjected to immunoprecipitation with anti-PHF2 and anti-PHF8 antibodies or pre-immune sera (Pre). One percent of input and 30% of immunoprecipitated samples were assayed by immunoblotting. The molecular weight marker is indicated on the right.

3.2. PHF2 and PHF8 localize to nucleoli

Given that the cellular localization of a protein will give a hint of its biological function, the distribution of GFP-tagged PHF2 (GFP-PHF2) and PHF8 (GFP-PHF8) in U2OS cells was examined by fluorescence microscopy. As shown in Fig. 3.2A, a bright green staining at nucleolar sites was observed in cells expressing GFP-PHF2 and GFP-PHF8. Nucleolar localization was confirmed

by co-immunostaining of UBF, a Pol I specific transcription factor and nucleolar marker protein. The overlapping staining of UBF with GFP-PHF2 and GFP-PHF8 demonstrated that both proteins are enriched in nucleoli. To monitor the localization of endogenous PHF2 and PHF8, U2OS cells were immunostained with antibodies against PHF2 and PHF8. Consistent with the localization of the GFP-PHF2 and GFP-PHF8, the endogenous proteins mainly localized within nucleoli and co-stained with UBF (Fig. 3.2B). The nucleolar localization of PHF2 and PHF8 suggests that these putative lysine demethylases may play a role in rDNA transcription.

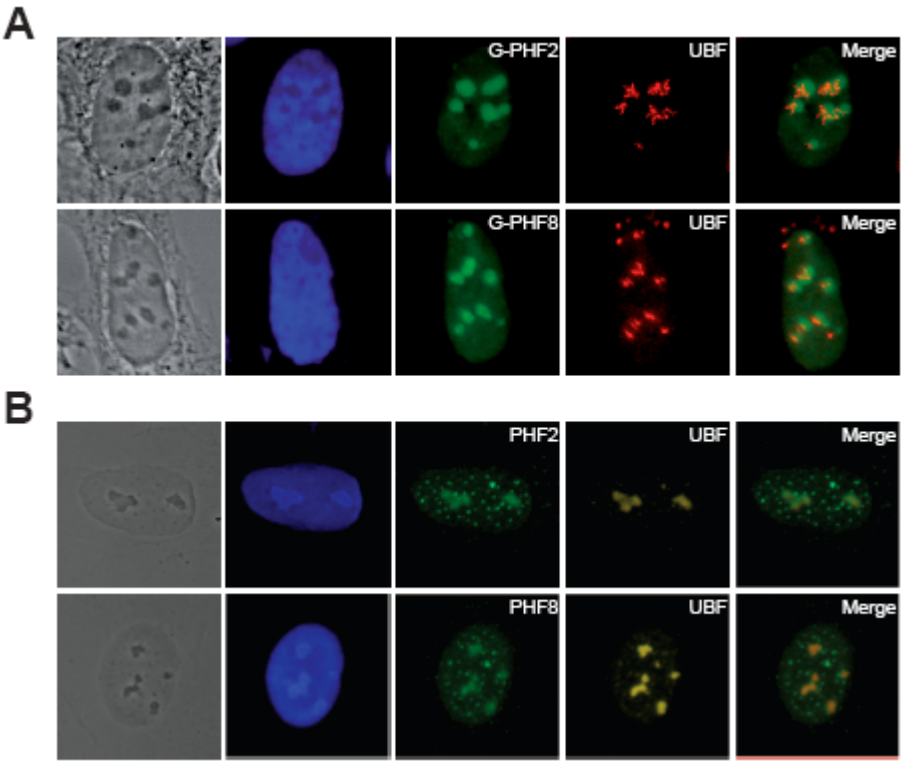

Figure 3.2. PHF2 and PHF8 localize to nucleoli
(A) GFP-tagged PHF2 and PHF8 colocalize with UBF in nucleoli. U2OS cells overexpressing GFP-tagged PHF2 (G-PHF2) or PHF8 (G-PHF8) were immunostained with anti-UBF antibodies. Images of phase contrast and DNA staining with Hoechst are shown in the first two panels.
(B) Endogenous PHF2 and PHF8 colocalize with UBF in nucleoli. The indirect immunofluorescence assays show the localization of endogenous PHF2, PHF8, and UBF in U2OS cells. Images of phase contrast and DNA staining are shown in the first two panels.

3.3. PHF2 and PHF8 are associated with rDNA

3.3.1. PHF2 and PHF8 bind to the entire rDNA repeat

The nucleolar localization of PHF2 and PHF8 raises the possibility that they are associated with rDNA. To test this, chromatin immunoprecipitation (ChIP) assays were performed. This technique allows the *in vivo* analysis of protein/DNA interactions in intact cells by formaldehyde-fixation of nucleoprotein complexes. After disruption of the cells, antibodies are used to isolate specific nucleoprotein complexes containing the immunoprecipitated proteins and the co-precipitated DNA. The DNA can be isolated and analyzed by PCR after reversal of the crosslink. To map the association of PHF8 with rDNA, cross-linked chromatin from HEK293T cells was incubated with anti-PHF8 antibodies or the pre-immune serum. The co-precipitated rDNA was analyzed by qPCR using primer pairs encompassing different regions of the rDNA repeat, including the enhancer region, the rDNA promoter, the 28S rRNA coding region and the intergenic spacer (IGS) which separates individual rDNA repeats (Fig. 3.3A). In all tested regions, significant amount of rDNA was co-precipitated with PHF8, but not with the pre-immune serum (Fig. 3.3B), demonstrating that PHF8 was associated with rDNA. In contrast, no significant binding of PHF2 to rDNA was detected with anti-PHF2 antibodies (data not shown), indicating that either PHF2 does not bind to rDNA or that the part of PHF2, which was used to generate the anti-PHF2 antiserum, is inaccessible due to cross-linking. To distinguish between both possibilities, binding of overexpressed HA-tagged PHF2 (HA-PHF2) to rDNA was examined by ChIP assays using anti-HA antibodies for immunoprecipitation. As depicted in Fig. 3.3B, HA-PHF2 was significantly enriched at rDNA whereas no rDNA bound to anti-HA antibodies in mock-transfected cells. Similar to PHF8, HA-PHF2 was equally enriched at all rDNA regions tested, suggesting that PHF2 and PHF8 are associated with the entire rDNA repeat, including the non-transcribed intergenic spacer.

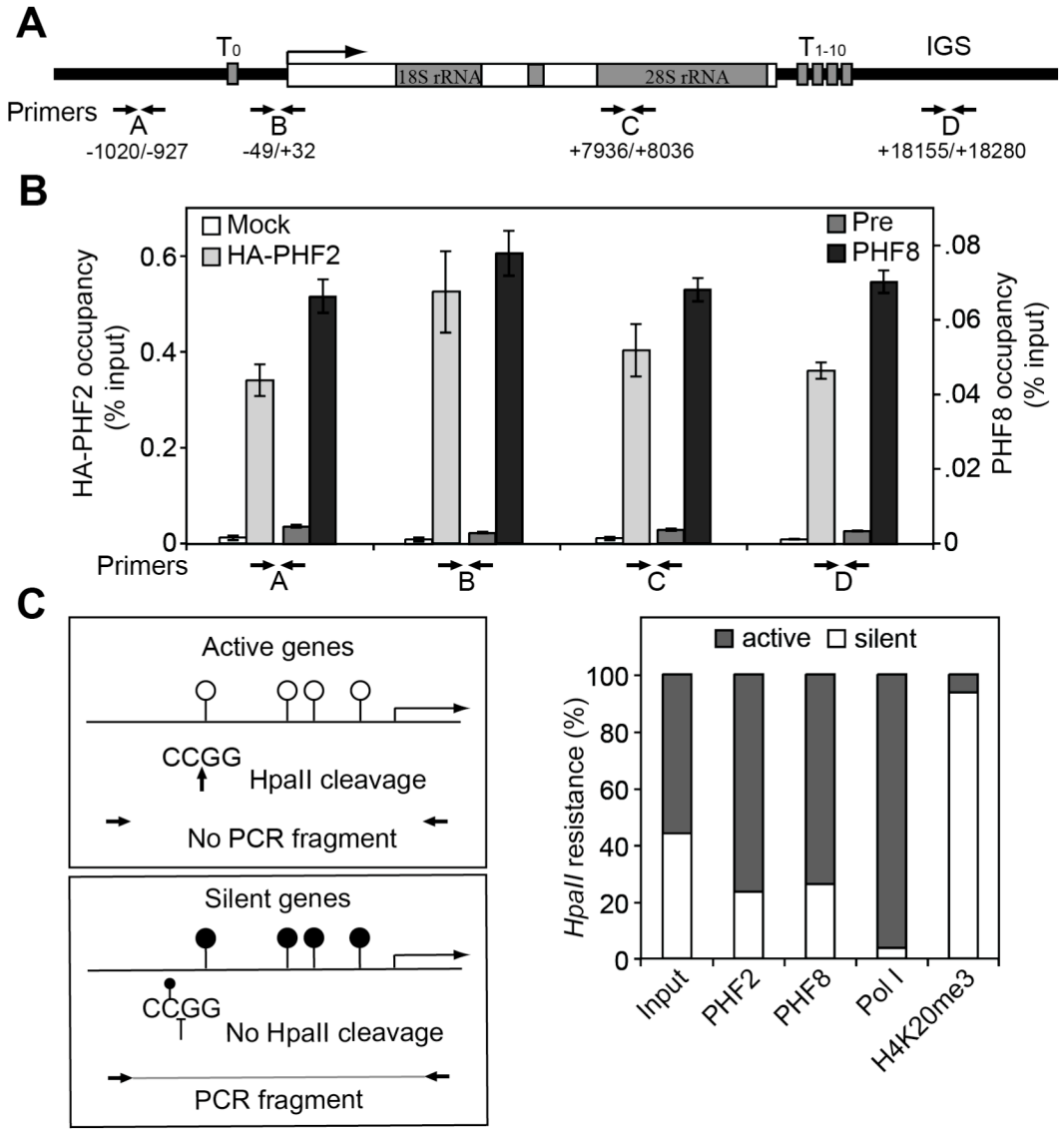

Figure 3.3. PHF2 and PHF8 are associated with rDNA

(A) The scheme outlines a representative mammalian rDNA repeat, illustrating the positions of the upstream terminator T_0, the rDNA promoter, the pre-rRNA coding region, the downstream terminators (T_{1-10}), and the intergenic spacer (IGS). Primer pairs used for qPCR in ChIP assays are indicated below.

(B) PHF2 and PHF8 are associated with rDNA. Cross-linked chromatin from HEK293T cells overexpressing HA-tagged PHF2 (HA-PHF2, light grey bars) or mock-transfected cells (white bars) was precipitated with anti-HA antibodies. Chromatin from HEK293T cells was incubated with antibodies against PHF8 (black bars) or the pre-immune sera (dark grey bars). The precipitated DNA was analyzed by qPCR using primers indicated in the scheme above. The enrichment of HA-PHF2 (scale on the left y-axis) and endogenous PHF8 (scale on the right y-axis) is reflected as the percentage of input DNA.

(C) PHF2 and PHF8 bind to active rDNA copies. The scheme on the left shows the principle of DNA methylation assay by *HpaII* digestion. Four *HpaII* restriction sites (5'-CCGG-3') are presented at the human rDNA promoter, which are unmethylated (represented as white balls) in active rRNA genes but methylated (represented as black balls) in silent genes. The qPCR primer pair flanking the *HpaII* sites is indicated with arrows. ChIP input DNA and DNA precipitated by indicated antibodies were either digested with *HpaII* or mock-digested before PCR amplification. The relative level of *HpaII*-resistant, inactive rDNA copies (white bars) and unmethylated, active copies (grey bars) was determined by qPCR.

3.3.2. PHF2 and PHF8 bind to active rRNA genes

In mammalian cells, rRNA genes consist of transcriptionally active and silent copies, which are distinguishable by their DNA methylation status. Whereas transcribed rDNA is unmethylated, silent rDNA harbors methylated cytosine residues at CpG sites. If this CpG methylation occurs at CCGG, the methylation-sensitive restriction enzyme *HpaII* will not cleave the DNA. Therefore, the resistance of genomic DNA to digestion with *HpaII* is indicative for CpG methylation and can be detected in PCR with primer pairs flanking one or more *HpaII* restriction sites. If a PCR-product can be amplified from the DNA upon incubation with *HpaII*, the DNA was methylated and thus resistant to digestion by HpaII. In contrast, if the PCR yields no product, the DNA was not methylated and thus cleaved by *HpaII* (Fig. 3.3C, left panel).

Using this technique, the association of PHF2 and PHF8 with active or silent rRNA genes was monitored by digestion of rDNA that was co-precipitated with PHF8 and HA-PHF2 in ChIP assays with *HpaII* followed by a subsequent PCR amplification of the rDNA promoter using primers that flanks the four *HpaII* restriction sites present at this region. To determine the overall ratio of active and silent rRNA genes in HEK293T cells, DNA isolated from soluble chromatin (ChIP input) was subjected to *HpaII* digestion. About 55% of rDNA were digested by *HpaII*, showing that these rRNA genes were unmethylated, whereas the rest 45% *HpaII*-resistant copies were methylated (Fig. 3.3C). As control, the CpG methylation status of rDNA associated with Pol I or H4K20me3, a transcriptional repressive histone mark, was monitored. As shown in Fig. 3.3C, more than 95% of rDNA associated with Pol I were digested by *HpaII*, demonstrating that Pol I binds and transcribes exclusively unmethylated rDNA. In contrast, only 5% of rDNA bound to H4K20me3 were cleaved by *HpaII*, showing that H4K20me3 is present predominantly at methylated rRNA genes. Notably, 70-80% of PHF2 and PHF8 were associated with unmethylated i.e. transcriptionally active rDNA copies. These results suggested that PHF2 and PHF8 might serve a positive role in rDNA transcription.

3.4. PHF2 and PHF8 interact with Pol I and UBF

The observation that PHF2 and PHF8 are preferentially associated with active rRNA genes suggests that they may cooperate with the Pol I transcription machineray to activate rDNA transcription. To examine whether PHF2 and PHF8 are associated with the Pol I transciption apparatus, co-immunoprecipitation assays were performed. For this, nuclear extracts from HEK293T cells overexpressing V5-tagged PHF2 (V5-PHF2) and PHF8 (V5-PHF8) were incubated with human autoimmune sera against Pol I and UBF (Zatsepina et al. 1993), and co-immunoprecipitation of V5-PHF2 and V5-PHF8 with Pol I and UBF was monitored on western blots. As shown in Fig. 3.4A, V5-PHF2 and V5-PHF8 were co-precipitated with antibodies against Pol I and UBF, but not with the control human IgGs. To confirm the association of PHF2 and PHF8 with Pol I and UBF, Fl-PHF2 and Fl-PHF8 were overexpressed in HEK293T cells and immunoprecipitated with anti-Flag antibodies. Consistently, Pol I and UBF were co-precipitated with Fl-PHF2 and Fl-PHF8, whereas in mock-transfected cells no binding of Pol I and UBF to the anti-Flag antibodies was observed (Fig. 3.4B). Thus, PHF2 and PHF8 are associated with Pol I and UBF *in vivo*, supporting the notion that these two putative lysine demethylases are involved in rDNA transcription. In addition, the interaction of PHF2 and PHF8 with Pol I and UBF may be required for their association with rDNA.

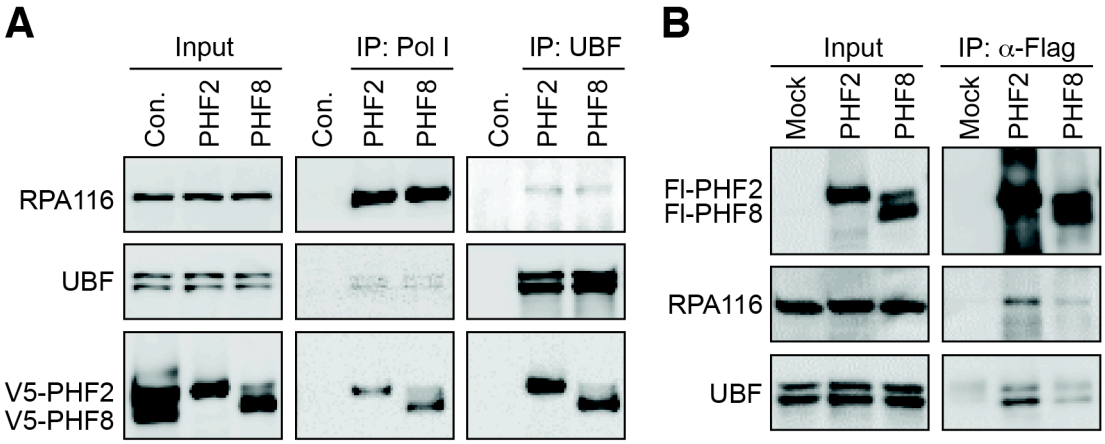

Figure 3.4. PHF2 and PHF8 interact with Pol I and UBF
(A) Overexpressed PHF2 and PHF8 co-precipitated with Pol I and UBF. Nuclear extracts from HEK293T cells overexpressing V5-tagged PHF2 (V5-PHF2) or PHF8 (V5-PHF8) were precipitated with antibodies against Pol I or UBF. As a control, equivalent amount of nuclear extracts from HEK293T cells overexpressing V5-PHF2 or V5-PHF8 were mixed and incubated with the control human IgGs. One percent of input and 30% of precipitated proteins were analyzed by immunoblotting with anti-V5, anti-RPA116 (the second largest subunit of Pol I complex) and anti-UBF antibodies.
(B) Pol I and UBF co-precipitate with Fl-PHF2 and Fl-PHF8. Nuclear extracts from HEK293T cells overexpressing Fl-PHF2 or Fl-PHF8 were precipitated with anti-Flag antibodies. One percent of input and 30% of precipitated proteins were assayed on western blots with the indicated antibodies.

3.5. PHF2 and PHF8 are required for Pol I transcription

3.5.1. Overexpression of PHF2 and PHF8 stimulates Pol I transcription

The observation that PHF2 and PHF8 interact with active rDNA repeats and the Pol I transcription machinery suggests that these enzymes might directly regulate rDNA transcription. To test this, HEK293T cells were either mock-transfected or transfected with expression plasmids encoding Fl-PHF2 and Fl-PHF8. Two days after transfection, RNA was isolated and the levels of pre-rRNA were quantified by qRT-PCR with a primer pair flanking the first processing site (+414/+419) of human pre-rRNA. Normalization of pre-rRNA abundance to β-actin mRNA levels revealed that pre-rRNA synthesis was stimulated by 30-50% upon overexpression of PHF2 and PHF8 (Fig. 3.5A, upper panel). Considering that also untransfected cells contribute to the average level of pre-rRNA, the actual change of pre-rRNA synthesis due to overexpression of PHF2 and PHF8 might be underestimated. To circumvent this

problem, reporter gene assays were performed. In the experiment shown in Fig. 3.5A (middle panel), cells were co-transfected with a Pol I-specific reporter construct and expression plasmids encoding Fl-PHF2 and Fl-PHF8. The reporter construct used was pHrP2-BH, a plasmid that contains an artificial rRNA minigene consisting of the human rDNA promoter followed by a short sequence of the pUC9 vector and two rDNA terminator elements. Transcripts from the reporter plasmid can be specifically detected by qRT-PCR. Notably, as compared to cells transfected with the reporter alone, reporter transcripts synthesis in cells expressing Fl-PHF2 was enhanced about 2.2 fold, whereas overexpression of Fl-PHF8 stimulated reporter transcripts synthesis by about 70%. This strong stimulation of reporter transcription confirms the observed enhancement of pre-rRNA synthesis and suggests that PHF2 and PHF8 are limiting factors for rDNA transcription. Thus, the gain-of-function assays suggests that PHF2 and PHF8 act as activators of rDNA transcription.

3.5.2. Depletion of PHF2 and PHF8 impairs pre-rRNA synthesis

If PHF2 and PHF8 activate Pol I transcription, then depletion of PHF2 and PHF8 should impair pre-rRNA synthesis. To test this, HEK293T cells were transfected with either small interfering RNA (siRNA) that specifically target PHF2 and PHF8 or with non-target control siRNA. Four days after transfection, the levels of cellular PHF2 and PHF8 were monitored on western blots. As shown in Fig. 3.5B (upper panel), PHF2 and PHF8 were significantly depleted in cells transfected with specific siRNA as compared to cells transfected with control siRNA. Notably, the level of PHF8 was not affected by depletion of PHF2 and the knockdown of PHF8 did not alter the level of PHF2, demonstrating the specificity of the individual siRNA. Pre-rRNA synthesis in these cells was measured on northern blots, using a ^{32}P-labeled RNA probe complementary to the first 183 nucleotides of unprocessed human pre-rRNA. After normalization with the levels of β-actin mRNA, relative pre-rRNA levels were compared, revealing a reduction of about 30-40% in cells depleted of PHF2 and PHF8 as compared to cells transfected with control siRNA. Therefore, PHF2 and PHF8 are required for rDNA transcription, and the level of pre-rRNA synthesis directly correlates with the amount of both enzymes.

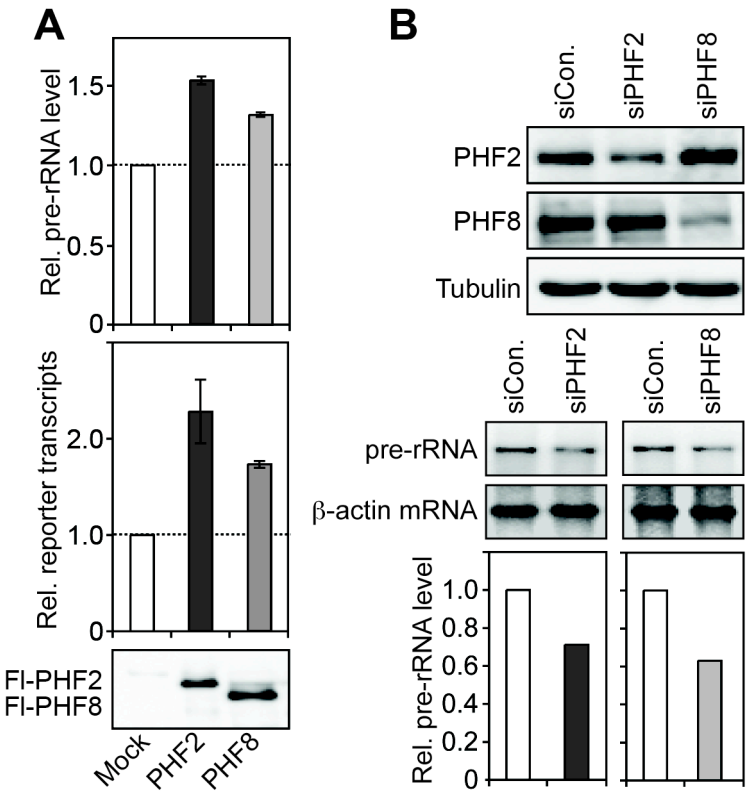

Figure 3.5. PHF2 and PHF8 activate Pol I transcription
(A) Overexpression of PHF2 and PHF8 stimulates rDNA transcription. HEK293T cells were transfected with expression vectors encoding Fl-PHF2 and Fl-PHF8 (upper panel), or together with the Pol I specific reporter construct pHrP2-BH (middle panel). The amounts of pre-rRNA and reporter transcripts were monitored by qRT-PCR and normalized to the level of β-actin mRNA. The western blot image in the bottom panel shows the expression level of Fl-PHF2 and Fl-PHF8. Error bars represent standard deviation of three independent experiments.
(B) Depletion of PHF2 or PHF8 reduces rDNA transcription. HEK293T cells were transfected with either siRNA oligos targeting PHF2 and PHF8 or control siRNA. The levels of pre-rRNA and β-actin mRNA were analyzed on northern blots (middle panel). The pre-rRNA levels were normalized to β-actin mRNA levels and represented in the bar diagram in the bottom panel. The cellular levels of PHF2, PHF8 and tubulin upon siRNA transfection are shown on western blots in the upper panel.

3.6. PHF2- and PHF8-dependent activation of rDNA transcription requires the PHD finger and JmjC domain

3.6.1. Generation of PHF2 and PHF8 mutants

PHF2 and PHF8 contain both a PHD finger and JmjC domain. Both domains are present in a variety of transcriptional regulators that affect gene expression by modulating the chromatin structure. The PHD finger has recently been shown to recognize the methylation status of lysine residues, such as H3K4me3 (Shi et al. 2006; Wysocka et al. 2006). The JmjC domain is capable to catalyze demethylation of mono-, di- and tri-methyl lysine residues *via* hydroxylation in an Fe(II)- and αKG-dependent manner (Tsukada et al. 2006). This raises the question whether the functions of these domains, i.e. binding to and removing methyl group from lysine residues, are required for PHF2 and PHF8-mediated activation of rDNA transcription. For this, the function of several PHF2 and PHF8 derivatives carrying mutations in these domains was investigated. To identify amino acids that are involved in binding to methylated lysine residues, the PHD fingers of PHF2 and PHF8 were aligned with ING2 and BPTF, proteins harboring PHD fingers that interact with H3K4me3 (Shi et al. 2006; Wysocka et al. 2006). This sequence alignment revealed conservation of defined residues involved in H3K4me3 binding (Fig. 3.6A), indicating that the PHD fingers of PHF2 and PHF8 might interact with H3K4me3 as well. Based on this alignment, a mutant was generated by site-directed mutagenesis in which tyrosine at position 7 was converted to alanine in the PHD finger and the respective mutants (PHF2-Y7A and PHF8-Y7A) were used in the designed experiments. Similar approach was used to generate mutants in that essential amino acids within the JmjC domain were replaced. A conserved iron-binding motif HXD/EXnH in the JmjC domain is present in all active JmjC domain-containing lysine demethylases (Fig. 3.6B). Mutations within this domain abolish the enzymatic activity. To generate a catalytically inactive mutant, the first iron-binding residue, histidine 249, was converted to alanine yielding mutant PHF2-H249A. For PHF8, three consecutive amino acids including the first two iron-binding residues (H247 and D249) and the residue I248 were replaced by alanine, yielding mutant PHF8-HID.

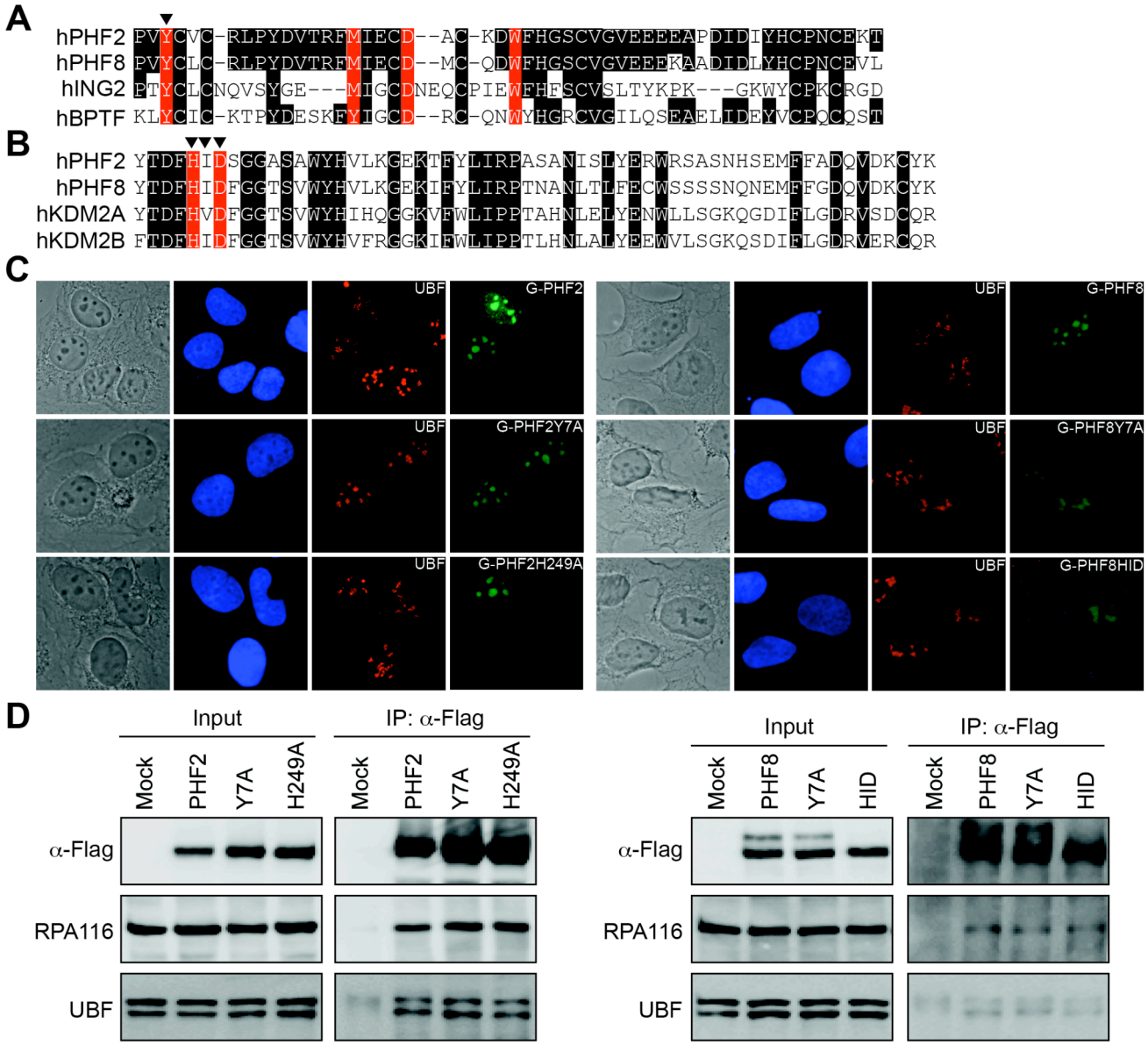

Figure 3.6. Mutations in the PHD finger and JmjC domains of PHF2 and PHF8 do not impair their nucleolar localization and interaction with Pol I and UBF

(A) Alignment of the PHD fingers of human PHF2 (5-56), human PHF8 (5-56), human ING2 (212-262) and human BPTF (2867-2918). Residues required for H3K4me3 binding are highlighted and the mutant used in this study is indicated by a triangle.

(B) Alignment of a portion of the JmjC domains of human PHF2 (aa 245-304), human PHF8 (aa 243-302), human KDM2A (aa 208-267) and human KDM2B (aa 238-297). The predicted first and second Fe(II)-binding residues are highlighted and the mutant used in this study is indicated by triangles.

(C) Immunofluorescence assays show that GFP-tagged wildtype and mutant PHF2 and PHF8 localize to nucleoli. U2OS cells overexpressing GFP-tagged wildtype and mutant PHF2 and PHF8 were immunostained with anti-UBF antibodies. Images of phase contrast and DNA staining with Hoechst are shown in the first two panels.

(D) Mutant PHF2 and PHF8 interact with Pol I and UBF. Nuclear extracts from HEK293T cells overexpressing wildtype and mutant Fl-PHF2 or Fl-PHF8 were incubated with anti-Flag antibodies. Two percent of input and 30% of precipitated proteins were analyzed by immunoblotting using indicated antibodies.

3.6.2. Mutant PHF2 and PHF8 localize to nucleoli and interact with Pol I and UBF

To analyze the role of the PHD finger and JmjC domain of PHF2 and PHF8 in their cellular localization, the subcellular distribution of the PHF2 (PHF2-Y7A and PHF2-H249A) and the PHF8 (PHF8-Y7A and PHF8-HID) mutants was monitored. For this, GFP-tagged wildtype and mutant PHF2 and PHF8 were expressed in U2OS cells and their localization was detected by fluorescence microscopy. As shown in Fig. 3.6C, similar to wildtype GFP-PHF2 and GFP-PHF8, mutant PHF2 (PHF2-Y7A and PHF2-H249A) and PHF8 (PHF8-Y7A and PHF8-HID) localized to nucleoli and co-stained with UBF. Thus, the nucleolar localization of PHF2 and PHF8 does not depend on a functional PHD finger and JmjC domain.

It has been shown above that PHF2 and PHF8 interact with Pol I and UBF (Fig. 3.4), suggesting that this interaction may be important for their function in rDNA transcription. Therefore, it was tested whether the association of PHF2 and PHF8 with the Pol I transcription machinery is compromised by introducing mutations in the PHD finger and JmjC domain. For this, nuclear extracts from HEK293T cells expressing Flag-tagged wildtype and mutant PHF2 and PHF8 were incubated with anti-Flag antibodies, and co-precipitation of Pol I and UBF was monitored by immunoblotting. As shown in Fig. 3.6D, similar amounts of Pol I and UBF were co-precipitated with wildtype and mutant Fl-PHF2 and Fl-PHF8, indicating that none of these mutations affected the interaction of PHF2 and PHF8 with the Pol I transcription machinery.

3.6.3. The PHD finger and JmjC domain are required for PHF2- and PHF8-dependent activation of rDNA transcription

Having shown that mutant PHF2 and PHF8 localize to nucleoli and interact with the Pol I transcription machinery, it was next assayed whether these mutants, like the wildtype proteins, are capable to activate rDNA transcription. For this, wildtype and mutant PHF2 and PHF8 were overexpressed in HEK293T cells and pre-rRNA synthesis was monitored by qRT-PCR. As detected by western blots, Flag-tagged mutant PHF2 and PHF8 were expressed

at similar levels as the wildtype proteins. Pre-rRNA synthesis was enhanced about 40% upon overexpression of wildtype Fl-PHF2, whereas neither the PHD finger mutant Fl-PHF2-Y7A nor the JmjC domain mutant Fl-PHF2-H249A was capable to stimulate Pol I transcription (Fig. 3.7A, upper panel). Likewise, overexpression of wildtype Fl-PHF8, but neither Fl-PHF8-Y7A nor Fl-PHF8-HID, augmented pre-rRNA synthesis (Fig. 3.7B, upper panel). Thus, mutations within the PHD finger as well as the JmjC domain abolished the transcription activation mediated by PHF2 and PHF8, underscoring the importance of these protein modules for the function of both proteins. To confirm this, reporter gene assays were performed. The Pol I specific reporter pHrP2-BH was co-transfected with wildtype and mutant Fl-PHF2 and Fl-PHF8 in HEK293T cells, and the synthesis of report transcripts was monitored by qRT-PCR. Consistent with PHF2 and PHF8 activating Pol I transcription, the levels of reporter transcripts were significantly enhanced upon overexpression of the wildtype Fl-PHF2 and Fl-PHF8. In contrast, mutations within the PHD finger and JmjC domain of PHF2 and PHF8 abolished their capability to activate transcription from the Pol I –specific reporter (Fig. 3.7A and Fig. 3.7B, middle panel). Taken together, these results reveal that the PHD finger and JmjC domain are indispensable for PHF2- and PHF8-dependent activation of rDNA transcription, although the nucleolar localization and the association with Pol I machinery are not affected by the compromised function of both domains.

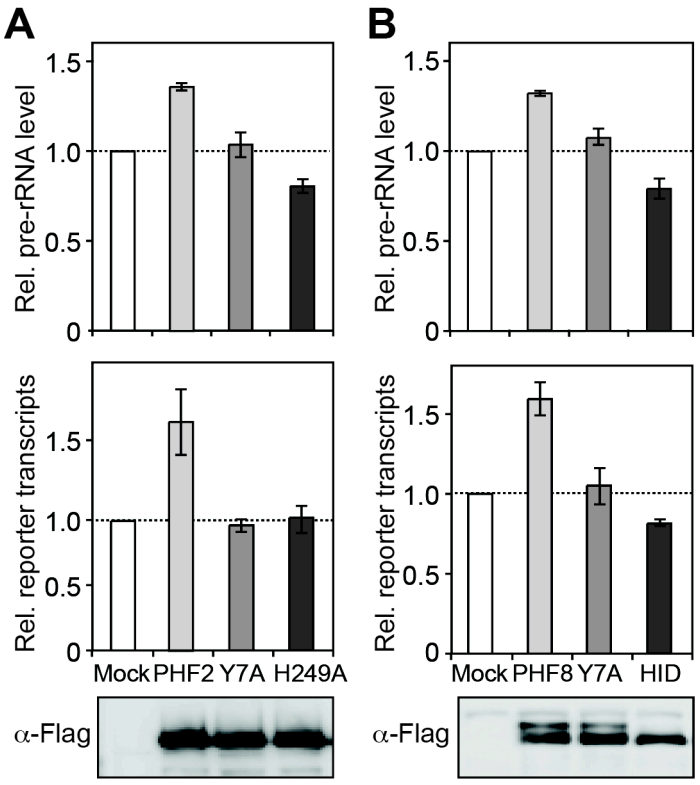

Figure 3.7. The PHD finger and JmjC domain are required for PHF2- and PHF8-dependent activation of Pol I transcription

(A) PHF2-dependent activation of Pol I transcription requires the PHD finger and JmjC domain. HEK293T cells were transfected with expression vectors encoding Flag-tagged wildtype and mutant PHF2 (upper panel), or together with the Pol I specific reporter construct pHrP2-BH (middle panel). The synthesis of pre-rRNA and reporter transcripts was monitored by qRT-PCR and normalized to β-actin mRNA levels. The western blot image in the bottom panel shows the expression levels of wildtype and mutant Fl-PHF2. Error bars represent standard deviation from three independent experiments.

(B) The PHD finger and JmjC domain are required for PHF8-mediated activation of rDNA transcription. HEK293T cells were transfected with expression vectors encoding Flag-tagged wildtype and mutant PHF8 (upper panel), or together with the reporter construct pHrP2-BH (middle panel). The synthesis of pre-rRNA and reporter transcripts was monitored by qRT-PCR. The western blot image in the bottom panel shows the expression levels of wildtype and mutant Fl-PHF8. The data are from three independent experiments.

3.7. PHF2 and PHF8 are associated with chromatin

The observation that mutations in the PHD finger and JmjC domain render PHF2 and PHF8 unable to activate pre-rRNA synthesis, suggests that both proteins may bind to H3K4me3 and act as lysine demethylases. To regulate Pol I transcription, both enzymes should not only interact with the Pol I transcription machinery, but also with chromatin. To test this, the association of PHF2 and PHF8 with chromatin was examined by biochemical fractionation under native condition. HEK293T cells were lysed in hypotonic buffer to separate nuclei from the cytoplasm. The nuclei were subsequently disrupted in low salt buffer to yield a soluble nucleoplasmic fraction and an insoluble chromatin fraction. Chromatin-bound proteins were extracted under high salt conditions and by nuclease treatment. The distribution of PHF2 and PHF8 in these subcellular fractions was monitored on western blots (Fig. 3.8A). As a control, a typical protein for each fraction was monitored in parallel. Tubulin, a cytosolic protein, was recovered mainly in the cytoplasmic fraction. TIF-IA, a Pol I specific transcription factor, was found mainly in the nucleoplasmic fraction but also in the cytoplasmic fraction, probably due to leakage during isolation of the nuclei. TIP5, a subunit of the chromatin remodeling complex NoRC, was exclusively detected in the chromatin fraction. The expected distribution of these marker proteins demonstrated that cellular fractionation was properly performed. Notably, PHF2 was mainly found in the chromatin fraction, whereas similar levels of PHF8 were detected in both the nucleoplasmic and chromatin fraction. Thus, PHF2 appears to be tightly associated with chromatin, whereas PHF8 is less strongly bound.

At the onset of mitosis, chromatin condenses to form chromosomes. The Pol I transcription is repressed and nucleoli disintegrate. Many rDNA-associated proteins, like Pol I, are replaced from chromatin during mitosis. However, some factors, like UBF, remain associated with rDNA during mitosis at nucleolar organization regions (NORs). To examine whether PHF2 and PHF8 remain associated with chromatin during mitosis, the distribution of GFP-PHF2 and HA-PHF8 in mitotic U2OS cells was examined by fluorescence microscopy. Notably, the GFP-PHF2 staining pattern matched the DNA staining with Hoechst (Fig. 3.8B), showing that GFP-PHF2 remained associated

with condensed chromatin in mitotic cell. In contrast, HA-PHF8 was mainly excluded from chromatin, demonstrating that HA-PHF8 was not or only weakly associated with chromatin during mitosis. This finding is consistent to the results from fractionation experiments showing that PHF2 binds more strongly to chromatin than PHF8. To examine whether PHF2 binds to NORs during mitosis, U2OS cells were co-immunostained with anti-UBF antibodies. As shown in Fig. 3.8B, UBF was detected as bright dots within the condensed chromosomes depicting the localization of NORs, whereas GFP-PHF2 did not match the staining of UBF but rather showed a diffuse staining along the chromosomes. Therefore, these results revealed that PHF2 is associated with chromatin but is not enriched in NORs during mitosis.

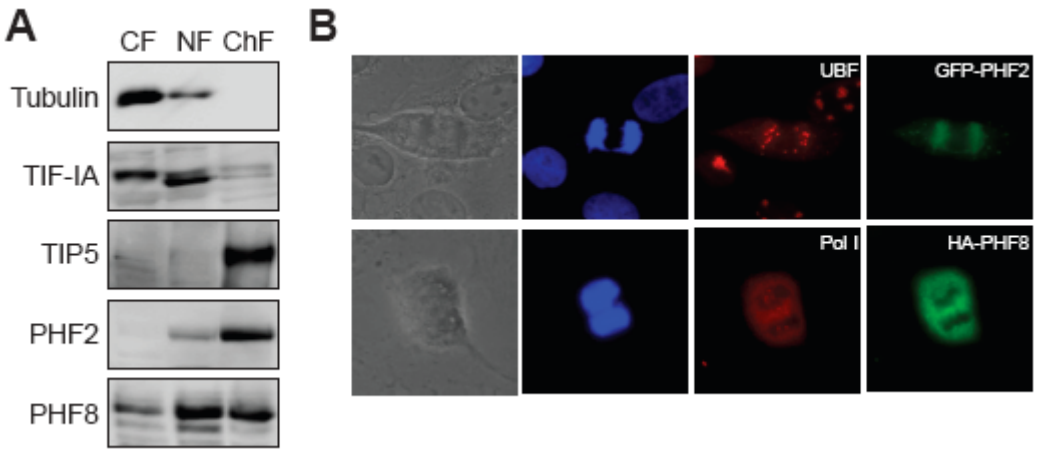

Figure 3.8. PHF2 and PHF8 are associated with chromatin
(A) PHF2 and PHF8 bind to chromatin. HEK293T cells were fractionated into cytoplasmic (CF), nucleoplasmic (NF) and chromatin fractions (ChF). Lysates of equivalent amounts of cells from each subcellular fraction were analyzed by immunoblotting using indicated antibodies.
(B) PHF2 stays associated with chromatin during mitosis. U2OS cells overexpressing GFP-PHF2 or HA-PHF8 were immunostained with antibodies against UBF, Pol I and HA epitope. Images of phase contrast and DNA staining with Hoechst are shown in the first two panels.

3.8. PHF2 binds to H3K4me3 via the PHD finger

PHD fingers have been shown to interact with methylated lysine residues on histone H3. The presence of PHD fingers in PHF2 and PHF8 indicates that these enzymes might directly interact with hitone H3. To test this, co-

immunoprecipitation assays were performed. Nuclear extracts from HEK293T cells expressing Fl-PHF2 and Fl-PHF8 were immunoprecipitated with anti-Flag antibodies, and co-precipitation of histone H3 was monitored by immunoblotting. As shown in Fig. 3.9A, significant amount of H3 was co-precipitated with Fl-PHF2, whereas only a minor fraction of histone H3 was co-precipitated with Fl-PHF8. Thus, PHF2 and to a lesser extent also PHF8, interact with histone H3 *in vivo*. The finding that PHF2 exhibited a stronger affinity to histone H3 than PHF8 is consistent with the observation that PHF2 binds more tightly to chromatin than PHF8. To analyze if Fl-PHF2 is also associated with histones other than H3, the Fl-PHF2 co-precipitated histones were also visualized by Coomassie blue staining. Besides histone H3, other core histones, i.e. H2A, H2B and H4 also co-precipitated with Fl-PHF2 in stoichiometric amounts, but not histone H1 (Fig. 3.9B), demonstrating that PHF2 interacts with nucleosomal core particles but not the linker histone.

To test if the association of PHF2 with histone H3 is mediated via methylated lysine residues, histone H3 that co-precipitated with Fl-PHF2 was examined on western blots using antibodies against different histone methylations. The relative enrichment of histone methylation marks in Fl-PHF2-associated histone H3 was calculated relative to the abundance of this mark in the nuclear extract. Importantly, H3K4me3 was specifically associated with Fl-PHF2 (>2 fold enrichment), whereas co-precipitation of other histone modifications, like H3K4me2, H3K9me2 and H3K36me2 mirrored the overall levels in the nuclear extract (Fig. 3.9C). Thus, these results revealed that PHF2 preferentially binds to H3K4me3 *in vivo*. Moreover, the enrichment of H3K4me3 in PHF2-associated histone H3 was impaired by mutation of tyr7, a residue in the PHD finger that is expected to be required to bind to H3K4me3 (Fig. 3.9D). As a control, the JmjC domain mutant PHF2-H249A showed similar affinity for H3K4me3 as the wildtype protein. Genome-wide analysis has shown that H3K4me3 is associated with the transcriptionally active genes. Consistently, H3K4me3 is associated with unmethylated, i.e. active rRNA genes. Thus, the specific association of PHF2 with H3K4me3 supports the view that PHF2 binds at transcriptionally active rDNA repeats and stimulates Pol I transcription.

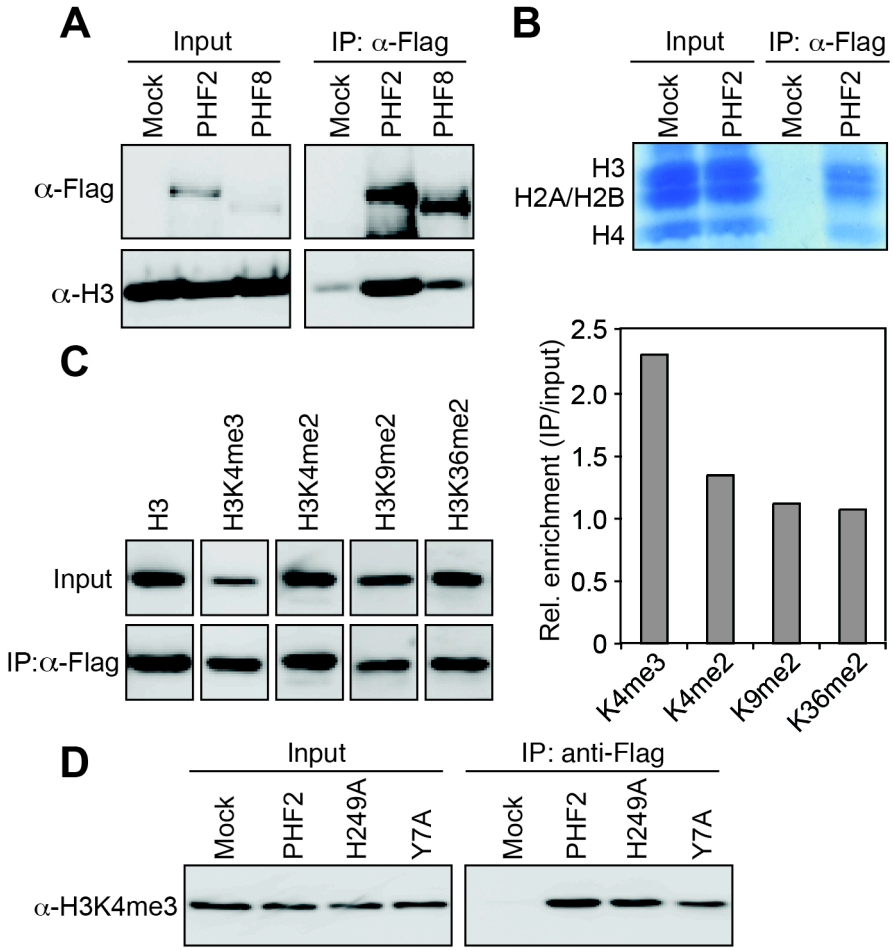

Figure 3.9. PHF2 interacts with H3K4me3 via the PHD finger
(A) PHF2 and PHF8 interact with histone H3. Nuclear extracts from HEK293T cells overexpressing Fl-PHF2 and Fl-PHF8 were immunoprecipitated with anti-Flag antibodies. 3.3% of input and 33% of precipitated proteins were analyzed on western blots.
(B) PHF2 is associated with core histones. Histones co-precipitated with Fl-PHF2 were visualized on SDS polyacrylamide gel stained with Coomassie blue. One percent of input and 50% of precipitated proteins were assayed.
(C) PHF2 preferentially binds to H3K4me3 *in vivo*. Fl-PHF2 was overexpressed in HEK293T cells and immunoprecipitated with anti-Flag antibodies. The co-precipitated histones and histones in the input samples were analyzed by immunoblotting using the indicated histone antibodies. 0.1% of input and 8% of precipitated proteins were analyzed on western blots. After normalization of the levels of histone H3, the relative enrichment of individual modifications in PHF2-bound histone H3 was shown on the right bar diagram.
(D) PHF2 binds to H3K4me3 via the PHD finger. HEK293T cells were transfected with constructs encoding Fl-PHF2, Fl-PHF2H249A and Fl-PHF2Y7A. Nuclear extracts from these cells were precipitated with anti-Flag antibodies, and bound proteins were analyzed by immunoblotting using anti-H3K4me3 antibodies. 0.5% of input and 13% of precipitated proteins were assayed by immunoblotting.

3.9. PHF8 demethylates H3K9me2 and H3K9me1

The data presented so far revealed that activation of rDNA transcription by PHF2 and PHF8 requires the functional JmjC domain, suggesting that both proteins function as lysine demethylases (KDMs) in the regulation of Pol I transcription. Recently, it has been shown that JmjC domain-containing proteins can remove methyl groups from different lysine residues on histone H3, such as K4, K9, K27 and K36 in an iron- and αKG-dependent manner (Tsukada et al. 2006; see review Cloos et al. 2008). Therefore, it was investigated whether PHF2 and PHF8 are capable to demethylate histones. First, the JmjC domains of PHF2 and PHF8 were aligned to two closely related lysine demethylases, KDM2A and KDM2B. KDM2A is capable to demethylate H3K36me2 (Tsukada et al. 2006), and KDM2B has been shown to target both H3K36me2 and H3K4me3 (He et al. 2008; Frescas et al. 2007; Tzatsos et al. 2009). As shown in Fig. 3.10A, the alignment shows that the three iron-binding and two αKG-binding residues in the JmjC domain of PHF8 are identical to KDM2A and KDM2B, suggesting that PHF8 is very likely a histone demethylase, too. These critical residues are also conserved in PHF2, except that a histidine is replaced by tyrosine at the third iron-binding residue within the JmjC domain (Fig. 3.10A).

Having shown that PHF8 augments rDNA transcription, we reasoned that the enzymatic activity of PHF8 might remove the repressive methyl groups from H3K9me. To test this, PHF8 was depleted in HEK293T cells by siRNA and changes in histone methylation at the rDNA promoter were monitored by ChIP assays. Notably, depletion of PHF8 in HEK293T cells increased the levels of H3K9me2 by 40% and H3K9me1 by 30% (Fig. 3.10B). In accord with an increase in the levels of H3K9me2 and H3K9me1 (H3K9me1/2), H3K9me3 levels were decreased. No significant change of another repressive mark, H4K20me3, was detected upon knockdown of PHF8. These results demonstrated that PHF8 is capable to specifically demethylate H3K9me2 and H3K9me1 at the rDNA promoter. Concomitant with an increase in H3K9me1/2 levels upon PHF8 depletion, H3K4me3 at the rDNA promoter decreased, suggesting that PHF8 might mediate a crosstalk between these repressive and active histone marks.

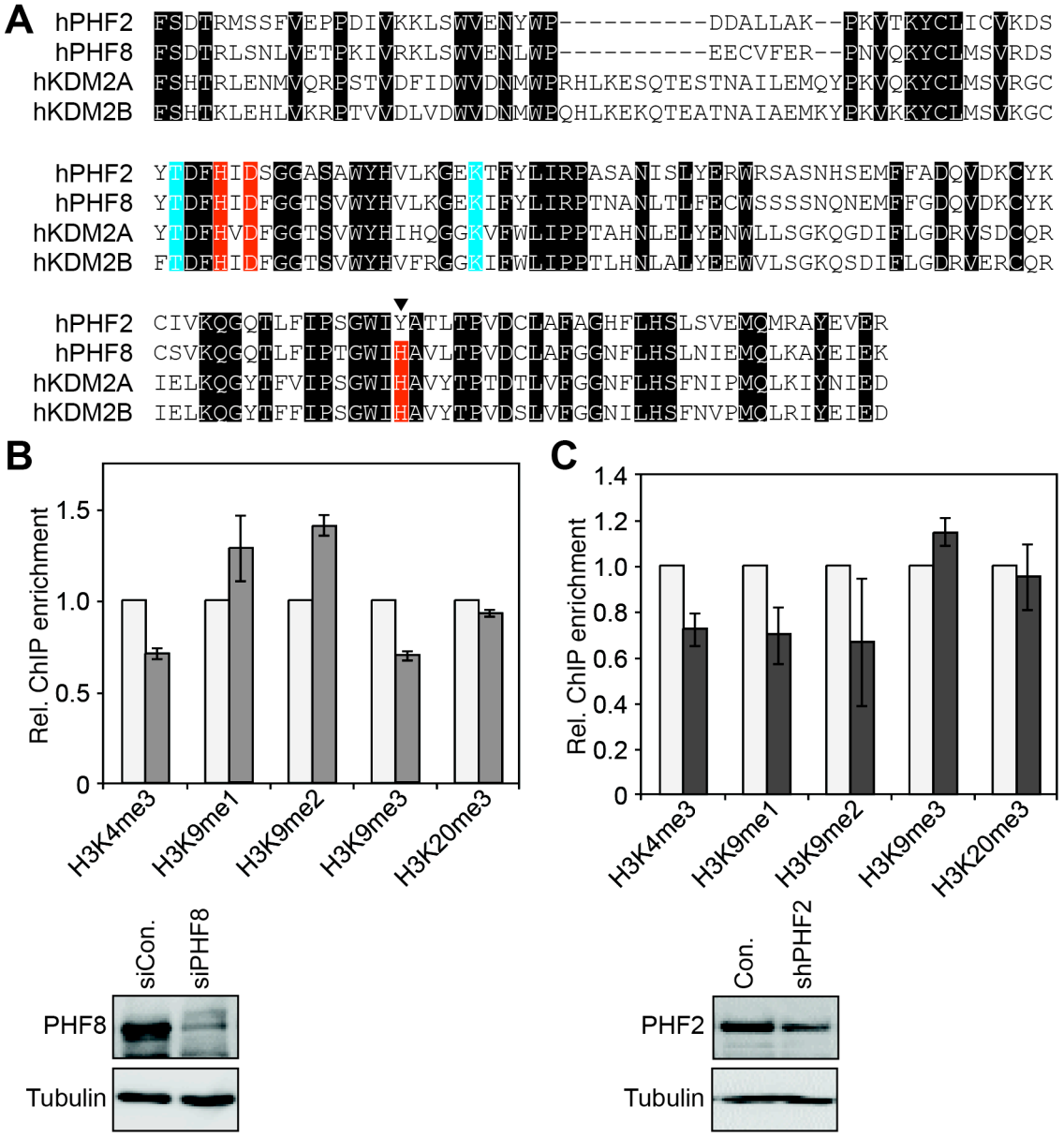

Figure 3.10. PHF8 demethylates H3K9me2 and H3K9me1 at rDNA

(A) Alignment of the JmjC domains of human PHF2 (aa 197-353), human PHF8 (aa 195-351), human KDM2A (aa 148-316) and human KDM2B (aa 178-346). The predicted Fe(II)-binding (red) and αKG-binding residues (blue) are highlighted. Substitution of histidine to tyrosine in the third Fe(II)-binding residue of the JmjC domain of PHF2 is indicated by a triangle.

(B) PHF8 demethylates H3K9me2 and H3K9me1 at rDNA. Chromatin from HEK293T cells transfected with either control siRNA (light bars) or siRNA against PHF8 (grey bars) was precipitated with the indicated histone antibodies. The precipitated DNA was analyzed by qPCR with primers covering the rDNA promoter. The western blot image below shows the levels of cellular PHF8 and tubulin upon siRNA transfection. Error bars represent standard deviation of three independent experiments.

(C) PHF2 does not demethylate H3K9me at rDNA. Chromatin from HEK293T cells transfected with either empty vector (pSuperior) (light bars) or plasmid encoding shRNA against PHF2 (dark bars) was precipitated with indicated histone antibodies. The precipitated DNA was analyzed by qPCR with primers covering the rDNA promoter. The western blot below shows the levels of cellular PHF2 and tubulin upon transfection. The data are from three independent experiments.

Like PHF8, PHF2 activates Pol I transcription in a JmjC domain-dependent manner. Therefore, I tested whether PHF2 is also capable to demethylate histones at rDNA. For this, PHF2 was depleted in HEK293T cells by transfection of a plasmid DNA encoding a small hairpin RNA (shRNA) that specifically targets PHF2 and changes in histone methylations at the rDNA promoter were monitored in ChIP assays. In contrast to knockdown of PHF8, depletion of PHF2 did not increase but rather decreased the levels of both H3K9me1 and H3K9me2 at the rDNA promoter, whereas no significant change of H3K9me3 and H4K20me3 was detected (Fig. 3.10C). Likewise, no increase in the levels of H3K27 and H3K36 methylation at rDNA was observed in PHF2-depleted cells (data not shown). Thus, PHF2 does not seem to activate Pol I transcription by changing H3K9 methylation at the rDNA promoter. In agreement with this, recombinant PHF2 did not exhibit histone demethylation activity *in vitro* (personal communication M, Yonezawa). However, upon knockdown of PHF2, the level of H3K4me3 at the rDNA promoter dropped to a similar level as in PHF8-depleted cells, demonstrating that both enzymes are required to maintain euchromatic state of actively transcribed rRNA genes.

3.10. Association of PHF2 with rDNA depends on PHF8

Given that both PHF2 and PHF8 localize to nucleoli, bind to active rRNA genes and stimulate Pol I transcription, these two enzymes might work in concert to facilitate rDNA transcription. To examine the functional relationship between PHF2 and PHF8, the interaction of these two proteins was monitored. Co-immunoprecipitation experiments in HEK293T cells showed that significant amounts of PHF8 were co-precipitated with Fl-PHF2 (Fig. 3.11A, left panel). In agreement with this, PHF2 could also be co-immunoprecipitated with V5-PHF8 (Fig. 3.11A, right panel). Thus, PHF2 and PHF8 interact *in vivo*, suggesting that both enzymes may be part of a multiprotein complex that activates rDNA transcription.

To gain further insight into the functional link between PHF2 and PHF8, either PHF2 or PHF8 was depleted in cells and the association of each protein with rDNA was examined by ChIP assays. As no antibody is available that immunoprecipitates endogenous PHF2 in ChIP assays, the association of

PHF2 with rDNA was monitored by overexpression of HA-PHF2 in HEK293T cells and precipitation with anti-HA antibodies. Notably, binding of HA-PHF2 to the rDNA promoter and the 28S rRNA coding region was decreased by 60% upon depletion of PHF8, whereas depletion of PHF2 did not reduce but rather increased the association of PHF8 with rDNA (Fig. 3.11B and Fig. 3.11C). The changes in rDNA occupancy were not due to differences in protein amounts because the level of cellular HA-PHF2 was not affected by knockdown of PHF8. Likewise, depletion of PHF2 did not change the level of PHF8. Therefore, these results demonstrated that PHF8 is required for the recruitment of PHF2 to rDNA.

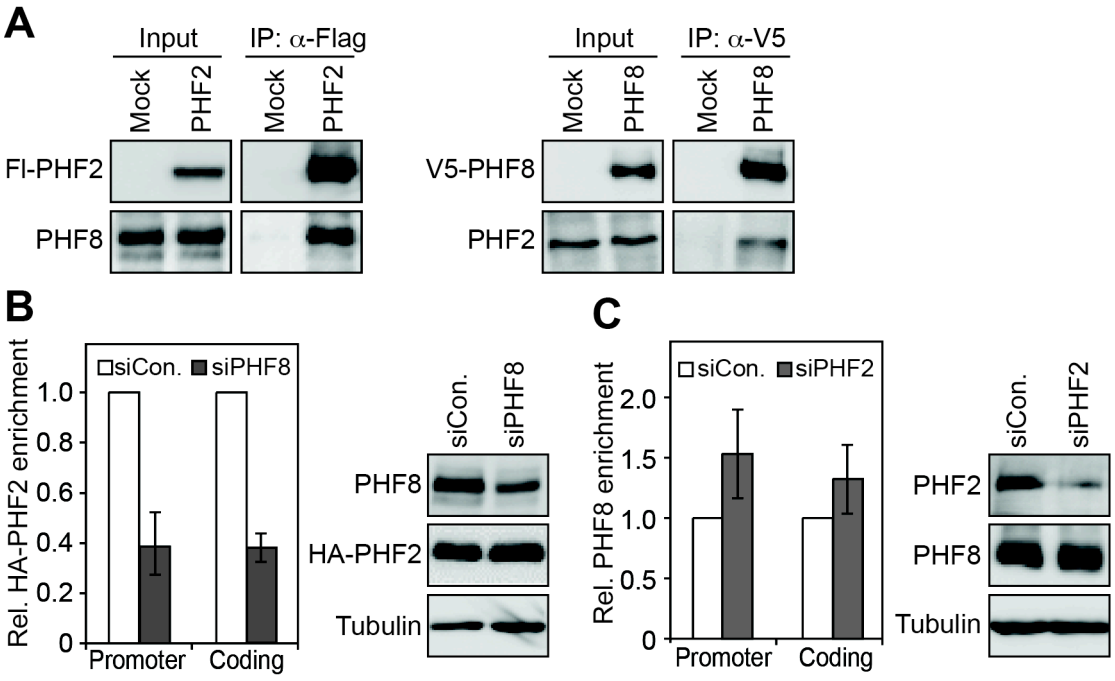

Figure 3.11. Association of PHF2 with rDNA depends on PHF8
(A) PHF8 interacts with PHF2 *in vivo*. Nuclear extracts from HEK293T cells overexpressing Fl-PHF2 or V5-PHF8 were incubated with anti-Flag or anti-V5 antibodies, respectively. Two percent of input and 30% of precipitated proteins were analyzed on western blots with indicated antibodies.
(B) Knockdown of PHF8 dissociates PHF2 from rDNA. The binding of PHF2 to the rDNA promoter and the 28S rRNA coding region in PHF8-depleted HEK293T cells was examined by ChIP assays. The western blot image at the right shows the levels of cellular PHF8, HA-PHF2 and tubulin upon siRNA knockdown.
(C) Knockdown of PHF2 enhances the association of PHF8 with rDNA. The binding of PHF8 to rDNA was analyzed by ChIP assays in PHF2-depleted HEK293T cells. The western blot image at the right shows the levels of cellular PHF2, PHF8 and tubulin upon siRNA knockdown.

3.11. PHF2 and PHF8 dissociate from rDNA upon cellular stress

Transcription of rRNA genes by Pol I is highly regulated to be responsive to specific environmental challenges, such as oxidative and ribotoxic stress. Having shown that both PHF2 and PHF8 are positive regulators of rDNA transcription, they may serve a role in confering environmental cues to the Pol I transcription machinery. Stress-induced signaling has been shown to repress rDNA transcription by inactivation of the Pol I-specific transcription factor TIF-IA (Mayer et al. 2005). However, it is not yet known whether cellular stress may also lead to alterations of the chromatin structure of rDNA. To examine whether PHF2 and PHF8 are involved in stress-dependent regulation or rRNA synthesis, the association of both proteins with rDNA was monitored upon cellular stress. For this, HEK293T cells were treated with anisomycin, a ribotoxic drug which inhibited pre-rRNA synthesis about 60% (Fig. 3.12A). Cross-linked chromatin from mock- or anisomycin-treated cells was precipitated with antibodies against HA-PHF2 and PHF8, and co-precipitated DNA was analyzed by qPCR using primers amplifying the rDNA promoter and the 28S rRNA coding region (Fig. 3.12B). In parallel, rDNA occupancy of Pol I and UBF were monitored. Consistent with anisomycin-dependent inhibition of rDNA transcription, the association of Pol I with rDNA was significantly impaired, whereas binding of UBF was not affected. Notably, the association of PHF2 and PHF8 with the rDNA promoter and the 28S rRNA coding region was reduced about 40% after anisomycin treatment, although that protein levels remained unaffected (Fig. 3.12C). These results suggested that the association of PHF2 and PHF8 with rDNA is regulated by stress signaling. In addition, the finding that stress-dependent release of PHF2 and PHF8 being comparable to the dissociation of Pol I from rDNA suggests that Pol I might regulate the recruitment of both proteins to rDNA.

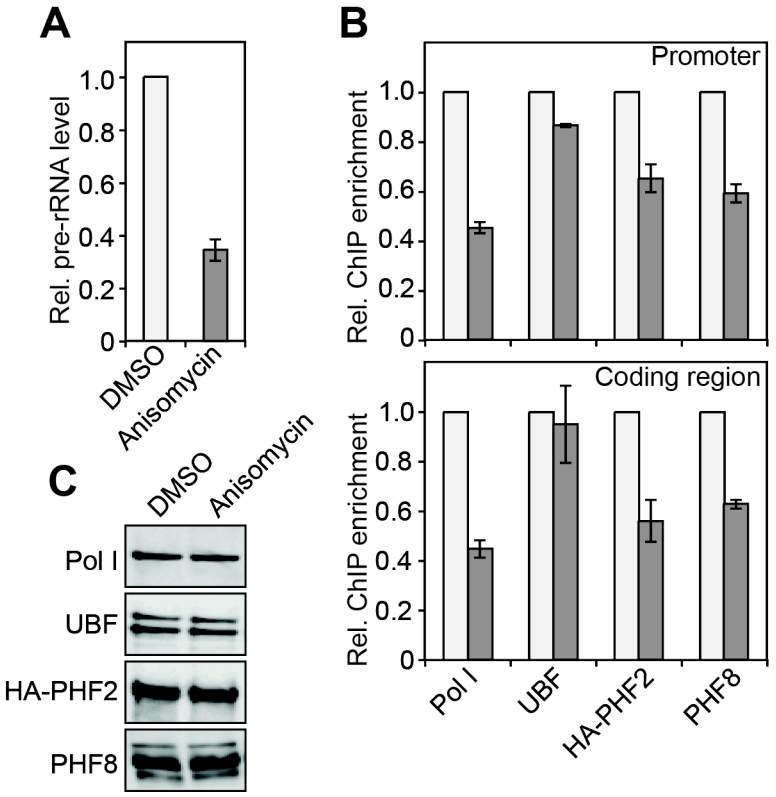

Fig. 3.12. The association of PHF2 and PHF8 with rDNA is regulated by cellular stress

(A) Anisomycin treatment represses pre-rRNA synthesis. HEK293T cells were treated with anisomycin (10 mM, 2 hr). Pre-rRNA levels were quantified by qRT-PCR and normalized to β-actin mRNA levels. The data are from three independent experiments.

(B) Anisomycin treatment impairs the association of PHF2 and PHF8 with rDNA. The bar diagrams show results from ChIP assays comparing rDNA occupancy of Pol I, UBF, HA-PHF2 and PHF8 in anisomycin-treated and DMSO-treated HEK293T cells. Error bars represent standard deviation from three independent experiments.

(C) Anisomycin treatment does not change protein levels of Pol I, UBF, HA-PHF2 and PHF8. HEK293T cells ovexpressing HA-PHF2 were treated with anisomycin. Protein levels were monitored on western blots with the indicated antibodies.

3.12. A disease-related PHF8 mutant does not localize to nucleoli and activate rDNA transcription

3.12.1. The JmjC domain of PHF8 is mutated in XLMR patients

Recently, *PHF8* has been shown to be involved in X-linked mental retardation (XLMR) Siderius type, a syndrome with manifest mild to borderline mental retardation with or without cleft lip/cleft palate (Siderius et al. 1999; Laummonier et al. 2005). Thus far, four mutations in *PHF8* have been identified in XLMR patients (Laummonier et al. 2005; Abidi et al. 2007; Koivisto et al. 2007). Intriguingly, all these mutations are linked to the JmjC domain, with one point mutation changing phenylalanine to serine (F279S) and three truncation mutations which either partly or completely delete this domain (Fig. 3. 13A). The deletion of critical residues within the JmjC domain that are required for the binding of the cofactor like iron and αKG in these XLMR-associated mutants demonstrates that they are defective of histone demethylase activity. Thus, these observations suggested that a defect in the JmjC domain abolishing the lysine demethylation activity of PHF8 is detrimental and might be a common cause of XLMR associated with *PHF8* mutation.

3.12.2. F279S mutation of PHF8 abrogates its nucleolar function

Notably, residue F279 is evolutionally conserved in PHF8 from vertebrates including human, dog, mouse and zebrafish but not in closely related JmjC domain-containing proteins, such as PHF2, KDM2A, KDM2B, indicating that it might confer a PHF8-specific function (Fig. 3.13B). Given that the XLMR phenotype is associated with a point mutation at position 279, this mutation has propably inactivated the demethylase activity of PHF8. If this was true, this mutant should compromise PHF8-dependent activation of rDNA transcription. Indeed, overexpression of PHF8-F279S in HEK293T cells did not enhance transcription from Pol I reporter plasmids and from endogenous rRNA genes (Fig. 3.13C). Moreover, in contrast to mutations within the PHD finger (Y7A) or on different positions within the JmjC domain (HID), GFP-PHF8-F279S

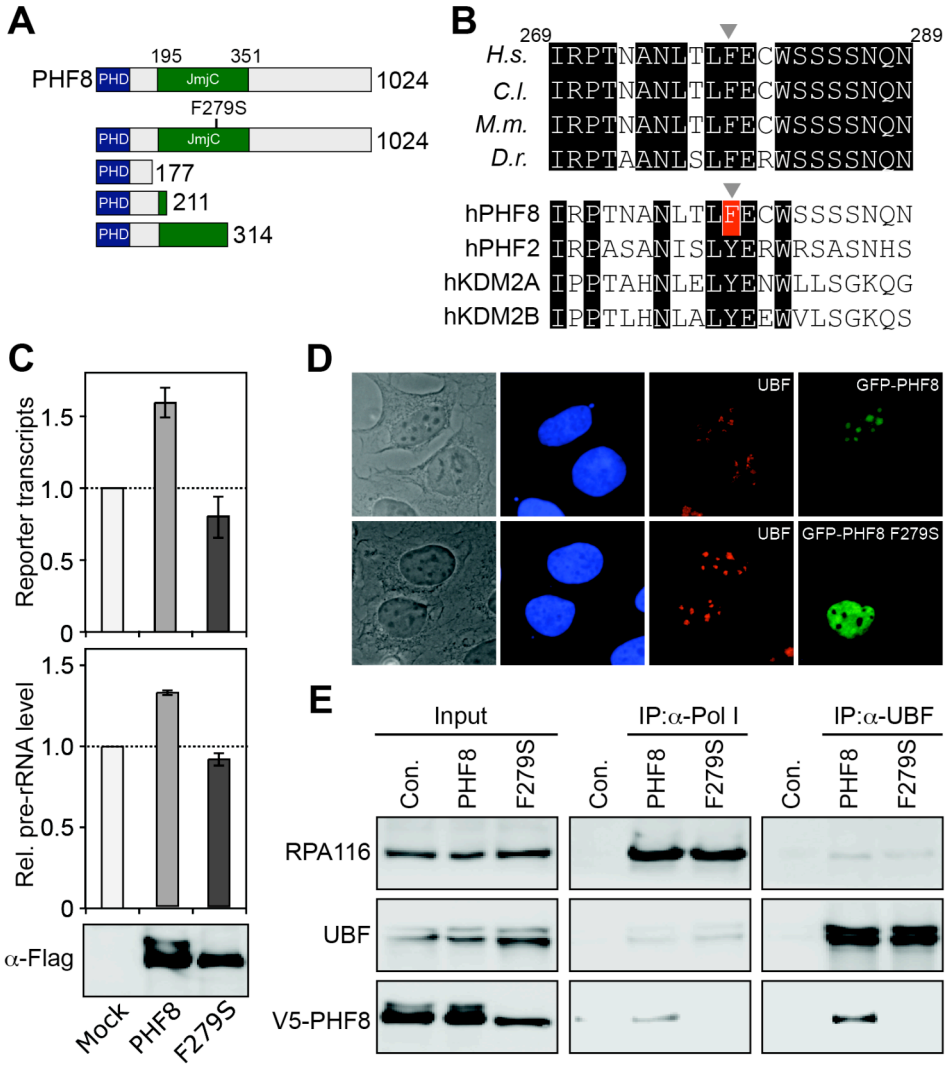

Figure 3.13. F279S mutation impairs the nucleolar function of PHF8

(A) Schemes show the wildtype PHF8 and four mutant PHF8 identified in XLMR patients. The numbers represent the position of amino acid.

(B) (Upper panel) Alignment of the amino acid sequences of PHF8 from human (H.s.), dog (C.l.), mouse (M.m.) and zebrafish (D.r.) showing the coservation of residue F279. The lower panel shows alignment of amino acid sequences around residue F279 of human PHF8, PHF2, KDM2A and KDM2B.

(C) PHF8-F279S does not activate rDNA transcription. HEK293T cells were transfected with expression vectors encoding Fl-PHF8 and Fl-PHF8-F279S (middle panel), or together with a Pol I-specific reporter plasmid (pHrP2-BH) (upper panel). The synthesis of reporter transcripts and pre-rRNA was monitored by qRT-PCR and normalized to β-actin mRNA levels. The western blot below shows the expression levels of Flag-tagged wildtype and mutant PHF8.

(D) GFP-PHF8-F279S does not localize to nucleoli. U2OS cells overexpressing GFP-tagged wild type and XLMR-associated mutant F279S were immunostained with anti-UBF antibodies. Images of phase contrast and DNA staining with Hoechst are shown in first two panels.

(E) F279S mutation impairs the association of PHF8 with the Pol I transcription machinery. Nuclear extracts from HEK293T cells expressing V5-PHF8 or V5-PHF8-F279S were precipitated with antibodies against Pol I and UBF, and the preciptated proteins were monitored by immunoblotting. As a control, equivalent amounts of lysates containing V5-PHF8 and V5-PHF8-F279S were mixed and incubated with the control human IgGs. One percent of input and 65% of precipitated proteins were assayed on western blots.

localized to nuclei but was excluded from nucleoli, indicating that the F279S mutation has impaired targeting of PHF8 to nucleoli (Fig. 3.13D). Significantly, mutation of F279 severely compromised the interaction between PHF8 and the Pol I transcription machinery (Fig. 3.13E), providing a molecular explanation for its incapability to promote Pol I transcription and its mislocalization. Thus, these results implicate that impairment of the nucleolar function of PHF8 may be responsible for the development of XLMR.

3.13. PHF8 interacts with the histone H3K4 methyltransferase MLL1

Knockdown of PHF8 causes a reduction of H3K4me3 at the rDNA promoter (Fig. 3.10B), indicating that PHF8 regulates H3K4 methylation. It is known that H3K4 is methylated by several histone methyltransferases including MLL1 that has been reported to localize within nucleoli (Caslini et al. 2000). To examine if there is a functional link between PHF8 and MLL1, the interaction between both proteins was analyzed. For this, MLL1 was immunoprecipitated from HEK293T cells expressing V5-PHF8. As shown in Fig. 3.14A (upper panel), V5-PHF8 was co-precipitated with MLL1, suggesting that PHF8 interacts with MLL1 *in vivo*. MLL1 is known to form a multiprotein complex comprising several core components, e.g. WDR5, RBBP5, and ASH2L (Shilatifard 2008). WDR5 has been shown to mediate the enzyme-substrate interaction by binding to H3K4me2 and to be required for the complex integrity (Wysocka et al. 2005; Dou et al. 2006). To examine whether PHF8 is capable to interact with other subunits of MLL1 complex, the interaction between PHF8 and WDR5 was monitored. As shown in Fig. 3.14A (middle panel), Fl-PHF8 was co-precipitated with V5-WDR5. Likewise, Fl-WDR5 could be co-immunoprecipitated with V5-PHF8 (Fig. 3.14A, lower panel). Thus, PHF8 interacts with both MLL1 and WDR5, indicating that PHF8 is associated with MLL1 complex. The association of PHF8 with MLL1 suggests a cooperative action of MLL1 and PHF8, MLL1 establishing the active mark H3K4me3 and PHF8 removing the repressive H3K9 methylation.

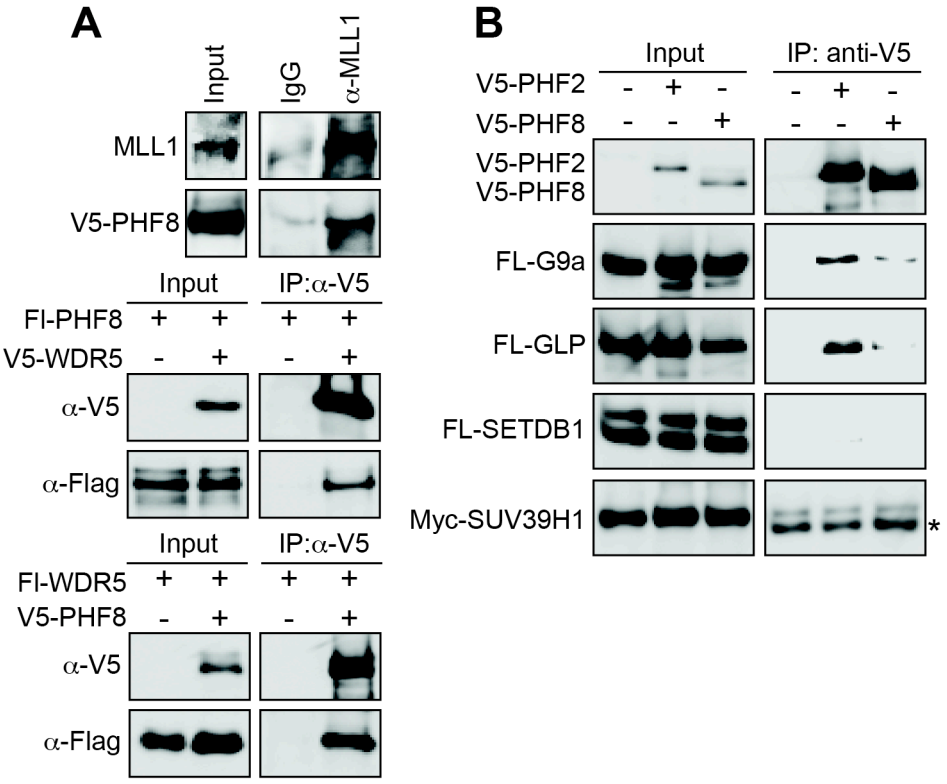

Figure 3.14. PHF2 and PHF8 interact with the histone H3K9 or H3K4 methyltransferases

(A) PHF8 interacts with MLL1 and WDR5. (Upper panel) Nuclear extracts from HEK293T cells overexpressing V5-PHF8 were incubated with anti-MLL1 antibodies or control rabbit IgGs. Two percent of input and 65% of precipitated proteins were analyzed on western blots. (Middle panel) Nuclear extracts from HEK293T cells overexpressing V5-WDR5 and Fl-PHF8 were incubated with anti-V5 antibodies. One percent of input and 65% of precipitated proteins were monitored by immunoblotting. (Lower panel) Nuclear extracts from HEK293T cells overexpressing V5-PHF8 and Fl-WDR5 were incubated with anti-V5 antibodies. One percent of input and 65% of precipitated proteins were analyzed on western blots.

(B) PHF2 interacts with G9a and GLP *in vivo*. HEK293T cells were co-transfected with expression vectors encoding V5-PHF2, V5-PHF8, and different tagged H3K9 methyltransferases, i.e. Flag-tagged G9a, GLP, SETDB1 and Myc-tagged SUV39H1. Nuclear extracts from these cells were precipitated with anti-V5 antibodies, and 2% of input and 50% of precipitated proteins were analyzed on western blots with the indicated antibodies. The heavy chain of IgGs is indicated by an asterisk.

3.14. PHF2 interacts with the histone H3K9 methyltransferase G9a and GLP

The finding that depletion of PHF2 leads to a decrease of H3K9me1/2 levels at the rDNA promoter suggests that PHF2 regulates H3K9 methylation. Methylation of H3K9 in heterochromatin is mediated by the histone methyltransferases SETDB1 and SUV39H1, whereas G9a and GLP are the enzymes responsible for H3K9 methylation in euchromatin. It was examined whether PHF2 interacts with any of these histone H3K9 methyltransferases. The association of PHF8 with these methyltransferases was monitored in parallel. For this, HEK293T cells were co-transfected with expression plasmids encoding V5-PHF2 or V5-PHF8 together with four different histone H3K9 methyltransferases (Flag-tagged G9a, GLP, SETDB1 and Myc-tagged SUV39H1), and lysates were incubated with anti-V5 antibodies. Co-immunoprecipitation of the respective methyltransferases with V5-PHF2 or V5-PHF8 was monitored on immunoblots. As shown in Fig. 3.14B, V5-PHF2 was co-precipitated with Fl-G9a and Fl-GLP, which is consistent with the finding that GLP and G9a form a heteromeric complex (Tachibana et al. 2005). In contrary, no clear association of Fl-SETDB1 and Myc-SUV39H1 with V5-PHF2 was observed. Thus, PHF2 interacts with the euchromatic histone H3K9 methyltransferases G9a and GLP, but not with the heterochromatic histone H3K9 methyltransferases SETDB1 and SUV39H1. Given that G9a-mediated methylation of H3K9 is required for rDNA transcription (Yuan et al. 2007), the association of PHF2 with G9a suggests that PHF2 might facilitate G9a to stimulate rDNA transcription. On the other hand, no clear interaction of V5-PHF8 with any of the tested histone H3K9 methyltransferases was observed (Fig. 3.14B). This data is consistent with the finding that PHF8 is associated with the histone H3K4 methyltransferase MLL1 complex and demethylates H3K9me1/2.

3.15. PHF2 interacts with the nucleosome remodeling and deacetylase complex NuRD

To further analyze the function of PHF2 on nucleolar chromatin, its association with other chromatin modifying enzymes was examined. For this, Fl-PHF2 was overexpressed and immunoprecipitated from HEK293T cells, and co-precipitated proteins were analyzed. As shown in Fig. 3.15A, two enzymatic components of the nucleosome remodeling and deacetylase complex NuRD, Mi2β and HDAC1, were found to be co-precipitated with Fl-PHF2, suggesting PHF2 is associated with NuRD complex *in vivo*. Interestingly, the ATP-dependent chromatin remodeler Mi2β has been shown to be associated with rDNA and to stimulate Pol I transcription (Shimono et al. 2005). Therefore, PHF2 might act in concert with NuRD complex to promote rRNA synthesis. If PHF2 interacts with NuRD complex, a subpopulation of PHF2 and NuRD complex should be associated in cell extracts. To test this, nuclear extract from HEK293T cells was loaded onto 12.5%-30% glycerol gradient and subjected to ultracentrifugation. Fractions were collected after centrifugation and the distribution of PHF2 and two subunits of NuRD complex, Mi2β and HDAC1 in these fractions was analyzed on western blots. Importantly, PHF2 co-peaked with Mi2β and HDAC1 at fraction 15 and 16 (Fig. 3.15B). The co-sedimentation of PHF2 with Mi2β and HDAC1 demonstrated that a significant portion of cellular PHF2 is associated with NuRD complex in a multiprotein complex, indicating that they might function as a complex to activate rDNA transcription via modulating the chromatin structure of rDNA.

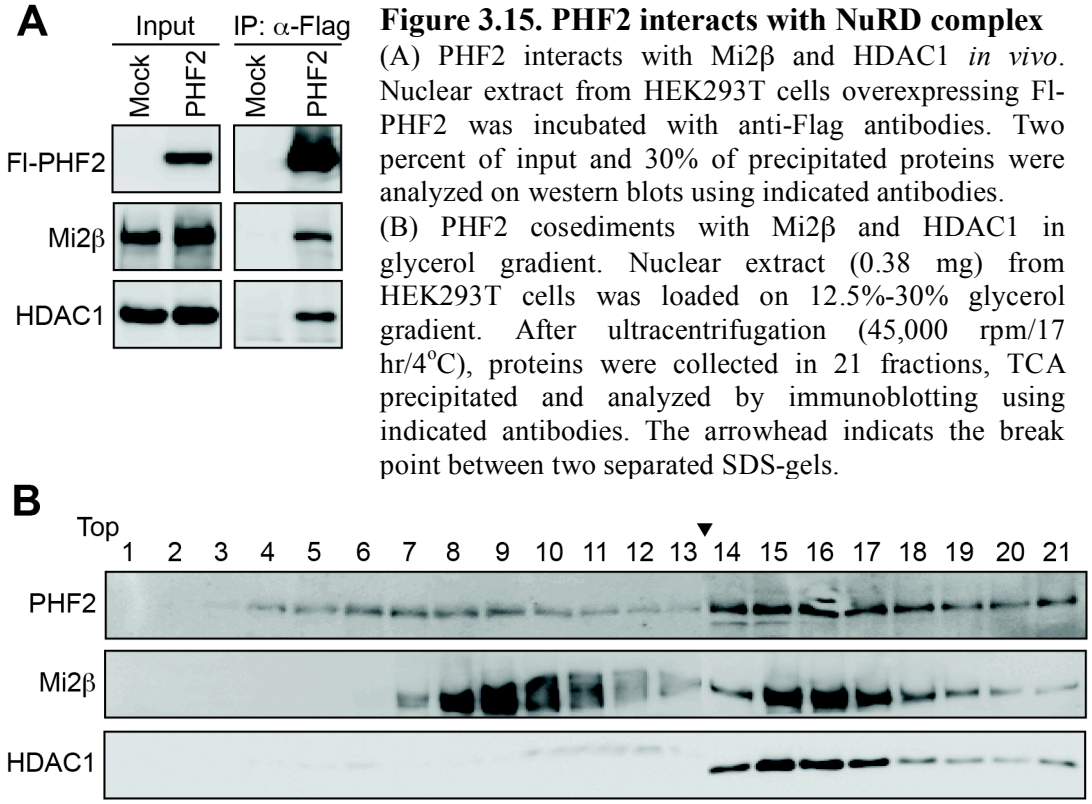

Figure 3.15. PHF2 interacts with NuRD complex
(A) PHF2 interacts with Mi2β and HDAC1 *in vivo*. Nuclear extract from HEK293T cells overexpressing Fl-PHF2 was incubated with anti-Flag antibodies. Two percent of input and 30% of precipitated proteins were analyzed on western blots using indicated antibodies.
(B) PHF2 cosediments with Mi2β and HDAC1 in glycerol gradient. Nuclear extract (0.38 mg) from HEK293T cells was loaded on 12.5%-30% glycerol gradient. After ultracentrifugation (45,000 rpm/17 hr/4^{o}C), proteins were collected in 21 fractions, TCA precipitated and analyzed by immunoblotting using indicated antibodies. The arrowhead indicats the break point between two separated SDS-gels.

3.16. PHF2 and KDM2B compete for rDNA occupancy

Recently, the JmjC domain-containing protein KDM2B has been reported to localize to nucleoli and to repress rDNA transcription via demethylation of the active histone mark H3K4me3 (Frescas et al. 2007). To reproduce these observations, nucleolar localization and rDNA occupancy of KDM2B were examined. Indirect immunofluorescence assays shown in Fig. 3.16A revealed that Flag-tagged KDM2B (Fl-KDM2B) localized to nucleoli and co-stained with UBF in U2OS cells. Consistent with KDM2B localizing to nucleoli and binding to rDNA, ChIP assays performed in HEK293T cells demonstrated that V5-tagged KDM2B (V5-KDM2B) was equally distributed at all rDNA regions tested, including the enhancer region, the rDNA promoter, the pre-rRNA coding region and intergenic spacer (Fig. 3.16B).

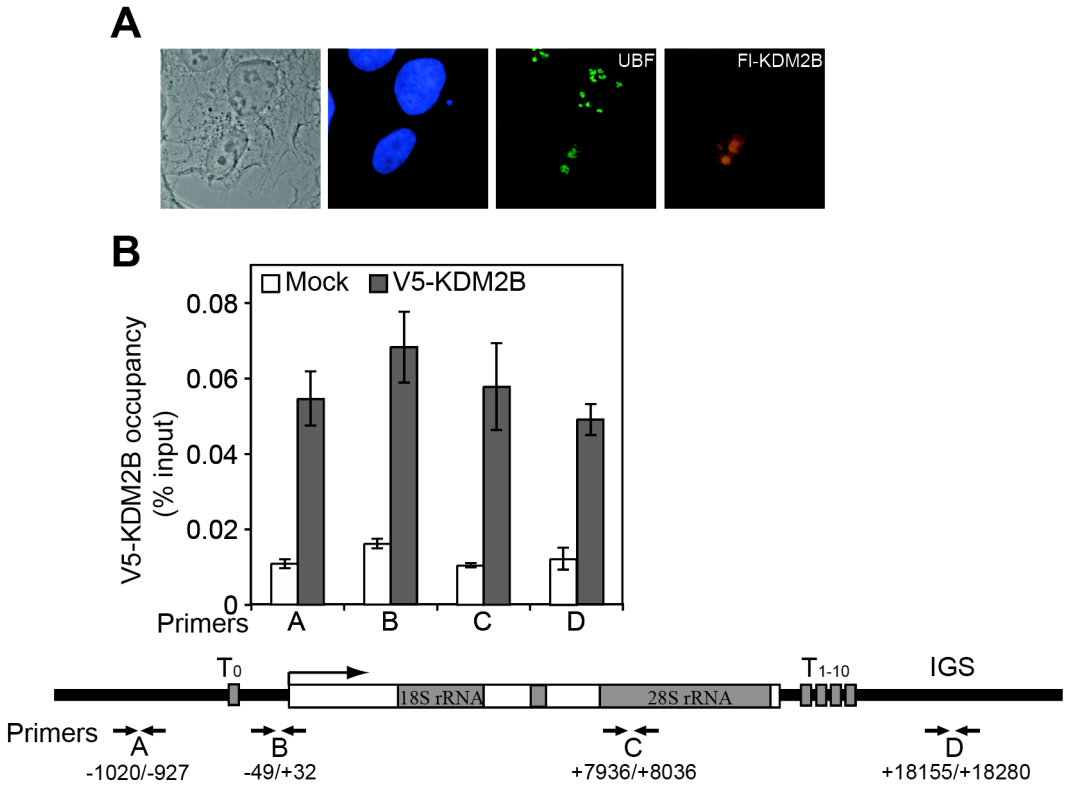

Figure 3.16. KDM2B localizes to nucleoli and binds to rDNA
(A) Fl-KDM2B colocalizes with UBF in nucleoli. U2OS cells overexpressing Fl-KDM2B were immunostained with anti-Flag-Cy3 and anti-UBF antibodies. Images of phase contrast and DNA staining with Hoechst are shown in the first two panels.
(B) KDM2B is associated with rDNA. Cross-linked chromatin from HEK293T cells overexpressing V5-KDM2B or mock-transfected was incubated with anti-V5 antibodies and precipitated DNA was amplified by qPCR using primers encompassing different regions of rDNA repeats indicated in the scheme below.

The observation that PHF2, PHF8 and KDM2B are present in nucleoli and regulate rDNA transcription raises the question about the functional relationship among these three JmjC domain-containing proteins. To examine whether these three nucleolar lysine demethylases physically interact, the interaction of KDM2B with PHF2 and PHF8 was examined by co-immunoprecipitation assays in HEK293T cells. As shown in Fig. 3.17 (left and middle panel), V5-KDM2B was co-precipitated with both Fl-PHF2 and Fl-PHF8. Consistently, both V5-PHF2 and V5-PHF8 could be co-precipitated with Fl-KDM2B (Fig. 3.17, right panel). Thus, KDM2B interacts with PHF2 and PHF8 *in vivo*.

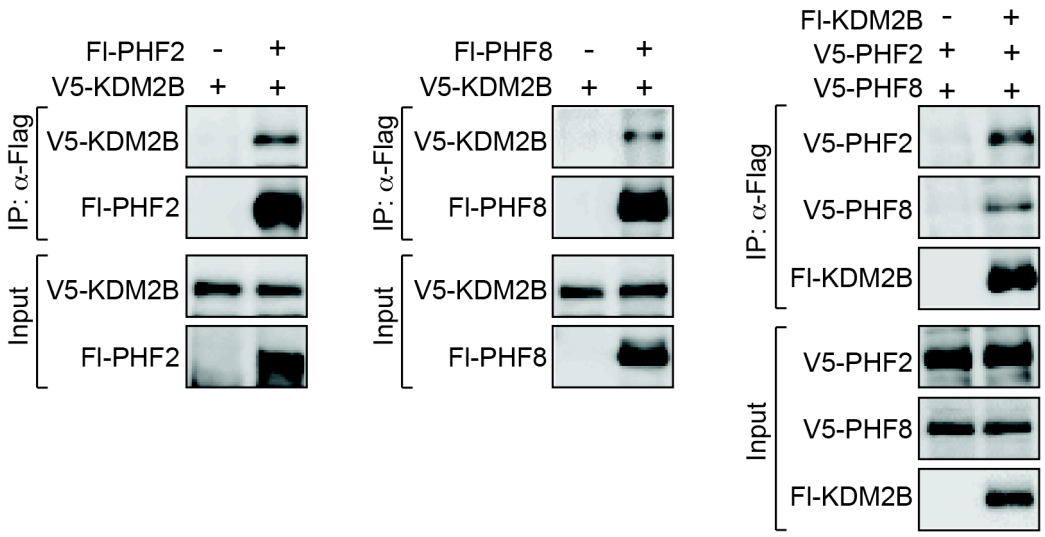

Figure 3.17. KDM2B interacts with PHF2 and PHF8
HEK293T cells were transfected with expression constructs encoding V5-KDM2B and Fl-PHF2 (left panel) or Fl-PHF8 (middle panel). Nuclear extracts from these cells were incubated with anti-Flag antibodies, and 2% of input and 33% of precipitated proteins were assayed by immunoblotting. (Right panel) HEK293T cells were transfected with expression plasmids encoding Fl-KDM2B, V5-PHF2 and V5-PHF8. Nuclear extracts from these cells were incubated with anti-Flag antibodies, and 2% of input and 33% of precipitated proteins were assayed on western blots.

To further explore the functional link among KDM2B, PHF2 and PHF8 at rDNA, KDM2B was depleted in HEK293T cells via siRNA and rDNA occupancy of PHF2 and PHF8 was examined by ChIP assays. As shown in Fig. 3.18A, the mRNA level of KDM2B was reduced by about 60% upon transfection of KDM2B-specific siRNA. Notably, the association of PHF2 with the rDNA promoter and the pre-rRNA coding region was enhanced >2- fold upon knockdown of KDM2B. The association of PHF8 with rDNA was also augmented, although to a lesser extent compared to PHF2 (Fig. 3.18A). The changes of rDNA occupancy of PHF2 and PHF8 were not due to the different levels of both proteins upon knockdown of KDM2B, as shown by western blot analysis. Thus, depletion of KDM2B leads to an increased association of PHF2 and PHF8 with rDNA, suggesting that a competition mechanism exists among KDM2B, PHF2 and PHF8 for rDNA occupancy. If so, depletion of PHF2 and PHF8 should enhance the association of KDM2B with rDNA. Indeed, depletion of PHF2 significantly enhanced rDNA occupancy of V5-KDM2B (Fig. 3.18B), but not the expression level of V5-KDM2B. However, no increase of rDNA occupancy of V5-KDM2B, but rather a slightly decrease, was observed upon

knockdown of PHF8, suggesting that PHF2, but not PHF8 is the direct competitor of KDM2B for rDNA occupancy. The competition between a transcriptional activator PHF2 and a repressor KDM2B indicates that PHF2 may partly activate rDNA transcription by replacing a repressor from rDNA.

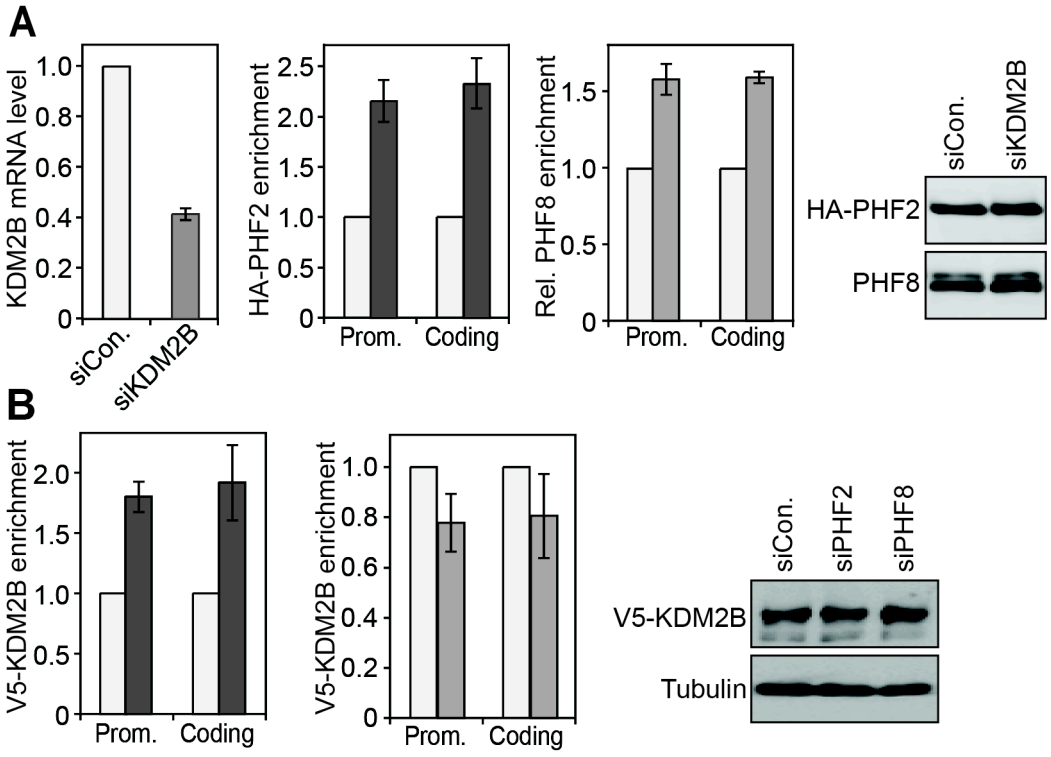

Figure 3.18. KDM2B competes with PHF2 for rDNA occupancy
(A) Knockdown of KDM2B augments the binding of PHF2 and PHF8 to rDNA. The binding of PHF2 and PHF8 to the rDNA promoter and the pre-rRNA coding region was monitored by ChIP assays with chromatin from HEK293T cells transfected with KDM2B-specific siRNA (dark bars) or the control non-target siRNA (light bars). qRT-PCR result at the left panel shows the level of KDM2B mRNA after normalizing to β-actin mRNA levels upon siRNA transfection. The western blot image at the right panel shows the levels of HA-PHF2 and PHF8 after siRNA transfection.
(B) Depletion of PHF2, but not PHF8 enhances the association of KDM2B with rDNA. The binding of V5-KDM2B to rDNA was monitored by ChIP assays using anti-V5 antibodies with chromtin from HEK293T cells depletion of PHF2 (left panel) or PHF8 (middle panel). The western blot image at the right panel shows the levels of V5-KDM2B and tubulin upon siRNA knockdown.

4. Discussion

The transcriptional activity of rRNA genes is reflected by specific euchromatic and heterochromatic modifications. Acetylation of histone H4 and methylation of H3K4 are characteristic for transcribed rRNA genes, whereas DNA hypermethylation at CpG residues, histone H4 hypoacetylation, and methylation of H3K9 and H4K20 correlate with transcriptional silencing (Santoro et al. 2002; Zhou et al. 2002). The ATP-dependent chromatin remodeling complex, NoRC, coordinates the activities of enzymes that modify histones and methylate DNA to establish a ‘‘closed’’ heterochromatic state (Santoro and Grummt 2005). In contrast to NoRC-dependent silencing, little is known about the mechanisms that establish and maintain the euchromatic state of active rDNA repeats. The recently identified histone demethylases are likely to play a crucial role, since they are able to remove the inhibitory methylation marks on histone H3. In the present work, the function of two putative JmjC domain-containing histone demethylases PHF2 and PHF8, which localize within nucleoli, has been studied. The results reveal that PHF2 and PHF8 function in a coordinated manner to maintain the euchromatic state of active rRNA genes.

4.1. PHF2 and PHF8 are targeted to active rDNA

Both endogenous and GFP-tagged PHF2 and PHF8 localize to nucleoli, suggesting that both proteins serve a role in regulation of nucleolar chromatin function and/or rDNA transcription. Indeed, protein-protein interaction experiments showed that PHF2 and PHF8 interact with Pol I and with UBF, a Pol I-specific transcription factor. This data suggests that the nucleolar localization of PHF2 and PHF8 is probably mediated by association with the Pol I transcription machinery. In support of this, a point mutant (PHF8-F279S) that does not interact with Pol I and UBF does not localize in nucleoli (Fig. 3.13C). On the other hand, PHF2 and PHF8 are also associated with untranscribed intergenic spacer (Fig. 3.3B) and therefore additional recruitment mechanisms should exist that facilitate the association of PHF2 and PHF8 with rDNA. The interaction of PHF2 and PHF8 with histones may explain the presence of both proteins at intergenic spacer that is compacted by nucleosomes

in both active and silent rDNA repeats. DNA methylation assays of PHF2 and PHF8-associated rDNA revealed that both proteins preferentially bind to unmethylated, active rRNA genes (Fig. 3.3C), which are characterized by the active histone mark H3K4me3. In vitro binding assays showed that the PHD fingers of PHF2 and PHF8 specifically bind to H3K4me3 (Fig. 3.9D and data not shown). Thus, the recruitment of PHF2 and PHF8 to active rDNA repeats is likely mediated by cooperative interaction with both Pol I and H3K4me3. The importance of this recruitment is underscored by the observation that mutations in the PHD fingers abolished PHF2 and PHF8-mediated activation of rDNA transcription. The targeting of PHF2 and PHF8 to active rDNA repeats reveals a common step-wise mechanism of recruitment of chromatin modifying enzymes to specific genes. First, interactions with gene specific DNA-binding factors recruit these enzymes to their target genes. Second, the local chromatin enviroment is recognized by the chromatin binding modules that are possessed by the enzymes themselves or by their associated proteins. With this, the chromatin modifying enzymes are capable to modulate chromatin in a temporal and spatial-dependent manner (Lan et al. 2008). For instance, the H3K4me3 demethylase SMCX/KDM5C (also known as JARID1C) has been shown to be associated with the sequence-specific REST complex, which targetes KDM5C to REST responsible genes. The PHD finger of KDM5C recognizes the repressive mark H3K9me3, which may provide additional selectivity for its recruitment. The coordinated action of the PHD finger and JmjC domain of KDM5C leads to repression of neuronal genes in non-neuronal tissues (Iwase et al. 2007; Tahiliani et al. 2007).

The association of PHF2 with rDNA was significantly reduced upon depletion of PHF8 (Fig. 3.11B). In contrast, depletion of PHF2 did not impair rDNA occupancy of PHF8 (Fig. 3.11C). This data indicates that PHF8 is required for the recruitment of PHF2. Knockdown of PHF8 resulted in a decrease of H3K4me3 and an increase of H3K9me1/2 at rDNA (Fig. 3.10B). Thus, these results suggested that the association with H3K4me3 facilitates binding of PHF2 to rDNA. The presence of H3K9me1/2, however, appears to be inhibitory for binding of PHF2 to rDNA. Therefore, PHF2 may serve as an auxiliary factor that cooperates with PHF8 to stimulate rDNA transcription.

4.2. PHF8 demethylates H3K9me1/2 at active rRNA genes

Consistent with a positive role in rDNA transcription, depletion of PHF8 increased the levels of the repressive marks H3K9me2 and H3K9me1 (H3K9me1/2) at the rDNA promoter (Fig. 3.10B), suggesting that PHF8 demethylates H3K9me1/2. In accord with this, *in vitro* demethylation assays revealed that PHF8 (1-690) purified from baculovirus-infected Sf9 insect cells demethylated H3K9me1 and H3K9me2 (personal communication M.Yonezawa). The JmjC domain-deficient mutant PHF8-HID was inactive in these assays, underscoring the specificity of the demethylation reaction. Given that the PHD finger of PHF8 interacts with H3K4me3, it was examined whether the presence of H3K4me3 may stimulate demethylation of H3K9me2. For this, a doubly modified histone H3 peptide that is trimethylated at lysine 4 and dimethylated at lysine 9 (H3K4me3/K9me2) was used as substrate for the demethylation assays. Coversion of H3K9me2 to mono- or unmodified form by PHF8 was markedly enhanced if the H3K4 was trimethylated. A point mutation in the PHD finger (PHF8-Y7A) that abolishes the interaction with H3K4me3 suppressed the stimulatory effect of H3K4me3 on PHF8-mediated demethylation of H3K9me2. This data indicates that binding of the PHD finger of PHF8 to H3K4me3 promotes demethylation of H3K9me2. The finding that demethylation of H3K9 depends on the presence of adjacent H3K4me3 underscores the cross-talk of histone modifications in chromatin-based processes. It has been demonstrated that the addition or removal of certain modifications may be dependent upon other existing modifications (Jenuwein and Allis 2001). This can occur both in cis, from within the same histone, or in trans, contributed from another histones. Consistently, a point mutation next to the PHD finger of the H3K4me3 demethylase SMCX/KDM5C has been shown to impair both the association of the PHD finger with H3K9me3 and the demethylase activity *in vitro* (Iwase et al. 2007). Moreover, the histone demethylase KDM4A contains a double tudor domain that is capable to recognize H3K4me2/3 and H4K20me2/3 (Kim et al. 2006), suggesting that stimulation of demethylase activity by pre-existing methylation marks may be a common mechanism for KDMs that contain methyl-lysine binding motifs.

Mammalian cells containing 400 copies of rRNA genes, about half of

them being actively transcribed. Therefore, ChIP assays monitor the average levels of histone marks both at active and silent rRNA genes. For this reason, the increase of H3K9me1/2 levels upon depletion of PHF8 can be caused by either inhibiting the demethylation of H3K9me1/2 at silent or active rDNA. Several lines of experimental evidences favor the latter possibility. First, PHF8 binds to active rRNA genes, which is likely due to the association with both the Pol I transcription machinery and H3K4me3. Second, *in vitro* demethylation assays reveal that H3K4me3 is required for efficiently removing H3K9me1/2 by PHF8. H3K4me3 is exclusively associated with active rRNA genes, whereas H3K9 methylation is present at both active and silent rDNA (Yuan et al. 2007). Third, depletion of PHF8 reduced the level of H3K4me3 at the rDNA promoter, suggesting a functional link between demethylation of H3K9me1/2 and trimethylation of H3K4. The association of PHF8 with the histone H3K4 methyltransfearse MLL1 complex (Fig. 3.14A) further supports the cross-talk between H3K4me3 and H3K9me1/2 demethylation. Taken together, PHF8 binds to active rRNA genes and maintains the euchromatic state of transcriptionally active rDNA repeats.

4.3. PHF2 does not demethylate histones

The finding that the JmjC domain-deficient mutant PHF2 (PHF2-H249A) does not activate rDNA transcription suggests that PHF2 may be an active lysine demethylase (Fig. 3.7A). However, depletion of PHF2 in HEK293T cells did not result in upregulation of any histone methylation mark tested (Fig. 3.10C and data not shown). In addition, recombinant PHF2 did not show any histone demethylation activity *in vitro* (personal communication M. Yonezawa). Therefore, PHF2 is probably not an active histone demethylase. However, it cannot be excluded that the point mutation (PHF2-H249A) affects the whole protein structure, thereby abrogating its function. If this is not the case, PHF2 may either demethylate non-histone substrates or possess another JmjC domain-dependent enzymatic activity rather than demethylation. A growing number of non-histone proteins, such as p53, TAF10 and G9a have been shown to be subjected to methylation at individual lysine residues (Sims et al. 2008). Similar to histone methylation, methylation of non-histone proteins is reversible. For

instance, lysine demethylase LSD1 is able to demethylate p53 at residue K370 (Huang et al. 2007). Two lysine residues in G9a and GLP have been shown to be methylated by G9a and an unkown methyltransferase (Sampath et al. 2007). Since both G9a and GLP interact with PHF2 (Fig. 3.14B), they are potential demethylation substrates for PHF2. Before the histone demethylation activity of the JmjC domain has been identified, this domain was suggested to be responsible for the enzymatic activity of iron- and αKG-dependent oxygenases (Trewick et al. 2005). For instance, the JmjC domain-containing protein FIH is an asparaginyl hydroxylase that targets residue Asp 803 of HIF-1α (Lando et al. 2002). Thus, it is likely that PHF2 may function as a hydroxylase.

The alignment of the JmjC domains of PHF2, PHF8, KDM2A and KDM2B revealed a substitution of histidine to tyrosine in the third iron-binding residue (Fig. 3.10A). Intriguingly, the same substitution occurs in the *S. pombe* JmjC domain-containing protein Epe1, which renders the enzyme inactive towards histone substrates (Tsukada et al. 2006). However, Epe1 requires predicted iron- and αKG-binding residues for *in vivo* function, suggesting that the functional JmjC domain is essential (Trewick et al. 2007).

4.4. PHF2 and PHF8 antagonize KDM2B at active rDNA

The maintaince of the balance of histone methylation requires the action of both histone methyltransferases and demethylases. PHF8 functions together with PHF2 at active rRNA genes to maintain them in a euchromatic state. On the other hand, KDM2B is capable to silence active rRNA genes by demethylating H3K4me3 (Frescas et al. 2007). While the distribution of KDM2B to nucleoli is mediated by a nucleolar localization sequence (NoLS), the binding to active rDNA might be conferred by a DNA-binding motif, the CXXC domain, which has been shown to have a strong preference for unmethylated CpG dinucleotides (Koyama-Nasu et al. 2007). The counteraction of PHF2, PHF8 and KDM2B offers a mechanism how the cell regulates the chromatin state of active rRNA genes (Fig. 4.1). PHF2 and PHF8 are targeted to rDNA by interaction with Pol I and UBF, and the recognition of H3K4me3 by their PHD fingers offers additional selectivity for active rRNA genes. The observation that depletion of PHF2 enhanced rDNA occupancy of KDM2B suggested that PHF2

is capable to antaganize the activity of the H3K4me3 demethylase KDM2B (Fig. 3.18A). This antagonization mechanism prevents erasion of the active mark H3K4me3. Importantly, the PHF8-associated MLL1 complex trimethylates H3K4 and the presence of H3K4me3 stimulates demethylation of H3K9me1/2 by PHF8. Therefore, a complex consisting of at least PHF8/MLL1/PHF2 is required to maintain and propagate the epigenetically active state of rRNA genes. On the other hand, downregulation of rDNA transcription not only leads to loss of rDNA occupancy of Pol I but also of PHF2 and PHF8. The dissociation of PHF2 from rDNA in turn may enable KDM2B to bind to rDNA. The changes of association of these chromatin modifying enzymes will establish heterochromatic histone modifications, i.e. will lead to decreased H3K4me3 and increased H3K9me1/2 levels at the rDNA promoter. However, this model of dynamic balance between PHF2, PHF8 and KDM2B still needs to be experimentally validated.

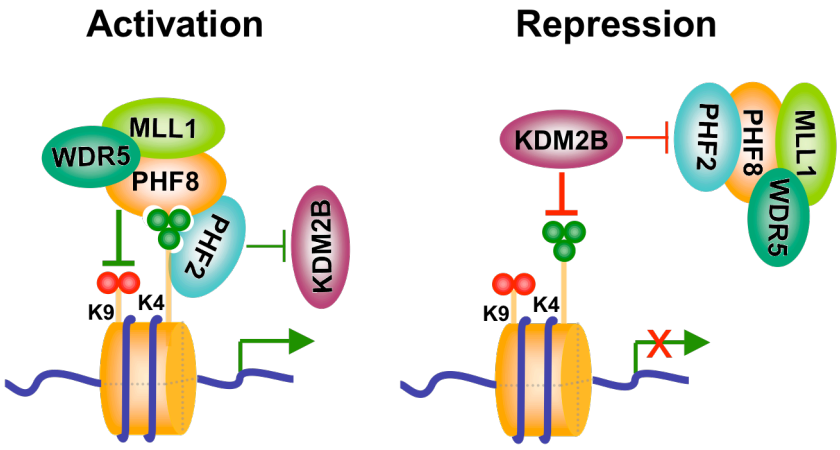

Figure 4.1. PHF2/PHF8/MLL1 and KDM2B regulate the chromatin state of the active rRNA genes
PHF8 and PHF2 bind to active rDNA repeats by recognition of H3K4me3 (green balls) with their PHD fingers. After recruitment, PHF8 removes the repressive mark H3K9me1/2 at the rDNA promoter (red balls), whereas PHF2 antaganizes the association of the H3K4me3 demethylase KDM2B. Moreover, PHF8 is associated with the histone H3K4 methyltransferase MLL1-WDR5 complex. The presence of H3K4me3 stimulates the demethylation of H3K9me1/2 by PHF8. Therefore, the cooperative action of PHF2/PHF8/MLL1 establishes and maintains euchromatic histone modifications at active rRNA genes. Upon repression of rDNA transcription, PHF2 and PHF8 dissociate from rDNA, whereas KDM2B is able to bind to active rRNA genes and demethylates the active mark H3K4me3. As a consequence, heterochromatic histone modifications are established, i.e. a decreased H3K4me3 and increased H3K9me1/2 levels.

4.5. PHF8 and XLMR

X-linked metal retardation is a common cause of moderate to severe intellectual disability in males. XLMR is very heterogeneous and over 60 genes have been linked to this syndrome. A subset of these genes seems to be involved in regulation of chromatin structure and gene expression, which include DNA binding transcription factors such as ARX and ZNF41 as well as methyl-CpG binding protein MeCP2 and the histone demethylase SMCX/KDM5C. In particular, mutations in *SMCX/KDM5C* and *PHF8* have been found in families with XLMR, suggesting a link between specific histone demethylases and human diseases. The finding that XLMR-associated SMCX/KDM5C mutations compromised H3K4me3 demethylation suggested that XMLR may be in part caused by aberrant histone methylation (Iwase et al. 2007; Tahiliani et al. 2007). In support of this notion, three of four identified XLMR-related PHF8 mutations result in partial or complete deletion of the JmjC domain, which apparently abrogate the demethylation activity. Moreover, an XLMR-associated point mutation within the JmjC domain of PHF8 (F279S) also abolished the histone demethylase acitivity (personal communication M. Yonezawa). This mutation was predicted to have a damaging influence on the function and structure of PHF8 (Koivisto et al. 2007), which may explain why a point mutant at a non-cofactor binding residue abolishes the demethylation activity of PHF8. Importantly, this point mutation also impaired nucleolar localization and transcription activation of PHF8, linking XLMR to dysfunction of rRNA synthesis. PHF8 is not only highly expressed in early stages of brain development, but also in the cerebellum and hippocampus in adult brain (Laumonnier et al. 2005), which are vital structures for memory and learning. Thus, XLMR-associated mutations of PHF8 impair ribosome biogenesis, which might cause proliferation defects of cells involved in cognition. Howerver, it cannot be excluded that PHF8 might also serve non-nucleolar functions in the cells, whose defect due to PHF8 mutation might also contribute to the development of XLMR. In particular, the mutant PHF8-F279S may serve a dominant negative function, which bind to H3K4me3 via its PHD domain at promoters of certain XLMR target genes. The lack of histone demethylation activity of PHF8-F279S may then keep these genes in transcriptional silent

state, which may in turn cause XLMR. Nevertheless, the present study offers a possible epigenetic mechanism to explain the role of PHF8 in XLMR.

References:

Abidi, F.E., Holloway, L., Moore, C.A., Weaver, D.D., Simensen, R.J., Stevenson, R.E., Rogers, R.C., and Schwartz, C.E. 2008. Mutations in JARID1C are associated with X-linked mental retardation, short stature and hyperreflexia. J Med Genet 45(12): 787-793.

Abidi, F.E., Miano, M.G., Murray, J.C., and Schwartz, C.E. 2007. A novel mutation in the PHF8 gene is associated with X-linked mental retardation with cleft lip/cleft palate. Clin Genet 72(1): 19-22.

Adams-Cioaba, M.A. and Min, J. 2009. Structure and function of histone methylation binding proteins. Biochem Cell Biol 87(1): 93-105.

Allis, C.D., Berger, S.L., Cote, J., Dent, S., Jenuwien, T., Kouzarides, T., Pillus, L., Reinberg, D., Shi, Y., Shiekhattar, R. et al. 2007. New nomenclature for chromatin-modifying enzymes. Cell 131(4): 633-636.

Baker, L.A., Allis, C.D., and Wang, G.G. 2008. PHD fingers in human diseases: disorders arising from misinterpreting epigenetic marks. Mutat Res 647(1-2): 3-12.

Bell, S.P., Learned, R.M., Jantzen, H.M., and Tjian, R. 1988. Functional cooperativity between transcription factors UBF1 and SL1 mediates human ribosomal RNA synthesis. Science 241(4870): 1192-1197.

Bhaumik, S.R., Smith, E., and Shilatifard, A. 2007. Covalent modifications of histones during development and disease pathogenesis. Nat Struct Mol Biol 14(11): 1008-1016.

Bradsher, J., Auriol, J., Proietti de Santis, L., Iben, S., Vonesch, J.L., Grummt, I., and Egly, J.M. 2002. CSB is a component of RNA pol I transcription. Mol Cell 10(4): 819-829.

Caslini, C., Alarcon, A.S., Hess, J.L., Tanaka, R., Murti, K.G., and Biondi, A. 2000. The amino terminus targets the mixed lineage leukemia (MLL) protein to the nucleolus, nuclear matrix and mitotic chromosomal scaffolds. Leukemia 14(11): 1898-1908.

Cedar, H. and Bergman, Y. 2009. Linking DNA methylation and histone modification: patterns and paradigms. Nat Rev Genet 10(5): 295-304.

Chang, B., Chen, Y., Zhao, Y., and Bruick, R.K. 2007. JMJD6 is a histone arginine demethylase. Science 318(5849): 444-447.

Chen, Z., Zang, J., Whetstine, J., Hong, X., Davrazou, F., Kutateladze, T.G., Simpson, M., Mao, Q., Pan, C.H., Dai, S. et al. 2006. Structural insights into histone demethylation by JMJD2 family members. Cell 125(4): 691-702.

Cloos, P.A., Christensen, J., Agger, K., Maiolica, A., Rappsilber, J., Antal, T.,

Hansen, K.H., and Helin, K. 2006. The putative oncogene GASC1 demethylates tri- and dimethylated lysine 9 on histone H3. Nature 442(7100): 307-311.

Cloos, P.A., Christensen, J., Agger, K., and Helin, K. 2008. Erasing the methyl mark: histone demethylases at the center of cellular differentiation and disease. Genes Dev 22(9): 1115-1140.

Conconi, A., Widmer, R.M., Koller, T., and Sogo, J.M. 1989. Two different chromatin structures coexist in ribosomal RNA genes throughout the cell cycle. Cell 57(5): 753-761.

Dou, Y., Milne, T.A., Ruthenburg, A.J., Lee, S., Lee, J.W., Verdine, G.L., Allis, C.D., and Roeder, R.G. 2006. Regulation of MLL1 H3K4 methyltransferase activity by its core components. Nat Struct Mol Biol 13(8): 713-719.

Fernandez, A.G., Gunsalus, K.C., Huang, J., Chuang, L.S., Ying, N., Liang, H.L., Tang, C., Schetter, A.J., Zegar, C., Rual, J.F. et al. 2005. New genes with roles in the C. elegans embryo revealed using RNAi of ovary-enriched ORFeome clones. Genome Res 15(2): 250-259.

Fodor, B.D., Kubicek, S., Yonezawa, M., O'Sullivan, R.J., Sengupta, R., Perez-Burgos, L., Opravil, S., Mechtler, K., Schotta, G., and Jenuwein, T. 2006. Jmjd2b antagonizes H3K9 trimethylation at pericentric heterochromatin in mammalian cells. Genes Dev 20(12): 1557-1562.

Frescas, D., Guardavaccaro, D., Bassermann, F., Koyama-Nasu, R., and Pagano, M. 2007. JHDM1B/FBXL10 is a nucleolar protein that represses transcription of ribosomal RNA genes. Nature 450(7167): 309-313.

Hasenpusch-Theil, K., Chadwick, B.P., Theil, T., Heath, S.K., Wilkinson, D.G., and Frischauf, A.M. 1999. PHF2, a novel PHD finger gene located on human chromosome 9q22. Mamm Genome 10(3): 294-298.

He, J., Kallin, E.M., Tsukada, Y., and Zhang, Y. 2008. The H3K36 demethylase Jhdm1b/Kdm2b regulates cell proliferation and senescence through p15(Ink4b). Nat Struct Mol Biol 15(11): 1169-1175.

Henikoff, S. 2008. Nucleosome destabilization in the epigenetic regulation of gene expression. Nat Rev Genet 9(1): 15-26.

Huang, J., Sengupta, R., Espejo, A.B., Lee, M.G., Dorsey, J.A., Richter, M., Opravil, S., Shiekhattar, R., Bedford, M.T., Jenuwein, T. et al. 2007. p53 is regulated by the lysine demethylase LSD1. Nature 449(7158): 105-108.

Iwase, S., Lan, F., Bayliss, P., de la Torre-Ubieta, L., Huarte, M., Qi, H.H., Whetstine, J.R., Bonni, A., Roberts, T.M., and Shi, Y. 2007. The X-linked mental retardation gene SMCX/JARID1C defines a family of histone H3 lysine 4 demethylases. Cell 128(6): 1077-1088.

Jensen, L.R., Amende, M., Gurok, U., Moser, B., Gimmel, V., Tzschach, A.,

Janecke, A.R., Tariverdian, G., Chelly, J., Fryns, J.P. et al. 2005. Mutations in the JARID1C gene, which is involved in transcriptional regulation and chromatin remodeling, cause X-linked mental retardation. Am J Hum Genet 76(2): 227-236.

Jenuwein, T. and Allis, C.D. 2001. Translating the histone code. Science 293(5532): 1074-1080.

Kim, J., Daniel, J., Espejo, A., Lake, A., Krishna, M., Xia, L., Zhang, Y., and Bedford, M.T. 2006. Tudor, MBT and chromo domains gauge the degree of lysine methylation. EMBO Rep 7(4): 397-403.

Klose, R.J., Kallin, E.M., and Zhang, Y. 2006. JmjC-domain-containing proteins and histone demethylation. Nat Rev Genet 7(9): 715-727.

Klose, R.J., Yamane, K., Bae, Y., Zhang, D., Erdjument-Bromage, H., Tempst, P., Wong, J., and Zhang, Y. 2006. The transcriptional repressor JHDM3A demethylates trimethyl histone H3 lysine 9 and lysine 36. Nature 442(7100): 312-316.

Klose, R.J. and Zhang, Y. 2007. Regulation of histone methylation by demethylimination and demethylation. Nat Rev Mol Cell Biol 8(4): 307-318.

Koivisto, A.M., Ala-Mello, S., Lemmela, S., Komu, H.A., Rautio, J., and Jarvela, I. 2007. Screening of mutations in the PHF8 gene and identification of a novel mutation in a Finnish family with XLMR and cleft lip/cleft palate. Clin Genet 72(2): 145-149.

Kouzarides, T. 2007. Chromatin modifications and their function. Cell 128(4): 693-705.

Koyama-Nasu, R., David, G., and Tanese, N. 2007. The F-box protein Fbl10 is a novel transcriptional repressor of c-Jun. Nat Cell Biol 9(9): 1074-1080.

Kustatscher, G. and Ladurner, A.G. 2007. Modular paths to 'decoding' and 'wiping' histone lysine methylation. Curr Opin Chem Biol 11(6): 628-635.

Lan, F., Collins, R.E., De Cegli, R., Alpatov, R., Horton, J.R., Shi, X., Gozani, O., Cheng, X., and Shi, Y. 2007. Recognition of unmethylated histone H3 lysine 4 links BHC80 to LSD1-mediated gene repression. Nature 448(7154): 718-722.

Lan, F., Nottke, A.C., and Shi, Y. 2008. Mechanisms involved in the regulation of histone lysine demethylases. Curr Opin Cell Biol 20(3): 316-325.

Lando, D., Peet, D.J., Gorman, J.J., Whelan, D.A., Whitelaw, M.L., and Bruick, R.K. 2002. FIH-1 is an asparaginyl hydroxylase enzyme that regulates the transcriptional activity of hypoxia-inducible factor. Genes Dev 16(12): 1466-1471.

Landry, J., Sutton, A., Hesman, T., Min, J., Xu, R.M., Johnston, M., and

Sternglanz, R. 2003. Set2-catalyzed methylation of histone H3 represses basal expression of GAL4 in Saccharomyces cerevisiae. Mol Cell Biol 23(17): 5972-5978.

Laumonnier, F., Holbert, S., Ronce, N., Faravelli, F., Lenzner, S., Schwartz, C.E., Lespinasse, J., Van Esch, H., Lacombe, D., Goizet, C. et al. 2005. Mutations in PHF8 are associated with X linked mental retardation and cleft lip/cleft palate. J Med Genet 42(10): 780-786.

Li, B., Carey, M., and Workman, J.L. 2007. The role of chromatin during transcription. Cell 128(4): 707-719.

Li, H., Ilin, S., Wang, W., Duncan, E.M., Wysocka, J., Allis, C.D., and Patel, D.J. 2006. Molecular basis for site-specific read-out of histone H3K4me3 by the BPTF PHD finger of NURF. Nature 442(7098): 91-95.

Li, J., Langst, G., and Grummt, I. 2006. NoRC-dependent nucleosome positioning silences rRNA genes. EMBO J 25(24): 5735-5741.

Loh, Y.H., Zhang, W., Chen, X., George, J., and Ng, H.H. 2007. Jmjd1a and Jmjd2c histone H3 Lys 9 demethylases regulate self-renewal in embryonic stem cells. Genes Dev 21(20): 2545-2557.

Martin, C. and Zhang, Y. 2005. The diverse functions of histone lysine methylation. Nat Rev Mol Cell Biol 6(11): 838-849.

Mayer, C., Bierhoff, H., and Grummt, I. 2005. The nucleolus as a stress sensor: JNK2 inactivates the transcription factor TIF-IA and down-regulates rRNA synthesis. Genes Dev 19(8): 933-941.

McStay, B. and Grummt, I. 2008. The epigenetics of rRNA genes: from molecular to chromosome biology. Annu Rev Cell Dev Biol 24: 131-157.

Miller, G., Panov, K.I., Friedrich, J.K., Trinkle-Mulcahy, L., Lamond, A.I., and Zomerdijk, J.C. 2001. hRRN3 is essential in the SL1-mediated recruitment of RNA Polymerase I to rRNA gene promoters. EMBO J 20(6): 1373-1382.

Murayama, A., Ohmori, K., Fujimura, A., Minami, H., Yasuzawa-Tanaka, K., Kuroda, T., Oie, S., Daitoku, H., Okuwaki, M., Nagata, K. et al. 2008. Epigenetic control of rDNA loci in response to intracellular energy status. Cell 133(4): 627-639.

Okada, Y., Scott, G., Ray, M.K., Mishina, Y., and Zhang, Y. 2007. Histone demethylase JHDM2A is critical for Tnp1 and Prm1 transcription and spermatogenesis. Nature 450(7166): 119-123.

Ooi, S.K., Qiu, C., Bernstein, E., Li, K., Jia, D., Yang, Z., Erdjument-Bromage, H., Tempst, P., Lin, S.P., Allis, C.D. et al. 2007. DNMT3L connects unmethylated lysine 4 of histone H3 to de novo methylation of DNA. Nature 448(7154): 714-717.

Panov, K.I., Friedrich, J.K., Russell, J., and Zomerdijk, J.C. 2006. UBF activates RNA polymerase I transcription by stimulating promoter escape. EMBO J 25(14): 3310-3322.

Pena, P.V., Davrazou, F., Shi, X., Walter, K.L., Verkhusha, V.V., Gozani, O., Zhao, R., and Kutateladze, T.G. 2006. Molecular mechanism of histone H3K4me3 recognition by plant homeodomain of ING2. Nature 442(7098): 100-103.

Percipalle, P., Fomproix, N., Cavellan, E., Voit, R., Reimer, G., Kruger, T., Thyberg, J., Scheer, U., Grummt, I., and Farrants, A.K. 2006. The chromatin remodelling complex WSTF-SNF2h interacts with nuclear myosin 1 and has a role in RNA polymerase I transcription. EMBO Rep 7(5): 525-530.

Pfau, R., Tzatsos, A., Kampranis, S.C., Serebrennikova, O.B., Bear, S.E., and Tsichlis, P.N. 2008. Members of a family of JmjC domain-containing oncoproteins immortalize embryonic fibroblasts via a JmjC domain-dependent process. Proc Natl Acad Sci U S A 105(6): 1907-1912.

Qian, C. and Zhou, M.M. 2006. SET domain protein lysine methyltransferases: Structure, specificity and catalysis. Cell Mol Life Sci 63(23): 2755-2763.

Ropers, H.H. 2006. X-linked mental retardation: many genes for a complex disorder. Curr Opin Genet Dev 16(3): 260-269.

Sampath, S.C., Marazzi, I., Yap, K.L., Krutchinsky, A.N., Mecklenbrauker, I., Viale, A., Rudensky, E., Zhou, M.M., Chait, B.T., and Tarakhovsky, A. 2007. Methylation of a histone mimic within the histone methyltransferase G9a regulates protein complex assembly. Mol Cell 27(4): 596-608.

Sanij, E., Poortinga, G., Sharkey, K., Hung, S., Holloway, T.P., Quin, J., Robb, E., Wong, L.H., Thomas, W.G., Stefanovsky, V. et al. 2008. UBF levels determine the number of active ribosomal RNA genes in mammals. J Cell Biol 183(7): 1259-1274.

Santoro, R. and Grummt, I. 2005. Epigenetic mechanism of rRNA gene silencing: temporal order of NoRC-mediated histone modification, chromatin remodeling, and DNA methylation. Mol Cell Biol 25(7): 2539-2546.

Santoro, R., Li, J., and Grummt, I. 2002. The nucleolar remodeling complex NoRC mediates heterochromatin formation and silencing of ribosomal gene transcription. Nat Genet 32(3): 393-396.

Seither, P. and Grummt, I. 1996. Molecular cloning of RPA2, the gene encoding the second largest subunit of mouse RNA polymerase I. Genomics 37(1): 135-139.

Shi, X., Hong, T., Walter, K.L., Ewalt, M., Michishita, E., Hung, T., Carney, D., Pena, P., Lan, F., Kaadige, M.R. et al. 2006. ING2 PHD domain links

histone H3 lysine 4 methylation to active gene repression. Nature 442(7098): 96-99.

Shilatifard, A. 2008. Molecular implementation and physiological roles for histone H3 lysine 4 (H3K4) methylation. Curr Opin Cell Biol 20(3): 341-348.

Shimono, K., Shimono, Y., Shimokata, K., Ishiguro, N., and Takahashi, M. 2005. Microspherule protein 1, Mi-2beta, and RET finger protein associate in the nucleolus and up-regulate ribosomal gene transcription. J Biol Chem 280(47): 39436-39447.

Siderius, L.E., Hamel, B.C., van Bokhoven, H., de Jager, F., van den Helm, B., Kremer, H., Heineman-de Boer, J.A., Ropers, H.H., and Mariman, E.C. 1999. X-linked mental retardation associated with cleft lip/palate maps to Xp11.3-q21.3. Am J Med Genet 85(3): 216-220.

Sims, R.J., 3rd and Reinberg, D. 2008. Is there a code embedded in proteins that is based on post-translational modifications? Nat Rev Mol Cell Biol 9(10): 815-820.

Sinha, S., Singh, R.K., Alam, N., Roy, A., Roychoudhury, S., and Panda, C.K. 2008. Alterations in candidate genes PHF2, FANCC, PTCH1 and XPA at chromosomal 9q22.3 region: pathological significance in early- and late-onset breast carcinoma. Mol Cancer 7: 84.

Sogo, J.M. and Thoma, F. 1989. Electron microscopy of chromatin. Methods Enzymol 170: 142-165.

Stefanovsky, V.Y., Pelletier, G., Bazett-Jones, D.P., Crane-Robinson, C., and Moss, T. 2001. DNA looping in the RNA polymerase I enhancesome is the result of non-cooperative in-phase bending by two UBF molecules. Nucleic Acids Res 29(15): 3241-3247.

Stefanovsky, V., Langlois, F., Gagnon-Kugler, T., Rothblum, L.I., and Moss, T. 2006. Growth factor signaling regulates elongation of RNA polymerase I transcription in mammals via UBF phosphorylation and r-chromatin remodeling. Mol Cell 21(5): 629-639.

Tachibana, M., Ueda, J., Fukuda, M., Takeda, N., Ohta, T., Iwanari, H., Sakihama, T., Kodama, T., Hamakubo, T., and Shinkai, Y. 2005. Histone methyltransferases G9a and GLP form heteromeric complexes and are both crucial for methylation of euchromatin at H3-K9. Genes Dev 19(7): 815-826.

Tahiliani, M., Mei, P., Fang, R., Leonor, T., Rutenberg, M., Shimizu, F., Li, J., Rao, A., and Shi, Y. 2007. The histone H3K4 demethylase SMCX links REST target genes to X-linked mental retardation. Nature 447(7144): 601-605.

Taverna, S.D., Li, H., Ruthenburg, A.J., Allis, C.D., and Patel, D.J. 2007. How chromatin-binding modules interpret histone modifications: lessons from professional pocket pickers. Nat Struct Mol Biol 14(11): 1025-1040.

Trewick, S.C., McLaughlin, P.J., and Allshire, R.C. 2005. Methylation: lost in hydroxylation? EMBO Rep 6(4): 315-320.

Tsukada, Y., Fang, J., Erdjument-Bromage, H., Warren, M.E., Borchers, C.H., Tempst, P., and Zhang, Y. 2006. Histone demethylation by a family of JmjC domain-containing proteins. Nature 439(7078): 811-816.

Tzatsos, A., Pfau, R., Kampranis, S.C., and Tsichlis, P.N. 2009. Ndy1/KDM2B immortalizes mouse embryonic fibroblasts by repressing the Ink4a/Arf locus. Proc Natl Acad Sci U S A 106(8): 2641-2646.

Tzschach, A., Lenzner, S., Moser, B., Reinhardt, R., Chelly, J., Fryns, J.P., Kleefstra, T., Raynaud, M., Turner, G., Ropers, H.H. et al. 2006. Novel JARID1C/SMCX mutations in patients with X-linked mental retardation. Hum Mutat 27(4): 389.

Vakoc, C.R., Mandat, S.A., Olenchock, B.A., and Blobel, G.A. 2005. Histone H3 lysine 9 methylation and HP1gamma are associated with transcription elongation through mammalian chromatin. Mol Cell 19(3): 381-391.

Vermeulen, M., Mulder, K.W., Denissov, S., Pijnappel, W.W., van Schaik, F.M., Varier, R.A., Baltissen, M.P., Stunnenberg, H.G., Mann, M., and Timmers, H.T. 2007. Selective anchoring of TFIID to nucleosomes by trimethylation of histone H3 lysine 4. Cell 131(1): 58-69.

Voo, K.S., Carlone, D.L., Jacobsen, B.M., Flodin, A., and Skalnik, D.G. 2000. Cloning of a mammalian transcriptional activator that binds unmethylated CpG motifs and shares a CXXC domain with DNA methyltransferase, human trithorax, and methyl-CpG binding domain protein 1. Mol Cell Biol 20(6): 2108-2121.

Wang, G.G., Song, J., Wang, Z., Dormann, H.L., Casadio, F., Li, H., Luo, J.L., Patel, D.J., and Allis, C.D. 2009. Haematopoietic malignancies caused by dysregulation of a chromatin-binding PHD finger. Nature.

Whetstine, J.R., Nottke, A., Lan, F., Huarte, M., Smolikov, S., Chen, Z., Spooner, E., Li, E., Zhang, G., Colaiacovo, M. et al. 2006. Reversal of histone lysine trimethylation by the JMJD2 family of histone demethylases. Cell 125(3): 467-481.

Wissmann, M., Yin, N., Muller, J.M., Greschik, H., Fodor, B.D., Jenuwein, T., Vogler, C., Schneider, R., Gunther, T., Buettner, R. et al. 2007. Cooperative demethylation by JMJD2C and LSD1 promotes androgen receptor-dependent gene expression. Nat Cell Biol 9(3): 347-353.

Wysocka, J., Swigut, T., Milne, T.A., Dou, Y., Zhang, X., Burlingame, A.L., Roeder, R.G., Brivanlou, A.H., and Allis, C.D. 2005. WDR5 associates with histone H3 methylated at K4 and is essential for H3 K4 methylation and vertebrate development. Cell 121(6): 859-872.

Wysocka, J., Swigut, T., Xiao, H., Milne, T.A., Kwon, S.Y., Landry, J., Kauer, M., Tackett, A.J., Chait, B.T., Badenhorst, P. et al. 2006. A PHD finger of NURF couples histone H3 lysine 4 trimethylation with chromatin remodelling. Nature 442(7098): 86-90.

Yamane, K., Toumazou, C., Tsukada, Y., Erdjument-Bromage, H., Tempst, P., Wong, J., and Zhang, Y. 2006. JHDM2A, a JmjC-containing H3K9 demethylase, facilitates transcription activation by androgen receptor. Cell 125(3): 483-495.

Yuan, X., Feng, W., Imhof, A., Grummt, I., and Zhou, Y. 2007. Activation of RNA polymerase I transcription by cockayne syndrome group B protein and histone methyltransferase G9a. Mol Cell 27(4): 585-595.

Zatsepina, O.V., Voit, R., Grummt, I., Spring, H., Semenov, M.V., and Trendelenburg, M.F. 1993. The RNA polymerase I-specific transcription initiation factor UBF is associated with transcriptionally active and inactive ribosomal genes. Chromosoma 102(9): 599-611.

Zhou, Y., Santoro, R., and Grummt, I. 2002. The chromatin remodeling complex NoRC targets HDAC1 to the ribosomal gene promoter and represses RNA polymerase I transcription. EMBO J 21(17): 4632-4640.